PROMOTING ANGIOGENESIS IN BIOARTIFICIAL GRAFTS TOWARDS ENHANCED MYOCARDIAL RESTORATION

ELIANA CECILIA MARTINEZ VALENCIA

(M.D., University of Antioquia)

A THESIS SUBMITTED

FOR THE DEGREE OF DOCTOR OF PHILOSOPHY

DEPARTMENT OF SURGERY

NATIONAL UNIVERSITY OF SINGAPORE

2010

PREFACE

This thesis is submitted for the degree of Doctor of Philosophy in the Department of Surgery, Yong Loo Lin School of Medicine, National University of Singapore. No part of this thesis has been submitted for any other degree or equivalent at another university or educative institution. The research work in this thesis is original unless reference is made to other works. Parts of this thesis have been published or presented in the following:

International Peer-Reviewed Publications

Martinez EC, Wang J, Gan SU, Singh R, Lee CN, Kofidis T. Ascorbic Acid Improves Embryonic Cardiomyoblast Cell Survival & Promotes Vascularization In Potential Myocardial Grafts In Vivo. Tissue Eng Part A. 2010; 16(4):1349-61.

Martinez EC, Wang J, Lilyanna S, Ling LH, Gan SU, Singh R, Lee CN, Kofidis T. Post-ischemic Angiogenic Therapy Using In-vivo Pre-vascularized Ascorbic Acid-Enriched Myocardial Artificial Grafts Improves Heart function in a Rat Model. Under Review. Submitted to Journal of Tissue Engineering and Regenerative Medicine.

Martinez EC, Kofidis T. Myocardial tissue engineering: the quest for the ideal myocardial substitute. Expert Rev Cardiovasc Ther. 2009 ;7(8):921-8.

Published Abstracts

Martinez EC, Wang J, Lilyanna S, Ling LH, Gan SU, Singh R, Lee CN, Kofidis T. Post-ischemic Angiogenic Therapy Using In-vivo Pre-vascularized Ascorbic Acid-

Enriched Myocardial Artificial Grafts Improves Heart function in a Rat Model Circulation, 2010; 122: A10834.

Martinez EC, Wang J, Gan SU, Singh R, Lee CN, Kofidis T. Ascorbic Acid Improves Embryonic Cardiomyoblast Cell Survival & Promotes Vascularization In Myocardial Grafts In Vivo. Tissue Engineering and Regenerative Medicine. 2009; 6(12): S273.

International Conference Presentations

Martinez EC, Wang J, Lilyanna S, Ling LH, Gan SU, Singh R, Lee CN, Kofidis T. Post-ischemic Angiogenic Therapy using In-vivo Pre-vascularized Ascorbic Acid-Enriched Myocardial Artificial Grafts Improves Heart function in a Rat Model. Poster Presentation, American Heart Association Scientific Sessions, Chicago, Nov 2010.

Martinez EC, Wang J, Gan SU, Singh R, Lee CN, Kofidis T. Ascorbic Acid Improves Embryonic Cardiomyoblast Cell Survival & Promotes Vascularization In Myocardial Grafts In Vivo. Poster Presentation. 2nd Tissue Engineering and Regenerative Medicine International Society (TERMIS) World Congress. Seoul, Sept 2009.

Awards

Martinez EC, et al. Post-ischemic Angiogenic Therapy using In-vivo Pre-vascularized Ascorbic Acid- Enriched Myocardial Artificial Grafts Improves Heart function in a Rat Model**.** Best Poster Presentation Award. Yong Loo Lin, School of Medicine Inaugural Graduate Scientific Congress 2011 - “Meet the Science Behind Medicine”. National University of Singapore, January 2011

Martinez EC. American Heart Association’s (AHA) Council on Basic Cardiovascular Sciences (BCVS) International Travel Grant.

ACKNOWLEDGEMENTS

I would like to express my deepest gratitude to my supervisor, Associate Professor Theo Kofidis, who allowed me to reach my full potential, and to grow as an independent scientist under his research structure. I am also grateful for his invaluable advice, mentorship and continuous support through the years. This research was supported by A/Prof. Kofidis' Start-up Grant (fund components: National Medical Research Council (NMRC) and Provost National University of Singapore).

I also extend my deepest gratitude to my boss, Professor Chuen Neng Lee, Head of the Department of Surgery, for encouraging me to pursue my PhD degree while working as a research fellow, and for his continuous support throughout.

My sincere appreciation goes to my colleagues at the Myocardial Restoration Lab, Mr. Wang Jing and Miss Shera Lilyanna, for their invaluable technical help. Special thanks to my collaborators Dr. Shu Uin Gan, Dr. Rageev Singh and Assoc. Professor Lieng Hsi Ling for their expertise and contributions to make this research possible; and to Professor Peter Little, Dr. Paul Macary and Dr. Veronique Angeli for allowing me to use cell culture and microscopy core facilities at the Life Science Institutes, National University of Singapore. My gratitude is extended to Dr. Ratha Mahendran for her guidance and constructive comments to this thesis, and to Ms. Cecilia Chao for her administrative help during thesis submission.

My love and thanks to my mother, Merling Valencia -who has been my best friend and greatest teacher-, for encouraging me to be the best that I can be, and for her never-ending love and support through the good and the challenging times. From the bottom of my heart, thank you Mum, for everything.

"Three passions, simple but overwhelmingly strong, have governed my life: the longing for love, the search for knowledge and unbearable pity for the suffering of mankind".

~ Russell Bertrand (1872-1970), Autobiography

TABLE OF CONTENTS

Myocardial restoration via cell therapy and cardiac tissue engineering is limited by impaired graft survival. To limit the sequelae of myocardial ischemia it is crucial to counteract oxidative stress while promoting neovascularization in the area of injury and within the bioengineered tissue. We hypothesized that: (1) supplementation with ascorbic acid (AA) improves donor cell viability in vitro and in vivo, as well as angiogenesis and remodeling of thick myocardial artificial grafts (MAG), suitable for implantation and myocardial repair; and (2) epicardial implantation of an ascorbic acid- enriched myocardial artificial graft, which has been pre-vascularized in the recipients' own body, promotes restoration of the ischemic heart.

In experiments conducted to test our first hypothesis, MAG were generated in vitro by populating an FDA-approved gelatin scaffold with GFP-Luciferase- expressing rat cardiomyoblasts (H9C2-GFP-Fluc). We found that MAG supplementation with ascorbic acid (5 or 50 µmol/L) improved cell survival significantly, reduced apoptosis, and enhanced H9C2 cell myogenic differentiation in vitro. Furthermore, a novel model of graft prevascularization – a renal pouch model, which provides the graft with blood vessels of autologous origin-, was developed in healthy Wistar rats. In our in vivo model using the renal pouch, AA enrichment improved donor cell survival and promoted neovascularization within the MAG.

To test our second hypothesis, an ascorbic acid- enriched pre-vascularized MAG was implanted as a patch into the same rat's ischemic heart following myocardial infarction (MI). MAG-treated animals (MAG group, n=6) were compared to untreated infarcted animals as injury controls (MI group, n=6) and sham operated rats as healthy controls (healthy group, n=7). Echocardiographic, hemodynamic, and histological assessments 4 weeks after implantation indicated that AA-enriched pre-

vascularized- grafts induced a robust angiogenic response in ischemic rat hearts, attenuated left ventricular (LV) remodeling and preserved LV function.

In conclusion, in the current study we have indentified ascorbic acid as a suitable supplement to enhance cell survival and neovascularization in tissue engineering based therapies. Furthermore, we demonstrated the importance of promoting angiogenesis for successful post-ischemic myocardial repair using three-dimensional cardiac patches.

With our approach, viability support (cell therapy and antioxidant effects), structural support (prevention of remodeling) and revascularization (stimulation of angiogenesis) have been addressed in the same setting in an acute model of myocardial repair. Also, the utilization of FDA approved compounds, as well as MAG vascularization with blood vessels of autologous origin, makes this strategy plausible for use in the clinical arena and applicable to various donor cell types (ideally of autologous origin), other organs and regenerative interventions.

2-D	two-dimensional
3-D	three-dimensional
AA	ascorbic acid
AV	arterio-venous
BLI	bioluminescence imaging
BMI	body mass index
BMMNC	bone marrow-derived mononuclear cells
DAPI	4',6-diamidino-2-phenylindole
CAD	coronary artery disease
CO	cardiac output
DIC	differential interference contrast
ECs	endothelial cells
ECM	extracellular matrix
EF	ejection fraction
EHT	engineered heart tissue
FAC	fractional area change
FDA	food and drug administration
FGF	fibroblast growth factor

Fluc	firefly luciferase
FS	fractional shortening
GAG	glycosaminoglycans
GFP	green fluorescent protein
hESC	human embryonic stem cells
HIF-1α	hypoxia-inducible factor-1α
HF	heart failure
HGF	hepatocyte growth factor
hMSCs	human mesenchymal stem cells
hpf	high power field
HUVECs	human umbilical vein endothelial cells
H&E	hematoxylin and eosin
IGF-1	insulin-like growth factor-1
IHD	ischemic heart disease
IP	intraperitoneal
IRP	isovolumetric relaxation period
IVDd	interventricular diameter in diastole
IVDs	interventricular diameter in systole
LAD	left anterior descending coronary artery
LV	left ventricular

LVEDP	left ventricular end-diastolic pressure
LVEDV	left ventricular end-diastolic volume
LVESV	left ventricular end-systolic volume
LVIDd	left ventricular internal dimensions in diastole
LVIDs	left ventricular internal dimensions in systole
MAG	myocardial artificial graft(s)
MAPK	mitogen activated protein kinase
MI	myocardial Infarction
MSCs	mesenchymal stem cells
NADPH	nicotinamide adenine dinucleotide phosphate
NRCMs	neonatal rat cardiomyocytes
OCT	optimal cutting temperature
PBS	phosphate buffered saline
PGLC	poly- (glycolide-co-caprolactone)
PLLA	poly (l-lactic acid)
PLGA	poly (l-lactic-co-glycolic acid)
RECA	rat endothelial cell antigen
ROS	reactive oxygen species
SC	subcutaneous
SD	standard deviation

SDF-1	stromal cell-derived factor-1
SEM	standard error of mean
SIS	small intestine submucosa
SV	stroke volume
TNF-α	tumor necrosis factor-α
TUNEL	Terminal deoxynucleotidyl transferase dUTP nick end labeling
VEGF	vascular endothelial growth factor
vWF	von Willebrand factor

CHAPTER 1 INTRODUCTION

1 Introduction

1.1 Background

Congestive heart failure resulting from myocardial infarction (MI) and ischemic loss of functional cardiomyocytes remains the leading cause of death in the developed world. Ischemic heart disease causes over 400,000 deaths per year in the USA alone [Lloyd-Jones, 2010]. Coronary artery disease is a major risk for heart failure in developed societies. Myocardial infarction and the irreversible loss of functional cardiomyocytes accompanied by scar tissue formation, typically lead to heart failure (HF). The global prevalence of patients developing heart failure has augmented due to the increase in the aging population and to improvements in survival post-myocardial infarction derived from therapeutic advances [Kannel, 2000, Miller, 2001]. Though advanced therapies to treat heart failure have reduced mortality of patients with moderate heart failure, heart transplantation remains the only therapy capable to improve life quality and survival in patients with end-stage heart failure [Boilson, 2010, Lietz, 2005, Miller, 2001]. Yet, the global shortage of available organ donors remains a limitation to broad utilization of heart transplantation and currently only few patients with terminal heart failure benefit from this strategy [Boilson, 2010].

Tissue engineering and regenerative medicine have emerged as strategies that may revolutionize existing therapies for failing organs. The main aim of tissue engineering is to replace injured tissues and regenerate organs through the assembly of cells with biomaterial scaffolds to be implanted into the area of injury [Langer, 1993, Leor, 2005, Vacanti, 2006]. Through this technology, functional bioartificial tissues can be manufactured to replace diseased native ones. Notably, during the past decade considerable research efforts in the field of regenerative medicine have been focused on finding the ideal cell type to mediate myocardial repair. Cell therapy has been explored as means to regenerate ischemic myocardium and an increasing body of

evidence suggests that several types of cells (including stem cells) have the capacity to partially restore infarcted myocardium following direct injection into the area of ischemic injury [Fukuda, 2003, Kofidis, 2004, Martinez, 2009, Nagaya, 2005, Zimmermann, 2007].

However, the success of cell therapy (i.e. intramyocardial delivery of stem cells or of any other cell type) and tissue engineered-based therapies is limited by poor cell survival in the ischemic area of the heart [Muller-Ehmsen, 2002, Reinecke, 2002], and low cell retention [Wang, 2010]. The infarcted myocardium is a harsh hypoxic environment that is not conductive to cell survival. It has been reported that more than 70% of donor cells die during the first 48 hr after injection in the ischemic heart [Muller-Ehmsen, 2002] . In addition, mechanical leakage and vascular wash out also contribute substantially to cell loss upon intramyocardial injection [Teng, 2006]. It has also been reported that poor cell retention due to early cell migration to other remote organs contributes to donor cell loss after injection [Toma, 2002, Zhang, 2007]. Cell retention and delivery in the area of injury may be improved by using the tissue engineering approach, as cells are seeded and entrapped into a biomaterial scaffold. Yet, the bioengineered myocardial graft strategy faces significant challenges towards its practical therapeutic application in the clinical arena. Many issues have to be addressed to prevent the deleterious effects that myocardial ischemia has on the heart structure. Injured cardiomyocytes are replaced by fibrous tissue (myocardial remodeling), which involves extensive changes in ventricular geometry [Pfeffer, 1990]. This ultimately contributes to heart failure progression and poor prognosis [White, 1987]. Furthermore, following graft implantation, cells in three-dimensional cardiac patches will be challenged by a pro-apoptotic environment and an intense inflammatory response arising from the surrounding ischemic tissue [Frangogiannis, 2008, Robey, 2008]. Likewise, hypoxia particularly in the core of the bioengineered graft, is detrimental to donor cell survival [Bursac, 1999]. Vascularization of 3-D grafts

is a fundamental goal in tissue engineering-based strategies for myocardial repair, as it is important to prevent necrosis within the core of the graft, and it plays an important role in cell survival and organization [Caspi, 2007]. However, bioengineering approaches to myocardial repair have mainly focused on allogeneic multicellular patches to achieve formation of primitive blood vessel (tube-like structures) [Bursac, 2009, Lesman, 2010a, Sekiya, 2006, Tan, 2009]. A major limitation in cardiac tissue engineering is the in vitro generation of three-dimensional constructs with a scale suitable for myocardial repair (i.e. more than 1 cm thick). As most bioreactors are unable to supply enough nutrients and have diffusional constraints on oxygen supply to engineered grafts in vitro [Radisic, 2007], the need for incorporation of blood vessels (i.e. via in vitro or in vivo-prevascularization), as well as the stimulation of in situ angiogenesis becomes obvious.

Most of the approaches explored for post-ischemic heart regeneration claim a positive effect on left ventricular (LV) function and mild stimulation of neoangiogenesis regardless of the cell type used for the therapy, and despite the massive early donor cell death after implantation [Bursac, 2009, Leor, 2005, Martinez, 2009]. Following MI, inflammation- and hypoxia- induced compensatory angiogenesis takes place. This process eventually fails and the subsequent impaired capillary growth as well as the resultant oxidative stress may be an important contributor to HF [Tabibiazar, 2001]. Cardiomyocytes are an important source of proangiogenic factors, and impaired angiogenesis has been shown to play a key role in the development of heart failure [Carmeliet, 1999, Hilfiker-Kleiner, 2006]. Furthermore, cardiac and vascular endothelial cells, release a variety of auto- and paracrine agents which may affect cardiac metabolism, contractility, and rhythmicity [Brutsaert, 2003, Narmoneva, 2004].

Thus, it is necessary to design strategies to counteract oxidative stress while promoting neovascularization in the area of injury and within the bioengineered

tissue. Given the relevance of hypoxia and oxidative stress for the fate of cardiac cells after ischemic injury as well as within thick bioengineered constructs, we postulate that ascorbic acid (AA) is a factor which might reduce cell death in myocardial grafts both in vitro and in vivo. This hydrophilic antioxidant scavenges toxic free radicals and other reactive oxygen species (ROS) efficiently [Arrigoni, 2002]. Furthermore, attenuation of hypoxia-induced apoptosis after ascorbic acid treatment in vitro has been demonstrated in HL-1 cardiomyocytes [Vassilopoulos, 2005], and endothelial progenitor cells [Fiorito, 2008]. Ascorbic acid also exerts a stimulatory effect on angiogenesis through increased type IV collagen synthesis by endothelial cells [Telang, 2007]. It has been shown that human umbilical vein endothelial cells (HUVECs) production of type IV collagen is enhanced when ascorbic acid is added in vitro. At physiological concentrations (up to 100 μmol/L), ascorbic acid induces tube formation by HUVECs in cultured extracellular matrix (ECM) [Telang, 2007]. Furthermore, large doses of ascorbic acid induce superior mesenchymal tissue healing in rats. The latter results from early angiogenesis induction and increased collagen synthesis [Omeroglu, 2008]. Finally, ascorbic acid is available ubiquitously, is an essential part of our diet at a global scale and can be easily administered in large doses as a therapeutic supplement in various formulations. However, the potential of ascorbic acid for cell therapy and cardiac tissue repair has not been exploited yet.

1.2 Ischemic Heart Disease and Heart Failure

1.2.1 Epidemiology

Ischemic heart disease (IHD) or myocardial ischemia is a disease characterized by decrease of blood supply to the myocardium usually due to coronary artery disease (CAD). The ischemic loss of cardiomyocytes derived from myocardial infarction and the subsequent development of heart failure constitute the most common cause of death worldwide. Ischemic heart disease claims more lives each year than cancer, chronic lower respiratory disease, and accidents together [Lloyd-Jones, 2010]. Heart failure affects more than 5 million patients, and IHD causes over 400,000 deaths per year in the USA alone [CDC, 2009, Lloyd-Jones, 2010] (Figure 1.1). It has been estimated that around 10% of all patients with heart failure have advanced disease, which is associated with high mortality and poor life quality. In Singapore, IHD has a significant one-year mortality of 20.8%, and is the major contributor to disease burden [WHO, 2010], and premature mortality burden [Phua, 2009].

Heart failure (HF) is a major healthcare burden with an incidence around 10 per 1000 persons older than 65 years [Goldberg, 2010]. It has been estimated that in 2010 about 470,000 Americans will have a new ischemic coronary event. According to recent statistics, the percentage of population aged 40-69 with a first MI who will have HF in 5 years is 7% of men and 12% of women. Whereas 22% of men and 25% of women of individuals >70 years will develop heart failure within 5 years after MI [Lloyd-Jones, 2010]. In spite of combination pharmacological therapy and advanced surgical treatment, 59% of men and 45% of women will die within 5 years after heart failure is diagnosed.

The main risk factors associated with heart failure are hypertension, Type 2 diabetes mellitus, hyperlipidemia, and smoking. The latter are also independent risk factors

for CAD, which constitutes the most common risk factor for heart failure [Goldberg, 2010].

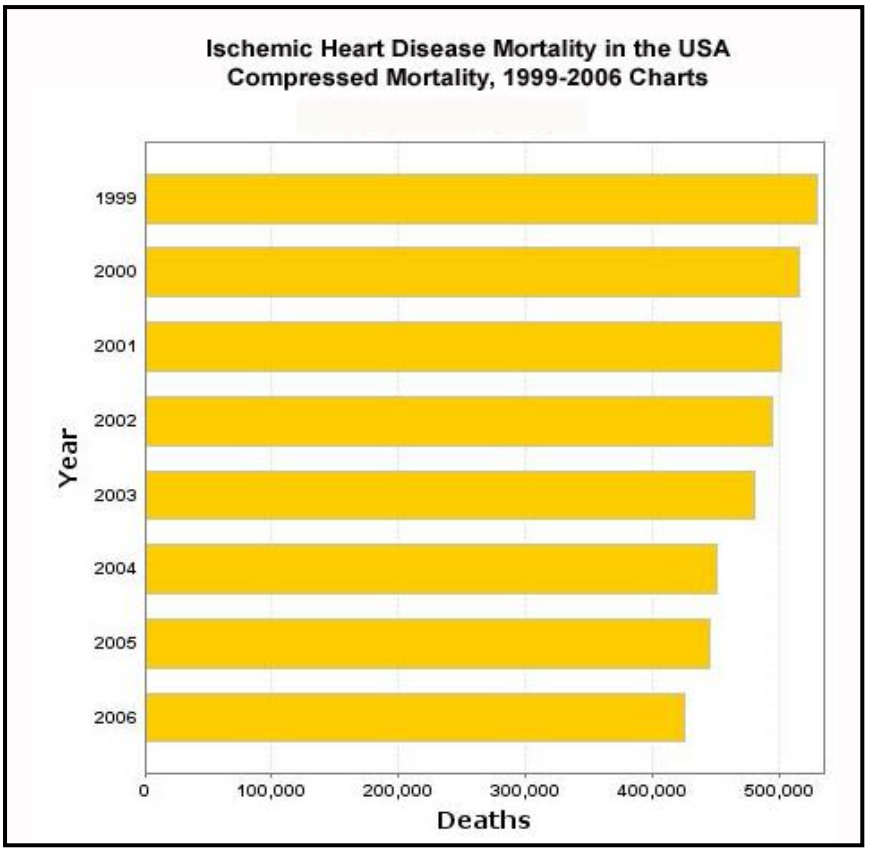

Figure 1.1 Ischemic heart disease mortality in the USA between 1999 and 2006, according to the Centre for Disease Control [CDC, 2009].

The global prevalence of patients developing heart failure has risen due to the increased number of the aging population and to improvements in survival post-myocardial infarction derived from therapeutic advances [Kannel, 2000, Miller, 2001].Neuroendocrine activation in heart failure has become the target of modern pharmacotherapy, and neurohormonal antagonists have now been established as the cornerstone of HF treatment strategies. The combined use of angiotensin converting enzyme (ACE) inhibitors and beta-blockers has shown to be safe and effective as initial therapy in patients with systolic heart failure or left ventricular

dysfunction following MI. On the other hand, recent clinical evidence suggests that "triple therapy" (i.e.beta-blocker, ACE inhibitor, plus an angiotensin receptor inhibitor or aldosterone antagonist can benefit certain patients with advanced systolic dysfunction [Jneid, 2007].

Though mortality in patients with moderate heart failure has been reduced through the utilization of advanced treatmentssuch as combined pharmacological therapy [Arroll, 2010], interventional and surgical revascularization, as well as the utilization of "destination therapies" (i.e. temporary mechanical support/ left ventricular assist devices used as palliative therapy in patients with end-stage heart failure who are not eligible for transplantation because of advanced age or comorbidities), heart transplantation remains the only therapy capable to improve life quality and survival in patients with end-stage heart failure [Boilson, 2010, Lietz, 2005, Miller, 2001].

Cardiac transplantation remains the final therapeutic option for the treatment of irreversible end-stage heart failure in all age groups [Koerner, 2000] with a true prospect for life extension and improvement of life quality. The most frequently reported indication for heart transplantation in the US is coronary artery disease (44.8%). The one-year survival for heart transplants in US is 82%, whereas the long-term survival (at 17 years) drops to 22% [Bennett, 2000]. Though cardiac transplantation may have complications related to immunosupression and long-term failure of transplanted organs [Hosenpud, 1997, Hunt, 1998], it remains the sole life-saving therapy for patients with end-stage HF not responsive to conventional medications or surgeries [Mancini, 2010]. However the global shortage of donor organs restricts cardiac transplantation [Boilson, 2010, Hosenpud, 2000], and with the scarcity of donors it is expected that the trend for transplantation of only the sickest patients requiring continuous inotropic and/or mechanical support will continue [Mancini, 2010].

1.2.2 Pathophysiology

1.2.2.1 Myocardial Dysfunction

Heart failure is defined as the structural and functional impairment of the heart such that it is unable to pump enough blood to fulfill tissue metabolic requirements at normal LV volumes and/or filling pressures. HF may develop as a result of (1) impaired ventricular contractility, (2) increased afterload (i.e. ventricular wall tension during contraction), and (3) impaired ventricular filling [Shah, 2007]. Systolic dysfunction resulting from loss of the ventricle's intrinsic inotropy (impaired ventricular contractility) is predominantly caused by ischemic heart disease, and is seen in about two thirds of patients with heart failure. Diastolic dysfunction is a ventricular filling impairment that is commonly caused by "stiffening" of the myocardium (the ventricle becomes less compliant).

In general, the changes in cardiac function associated with heart failure include systolic dysfunction, diastolic dysfunction, or the presence of both, which ultimately lead to a fall in cardiac output (that is the volume of blood ejected by the left ventricle per minute). Cardiac dysfunction induces compensatory mechanisms aimed at maintaining cardiac output and organ perfusion. The compensatory effect is achieved through neurohumoral and autonomic changes that induce cardiac muscle remodeling and hypertrophy, as well as vasoconstriction and augmented intravascular volume [Jackson, 2000]. Furthermore, the Frank Starling mechanism is activated to increase stroke volume, through the elevation of the LV end-diastolic pressure. This compensatory increase in left ventricular end-diastolic pressure and the subsequent increase in circulating volume may result in pulmonary venous congestion and fluid transudation to the lungs (pulmonary edema).

1.2.2.2 Ventricular Remodeling

Remodeling is defined as adaptive changes that affect the organization of the myocardium allowing the heart to adjust to alterations in mechanical, chemical and electrical signals [Souders, 2009]. Remodeling takes place following extensive myocardial infarction and the ensuing impairment in cardiac contractility. During the scar maturation phase after myocardial infarction, vascular cells undergo apoptosis as a collagen-based scar is formed. The extent of remodeling depends on the size of the infarct, but is also directly affected by the structural changes associated with infarct healing [Frangogiannis, 2008]. Neurohormonal activation leads to regional hypertrophy of the non-infarcted segment, with expansion of the infarcted area (regional LV wall thinning and dilatation) [Jackson, 2000]. The underlying mechanism leading to this enlarged left ventricular size and geometrical change (spherical shape) likely stems from the loss of muscle mass and a resultant stretch of compensatory remote fibers within unscarred muscle [Buckberg, 2006a]. The initial effect of compensatory hypertrophy in the non-ischemic myocardium normalizes wall stress and has a short-term beneficial effect on LV function [Margulies, 2002]. However, the increased collagen deposition and decreased capillary density associated with the LV remodeling process may contribute to long-term LV dysfunction through increased LV dilation, decreased cardiac output, along with increased hemodynamic overloading, and myocardial arrhythmogenicity [Mann, 2010]. The renin-angiotensin system (RAS) plays an important role in hemodynamic hemostasis through short-term vascular and renal effect. Chronic RAS activation has involved in the pathogenesis of cardiac remodeling and failure.

1.2.3 Molecular and Cellular Mechanisms in Heart Failure

At the molecular level, pathological heart hypertrophy is characterized by re-activation of fetal stage genes that regulate cardiac contractility and Calcium usage [Hilfiker-Kleiner, 2006]. Likewise, the activation of signaling pathways in response to stress signals has been associated with adaptive and maladaptive hypertrophy, cardiac fibrosis and apoptosis, all of which promote heart failure.

The main cellular constituents of the heart consist of fibroblasts and cardiomyocytes. However, other cell types such as endothelial cells and vascular smooth muscle cells play an important role in cardiac homeostasis and the heart's responses to electrical, mechanical and chemical factors. Furthermore, transient cell populations (i.e. lymphocytes, mast cells, and macrophages) can interact with the permanent cell types and affect cardiac function [Souders, 2009]. Following cardiac injury, fibroblasts play a key role in the remodeling process due to their ability to produce ECM. Post-ischemic chemical signals (e.g. cytokines, and growth factors) produce changes in fibroblast gene expression, and induce cell migration to the area of ischemia to support wound healing and scar formation. Initially, this process is critical to the reparative wound healing response; yet, over time, these changes produce fibrosis and reduce cardiac function [Souders, 2009].

A growing body of evidence suggests that inflammatory signaling and bioactive molecules (cytokines) also contribute to the development of heart failure. It has been shown that TNF-α induces apoptosis in cardiomyocytes [Krown, 1996], and is a cardio-depressant [Muller-Werdan, 1997]. Levels of circulating TNF-α are increased in patients with heart failure and is a marker for bad prognosis due to its toxic effects on the heart and the circulation [Mann, 2001]. Neurohormonal and sympathetic activation are the pathophysiological hallmark of acute and chronic HF. The renin-angiotensin system is a key mediator in cardiac remodeling, and encompasses a

cascade of enzymatic reactions resulting in the formation of Angiotensin II (Ang II). Ang II causes vasoconstriction and has multiple pro-fibrotic effects in the heart that include promotion of fibroblast proliferation and adhesion, as well as synthesis of extracellular matrix proteins through activation of the Ang II type I receptor (AT1R). Also, TGFβ1 acts downstream of Ang II promoting cardiac fibrosis [Schnee, 2000]. Aldosterone is another important component of the RAS. Stimulated by Ang II, aldosterone is released to maintain fluid balance. Its increased levels during heart failure lead to water and sodium retention [Swedberg, 2000]. Furthermore, aldosterone plays a key role in adverse remodeling, collagen synthesis and endothelial dysfunction [Dawson, 2004, Falkenstein, 2000]. Likewise, increased plasma levels of the vasoactive peptides urocortin-1 and entodothelin-1 have been associated with severe diastolic ventricular dysfunction and poor prognosis [Tang, 2010]. On the other hand, natriuretic peptides including atrial natriuretic peptide, brain natriuretic peptide, and C- type natriuretic peptide are up-regulated during cardiac stretch and cardiac injury, and seem to have a protective effect through inhibition of cardiac remodeling through regulation of fibroblast proliferation [Jarvis, 2006].

1.2.4 Oxidative Stress during Heart failure

Evidence has demonstrated the increased myocardial production of reactive oxygen species (ROS) during heart failure [Sam, 2005]. ROS include the free radicals superoxide anion ($O_2^{\bullet -}$) and hydroxyl ($OH^{\bullet}$) as well as hydrogen peroxide (H_2O_2). The process of remodeling may also be driven by (ROS)-dependent pathways. Cellular levels of ROS and therefore their deleterious effects are regulated by various antioxidant systems (e.g. catalase, superoxide dismutases, glutathione peroxidases, and various vitamins) [Nabeebaccus, 2010]. The imbalance between ROS and

antioxidants is known as oxidative stress. The latter is likely to be involved in critical aspects related to the development and progression of heart failure [Hilfiker-Kleiner, 2006]. In particular it seems that NADPH oxidase-derived ROS play an important role in cardiac remodeling through activation of mitogen kinases (e.g. Akt, Ras/MAPK) and transcription factors (e.g. STAT, NFκB) that produce cardiac hypertrophy. Similarly, NADPH oxidase-derived ROS activate pro-fibrotic genes that contribute to fibrosis and subsequent dilation [Nabeebaccus, 2010]. Moreover, ROS produce mitochondrial dysfunction leading to cardiomyocyte apoptosis. Activation of apoptotic pathways are involved in cardiomyocytes' cell loss not only during acute ischemia, but also during heart failure. In contrast to the copious amount of cells that undergo apoptosis during acute ischemia; heart failure is associated with low but abnormally sustained levels of cardiomyocyte apoptosis. Furthermore, evidence suggests that apoptosis also has an effect on cardiomyocyte remodeling and contractility [Hilfiker-Kleiner, 2006].

1.2.5 Angiogenesis in the Ischemic Heart

Angiogenesis is defined as the sprouting of blood vessels from pre-existing capillaries. Following myocardial ischemia, transient enhancement of blood flow can originate from angiogenesis or from the recruitment of coronary collaterals [Tabibiazar, 2001]. Following MI, inflammation- and hypoxia- induced compensatory angiogenesis takes place. The major triggers of this process include mechanical (e.g. increased blood flow and sheer stress and stretch of the myocardium due to increase in LVEDV), chemical (e.g. hypoxia-induced up-regulation of VEGF) and molecular factors (e.g. pro-angiogenic growth factors and inflammation) [Al Sabti, 2007]. Pre-clinical studies have shown that the presence of inflammatory cells, such as macrophages and neutrophils is sufficient to produce angiogenesis [Lin, 2006,

Sunderkotter, 1991]. The recruitment of inflammatory cells following myocardial infarction (i.e. macrophages, monocytes and platelets), induces the expression of VEGF and FGF. On the other hand, VEGF can stimulate and recruit other macrophages to increase inflammatory response, and in this way, stimulate more angiogenesis [Al Sabti, 2007]. However, this process of compensatory post-ischemic angiogenesis eventually fails and the subsequent impaired capillary growth as well as the resultant oxidative stress may be an important contributor to HF [Tabibiazar, 2001]. Cardiomyocytes are an important source of proangiogenic factors, and impaired angiogenesis has been shown to play a key role in the development of heart failure in animal models [Carmeliet, 1999, Hilfiker-Kleiner, 2006].

1.3 Cardiac Tissue Engineering and Cell Therapy

The heart is an organ with restricted regenerative capacity. Though a new paradigm which confers self-regeneration potential to the heart -an organ believed to be terminally differentiated-, has been introduced by the identification of cardiac stem cells [Beltrami, 2003, Messina, 2004], its regenerative capability cannot compensate for cell loss during MI and HF. Tissue engineering and regenerative medicine have emerged as strategies that may revolutionize existing therapies for the failing heart. The main aim of tissue engineering is to replace injured or damaged tissues and regenerate organs through the assembly of cells into biomaterial scaffolds to then be implanted into the area of injury [Langer, 1993, Leor, 2005, Vacanti, 2006]. Through this technology, functional bioartificial tissues can be manufactured to replace diseased native ones.

Cell therapy has also been explored as means to regenerate ischemic myocardium. This approach focuses on re-population of the ischemic heart with healthy cells via direct injections into the scarred myocardium. During the past decade substantial

research efforts in the field of regenerative medicine have been focused on finding the ideal cell type to mediate myocardial repair [Martinez, 2009]. A growing body of evidence suggests that several types of cells have the capacity to partially restore infarcted myocardium [Fukuda, 2003, Kofidis, 2004, Martinez, 2009, Nagaya, 2005, Zimmermann, 2007]. Pre-clinical evidence has widely supported the paracrine hypothesis of stem cell action, which proposes that the beneficial effects of adult stem cell implantation is attributable to cardioprotection that leads to repair of ischemic myocardium rather than de *novo* regeneration by cardiomyogenic differentiation [Gnecchi, 2005]. On the other hand, most clinical trials so far have focused on using both autologous skeletal myoblasts and diverse bone marrow-derived cell subsets (mononuclear cells, hematopoietic progenitors, mesenchymal stem cells) in acute myocardial infarction, refractory angina and chronic heart failure patients [Dobert, 2004, Menasche, 2010, Schachinger, 2004, Schaefer, 2009, Wollert, 2004]. Yet, pre-clinical and clinical studies using bone marrow adult stem cells have failed to demonstrate that cell therapy elicits a sustained large-scale long-term positive effect on heart function [Meyer, 2009, Schaefer, 2009], while therapies using skeletal myoblasts have lead to sustained ventricular arrhythmias [Menasche, 2005].

The therapeutic success of post-ischemic stem cell implantation - and virtually of any other cell type- is limited by poor cell survival in the ischemic myocardium [Muller-Ehmsen, 2002, Reinecke, 2002], and low cell retention [Wang, 2010]. The ischemic or failing heart encloses a harsh hypoxic environment that is not conductive to cell survival, and it has been reported that more than 70% of cells die during the first two days after injection into the heart [Muller-Ehmsen, 2002]. Furthermore, post-injection mechanical leakage and vascular wash out may also account for a large amount of cell loss [Teng, 2006]. Poor cell retention due to early stem cell migration to other remote organs such as lungs, liver, and spleen immediately after injection has also

been observed [Dai, 2009, Toma, 2002, Zhang, 2007]. However, these issues may be improved by using the cardiac tissue engineering approach, as this strategy may offer homogeneous cell delivery in a three-dimensional environment while providing structural support (scaffold) to the myocardial area of ischemic injury [Bursac, 2009, Dai, 2009, Leor, 2005, Martinez, 2009, Wang, 2010].

1.3.1 Cardiac Tissue Engineering Strategies

Strategies of cardiac tissue engineering are classified as 1) in vitro and 2) in vivo. The in vitro strategy involves the fabrication of a three-dimensional bioengineered myocardial patch in a culture dish or bioreactor. Tissues are constructed from a cell-seeded scaffold or biomaterial gel, as well as by the generation of scaffold-free cell sheets. The in vivo tissue engineering approach involves in situ generation of tissue by either implanting cell seeded or acellular scaffolds in the epicardium, or by injecting hydrogels with or without cells intramyocardially [Kofidis, 2005, Leor, 2005]. The in vitro approach offers good control of construct shape and size but it is limited by size constraints, since three dimensional constructs generated in vitro may undergo core necrosis in vitro or after transplantation in the area of ischemic injury.

1.3.1.1 Tissue Engineered Three Dimensional Approaches in Myocardial Restoration

A number of works have emerged during the last decade and various biomaterials and cell types have been used to construct three dimensional grafts destined for myocardial repair. In vivo studies indicate that regardless of the kind of cells or scaffold material used, three-dimensional tissue implantation into the area of myocardial injury improves heart function to some extent [Martinez, 2009]. A summary of the various strategies used to fabricate 3-D cardiac patches for

myocardial repair and their advantages and disadvantages are displayed in Table 1.1. Heart function improvement following the epicardial implantation of a bioengineered graft containing adult stem cells –or any other cell type-, is not likely to be associated with induction of cardiomyocyte regeneration, cell engraftment or cell differentiation. The beneficial effect of bioengineered patches on cardiac function seems to be mediated by proangiogenic and paracrine mechanisms which may attenuate left ventricular remodeling [Frangogiannis, 2008].

1.3.1.1.1 Myocardial Patches- Porous Biomaterials

Tissue engineers utilize scaffold materials that are biocompatible and biodegradable to generate patches for epicardial implantation in the area of myocardial injury. Cells can be seeded in a porous material which will thereby provide structural support. Three dimensional porous scaffolds promote neo-tissue formation by providing surface that facilitates cell attachment, migration, proliferation and generation of tissue through the region where it is required [Muschler, 2004]. For the fabrication of porous scaffolds, single or combined biomaterials are used [Leor, 2000, Piao, 2007, Vacanti, 2006]. In some cases, Engelbroth-Holm-Swarm mouse sarcoma-derived extracellular matrix (i.e. Matrigel™) is added to assist cell retention within the scaffolds [Caspi, 2007]. Researchers have used various strategies using diverse scaffold materials and cell types to fabricate 3-D cardiac patches: e.g. alginate scaffolds seeded with fetal rat cardiac cells [Leor, 2000]; PGL mesh - embedded fibroblast grafts (Dermagraft ®) [Kellar, 2001]; Poly- glycolide-co-caprolactone (PGLC) patches seeded with bone marrow-derived mononuclear cells [Piao, 2007]; hESC-derived endothelial cells and embryonic fibroblasts embedded in porous polymer scaffolds (PLLA/PLGA) using Matrigel™ [Caspi, 2007]. Most of these strategies have been applied in animal (rodent) models of myocardial repair i.e.

epicardial patch implantation after myocardial infarction is induced. Regardless of the approach and cell type utilized, patch implantation leads to neovascularization in the graft and scar areas. Moreover, the grafts attenuate left ventricle (LV) dilation and improve heart function.

1.3.1.1.2 Myocardial Patches- Hydrogel/ ECM – Based Tissues

In this strategy, cells are mixed with soluble hydrogel matrices (e.g. collagen, fibrin) and entrapped in the 3-D structure upon matrix solidification [Zimmermann, 2009].

Human mesenchymal stem cells (hMSCs) have been embedded into rat tail collagen type I to produce a patch that was implanted on the rat epicardium immediately after myocardial infarction [Simpson, 2007]. Donor hMSCs were not detectable at 4 weeks after graft implantation, but patch application induced improvements in LV remodeling. Furthermore, a marked increase of blood vessels was detected in the infarct area of treated animals. In contrast, acellular control-patches did not improve heart function or remodeling parameters, so early remodeling changes in the patch-treated animals were assumed to be hMSCs-mediated and not matrix related. Notably, Zimmermann et al. showed the feasibility of generating large contractile engineered heart tissue (EHT) grafts in vitro, made of neonatal rat cardiac cells (mixed cell population) embedded in a collagen type I/ Matrigel™ scaffold and shaped into a ring and conditioned by mechanical stretching that can survive after implantation and enhance contractile function of infarcted hearts [Zimmermann, 2006]. EHT-derived cardiomyocytes engrafted with the host myocardium and capillary networks were identified in the area of injury. The authors observed that donor cells were recruited and integrated into host vessels during neovascularization [Naito, 2006].

1.3.1.1.3 Scaffoldless Systems- Cell Sheets

Strategies to produce scaffoldless systems for myocardial engineering have been recently established. A novel technique to fabricate pulsatile cardiac grafts via 3-D cell sheet manipulation using thermo-responsive culture surfaces was introduced by Okano's group [Shimizu, 2002]. Later, it was demonstrated that cardiac cell sheets made of neonatal rat cardiomyocytes (NRCMs) have intrinsic angiogenic potential, since they express angiogenesis-related genes and form endothelial cell networks in vitro [Sekine, 2008, Sekiya, 2006]. After a three-step subcutaneous implantation into nude rats, grafts completely synchronized and all tissues survived without necrosis while a well-organized microvascular network was created [Shimizu, 2006]. The cell sheet approach has been recently used as a strategy aiming to repair the heart after myocardial infarction. Sekine et al. created triple-sheet myocardial tissues made of co-cultured NRCMs and endothelial cells (ECs) and implanted it as an epicardial patch in infarcted rats [Sekine, 2008]. The authors found that greater number of capillaries, decrease in fibrosis and improvement of cardiac function were proportional to the amount of ECs contained in the layered tissue grafts. More importantly, they found that donor blood vessels bridged into the host's infarcted myocardium. These results suggest that neovascularization reduces remodeling and contributes to the improvement of cardiac function.

1.3.1.1.4 Decellularized Matrix and Biological Patches

By decellularization of mammal organs, any potentially immunogenic material is cleared, and the remaining extracellular matrix is then recellularized and implanted as an epicardial patch. Porcine small intestine submucosa (SIS) seeded with mesenchymal stem cells (MSCs) [Tan, 2009], as well as sliced acellular bovine pericardium sandwiched with folded MSCs sheets (i.e. five layers) [Chen, 2008, Wei, 2008] have been used to create patches for myocardial repair. Implantation of such

re-cellularized biological patches into the area of ischemic injury lead to improvement of LV contractile function and remodeling, and increased blood vessel density.

Notably, Ott et al. described the decellularization of whole rat hearts as a platform to engineer a bioartificial heart [Ott, 2008]. Though this strategy has not been tested in pre-clinical models of myocardial repair, the organ decellularization and recellularization approach might be a promising technology for organ tissue engineering once the conditions for in vitro reseeding and organ maturation are optimized.

1.3.1.1.5 In vivo Myocardial Engineering and Graft pre-vascularization

The in vivo tissue engineering approach involves in situ generation of tissue or the utilization of the body as a "bioreactor" to mature and pre-vascularize cardiac grafts in vivo.

Birla et al. introduced an in vivo model of angiogenesis to promote survival, organization and functionality of myocardial cells in 3-D- fibrin constructs. [Birla, 2005, Birla, 2009]. Neonatal rat cardiomyocytes were suspended in a fibrin gel and seeded into silicone tubing that was implanted on top of the femoral vessels of adult rats. Three weeks after implantation, the resulting graft showed well organized cardiac cells and neovascularization and displayed normal myocardial tissue contractile properties. In another approach, Morrit and colleagues introduced an in vivo 3-D cell culture chamber containing an AV-loop in the rat groin and that was seeded with a mixture of neonatal rat cardiomyocytes and Matrigel™ [Morritt, 2007]. After 4 and 10 weeks in vivo, vascularized, spontaneously beating, 3-D cardiac tissue was obtained. These vacularized grafts have not been used for myocardial repair yet. Also, the harvest of femoral vessels with the graft and the utilization of tumor-derived ECM (Matrigel) may be limitations for future clinical application of this strategy.

Omental wrapping or omentopexy, is a technique introduced in the mid 30's to treat heart ischemia, by promoting 're-vascularization' from a pedicle with omental vessels to coronary arteries [O'Shaughnessy, 1937]. Tissue engineers have been recently using this classic concept to promote neovascularization in myocardial grafts. Ueyama et al. combined the omentopexy and 0.7 mm FGF-enriched hydrogel sheets for cardiac repair [Ueyama, 2004]. The procedure was used as a restorative therapy placing the FGF- hydrogel sheet on top of the area of ischemia followed by omental wrapping in rabbits. A better fractional area change was detected in the FGF-omentum treated group, and communication between the gastroepiploic artery and to the coronary artery was documented by angiography. In a unique study, Shao and associates used autologous hepatic tissue combined with omental wrapping to promote angiogenesis and restore cardiac function in rats [Shao, 2008]. This strategy stimulated angiogenesis, reduced adverse LV remodeling after MI and improved cardiac function. Enhancement in vascularization was associated withthe expression of proangiogenic growth factors (i.e. HGF, bFGF and VEGF).

Interesting results have also been obtained by Cohen's group, which has explored strategies aiming at in vivo prevascularization of cardiac patches for myocardial repair via the omentum [Dvir, 2009], or the peritoneum [Amir, 2009]. In a model of post-ischemic myocardial repair, a patch was constructed by seeding a porous alginate scaffold with neonatal rat cardiomyocytes mixed with growth factor-reduced Matrigel™ and a cocktail of pro-survival and angiogenic factors (i.e. IGF-1, SCD-1 and VEGF) [Dvir, 2009]. After 2 days in culture, the factor-supplemented grafts were implanted in the omentum of rats and allowed to prevascularize for 7 days, followed by graft implantation onto the infarcted heart of allogeneic rats for 28 days. The factor mixture incorporation favored sarcomeric organization of cardiac cells and improved cell viability within the grafts in vitro and in vivo. Furthermore, the implanted omentum- pre-vascularized patch engrafted with the host myocardium and increased

scar thickness and thereby prevented further dilation. Some drawbacks of this strategy include the utilization of an allogeneic model of graft prevascularization and implantation. Besides, the utilization of Matrigel™ (even in the growth factor-reduced form) is a limitation, since this is a product unlikely to receive FDA approval, and hence it is not suitable for clinical use [Polykandriotis, 2008]. On the other hand, the omentum has been increasingly appreciated as an important intra-abdominal structure that has an innate immune function and plays an important role in peritoneal defense. Thus, some clinicians have even warranted careful consideration before the omentum is removed [Platell, 2000]. Furthermore, removal of the omentum (omentectomy), as well as its utilization for graft pre-vascularization could be limited in patients that have undergone major abdominal procedures.

Table 1.1 Summary of advantages and disadvantages of 3-D approaches for myocardial restoration [Martinez, 2010].

Approach	Advantages	Disadvantages
Myocardial Patches- Porous biomaterials	-Porous materials provide structural support to the seeded cells. -Increased cell retention when used in combination with ECM. -Graft mechanical and electrical pre-conditioning is feasible. - Increase neovascularization upon implantation in the area of injury. -Improvement of LV remodeling and heart function. -LV structural support.	-Irregular cell seeding and distribution. -Limited cell survival within the grafts. -Biodegradable materials that trigger inflammatory response. -Immunogenicity when tumor-derived ECM (Matrigel™) is added to the construct. -Epicardial patch application lacks integration with the host myocardium. -Involves open chest surgery for graft implantation.
Myocardial Patches- Hydrogel/ECM-based Tissues	-Cell retention within the scaffold. Uniform cell seeding can be achieved. -Graft mechanical and electrical pre-conditioning are feasible. - Increase neovascularization upon implantation in the area of injury. -Improvement of LV remodeling and heart function. LV structural support. - Cardiac cell engraftment into the host myocardium has been reported.	-Limited cell survival within the grafts. -Immunogenicity when animal products and tumor-derived ECM (Matrigel™) are used. -Amount of cardiac cell engraftment is yet limited. -Epicardial patch application lacks integration with host myocardium. -Involves open chest surgery for graft implantation.
Scaffoldless Systems- Cell Sheets and Microtissues	- It does not induce immunogenic and inflammatory responses from ECM. -Angiogenic potential in vitro. -Increase neovascularization upon implantation in the area of injury. -Blood vessels integration with host myocardium has been reported. -Improvement of LV remodeling and heart function.	-Limited size (3 cell sheet layers). -Graft mechanical pre-conditioning could be limited. -Involves open chest surgery for graft implantation.
Decellularized Matrix and Biological Patches	-Any potential immunogenic material is cleared during decellularization. -Graft mechanical and electrical pre-conditioning are feasible. -Increase neovascularization upon implantation in the area of injury. -Improvement of LV remodeling and heart function. LV structural support. -Autologous vascularization when the omentopexy approach is used.	-Irregular cell seeding and distribution. -Cell differentiation and engraftment has been documented, but is yet limited. -Involves open chest surgery for graft implantation.
In vivo Myocardial Engineering	-In vivo autologous graft neovascularization and maturation.	-This approach has not been evaluated for myocardial repair

1.3.2 Challenges of Cardiac Tissue Engineering:

The uniqueness of the heart and the limitations for its reproduction by means of tissue engineering, derive from its characteristics (Figure 1.2). It is an organ with limited regenerative potential and a complex structure comprised by a helix of distinctively arranged muscular bands [Buckberg, 2002, Buckberg, 2006b]. The normal functional capacity of the heart allows it to pump about 15,000 liters blood per day. In a lifetime, it beats over 2.5 billion times and pumps over 200 million liters of blood. The heart is asymmetric (i.e. left and right chambers are not symmetric), anisotropic (i.e. it has different microstructure) and highly angiotropic (i.e. contains a great amount of blood vessels). Besides, the heart is a multidimensional organ that has more than the usual three dimensions, in which tissue engineering is perceived. The fourth dimension of the heart is its pump-function over time. Furthermore, the heart rhythm is another feature (a temporal dimension) that needs to be replicated.

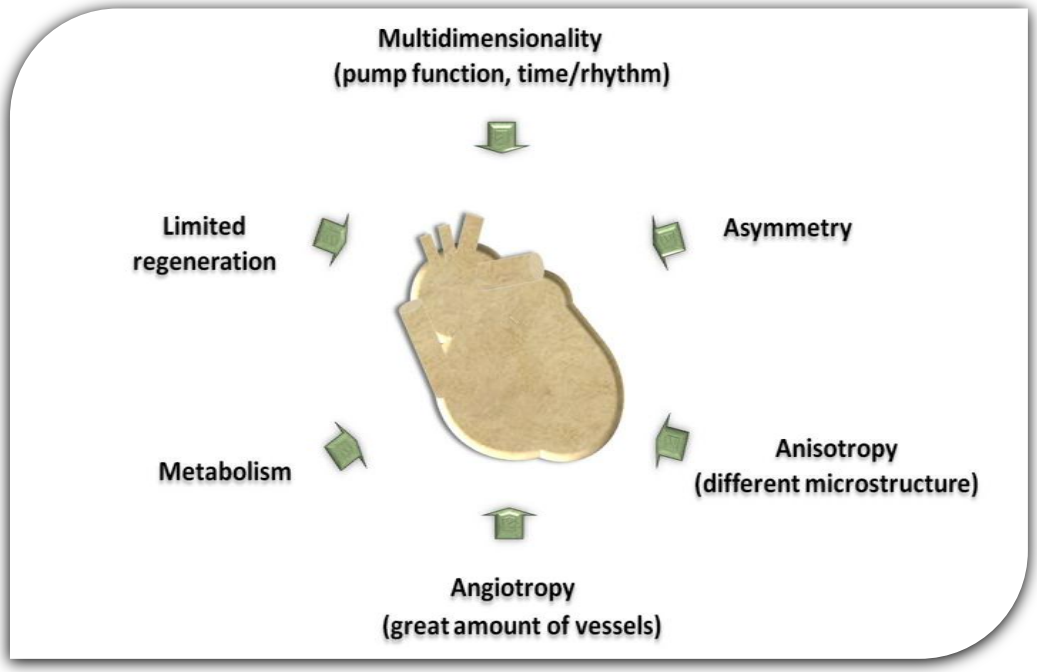

Figure 1.2 Limitations of myocardial restoration due to the uniqueness of the heart.

To date, the ideal cell type to assemble three-dimensional cardiac patches has not been found. However, autologous adult stem cells have become an increasingly appealing source for cardiac tissue engineering, as these cells may hold realistic clinical potential. Though outcomes derived from animal studies using adult stem cell- based cardiac tissue engineering for myocardial repair have reported similar encouraging results (Table 1.2), the degree of donor cell engraftment and survival is limited, and the cardiomyogenic trans-differentiation of most types of adult stem cells remains controversial [Martinez, 2011]. The evaluation of tissue engineering-based therapies in clinical trials has been limited. Chachques and collaborators assessed a combined therapy involving cell therapy (i.e. intramyocardial injections) followed by the epicardial implantation of a collagen scaffold seeded with autologous bone marrow cells in patients undergoing coronary artery bypass surgery (CABG) [Chachques, 2008]. This nonrandomized, controlled phase I clinical trial (MAGNUM-trial) included 10 patients that underwent CABG and received BMMNC injections, and 10 patients that additionally to surgery and BMMNC injections underwent epicardial BMMNC-patch application. The combined therapy limited LV remodeling and improved diastolic function. However, obvious limitations of this study include the association of a tissue engineering approach with CABG surgery and cell injections, which makes it difficult to attribute any beneficial effect on LV function exclusively to the implanted patch.

On the other hand, while extensive pre-clinical efforts have been focused on finding the “ideal cell type” for myocardial regeneration, many equally important aspects need to be addressed in light of the complex structure of the heart and the series of deleterious and fulminant events leading to heart failure. Besides the lack of a large-scale human cardiac cells source [Zimmermann, 2009], one of major limitations in cardiac tissue engineering is the in vitro generation of three-dimensional constructs with a scale suitable for myocardial repair (i.e. more than 1 cm thick). As most

bioreactors are unable to supply enough nutrients and oxygen to bioengineered grafts in vitro [Radisic, 2007]. Furthermore, following graft implantation, cells in 3D cardiac patches will be challenged by a pro-apoptotic environment and an intense inflammatory response arising from the surrounding ischemic tissue [Frangogiannis, 2008, Robey, 2008]. Likewise, hypoxia particularly in the core of the bioengineered graft is a factor that is detrimental to donor cell survival [Bursac, 1999].

Promoting vascularization of 3-D grafts is a fundamental goal in tissue engineering-based strategies for enhanced myocardial repair. Neovascularization is important to prevent cardiac graft's core necrosis, and it plays an important role for cell survival and organization. Research efforts towards ex vivo and in vivo vascularization of bioengineered cardiac patches have been recently reported [Caspi, 2007, Dvir, 2009, Lesman, 2010b, Morritt, 2007]. The formation of capillaries within ex vivo generated cardiac muscle derived from human embryonic stem cells has been documented [Caspi, 2007]. It has been shown that when transplanted in vivo (into healthy rodent hearts) the human vessels within the graft can become functional and contribute to tissue perfusion [Lesman, 2010b]. However, this approach has not been evaluated yet in pre-clinical studies aiming at post-ischemic myocardial repair. Also, the utilization of hESC-derived cardiomyocytes could be a limitation for immediate clinical application of this strategy, as further studies are required to ensure the safety of embryonic stem cells and their derivatives. On the other hand, data from work involving in vitro generation of human endothelial cell-derived capillary networks within biodegradable polymer matrices indicate that these in vitro bioengineered blood vessels may become leaky after transplantation [Nor, 2001]. In summary, novel cardiac tissue engineering concepts that incorporate functional blood vessels and stimulate in situ angiogenesis through methods that can realistically be translated into the clinical arena are clearly needed to achieve successful cardiac repair by tissue engineering.

Table 1.2 Outcomes of pre-clinical studies using adult stem cell- based cardiac tissue engineering for myocardial repair [Martinez, 2011]. *

Adult Stem Cell Type	Tissue Engineering Approach/ Biomaterial	Animal Model/ Time of treatment after injury	Outcome						Ref.
			Stem cell engraftment / Migration to scar	Expression of cardiac markers by donor cells	Expression of vascular markers by donor cells	Enhanced Angiogenesis	LV function improvement	LV remodeling attenuation	
Bone Marrow Cells	Muscle patch	MI in mice - Chronic	+ (8%)	*	*	+	+	+	[Barandon, 2004]
	Polyglycolic acid cloth patch	MI in rats- Chronic	-	*	*	+	+	+	[Fukuhara, 2005]
Bone Marrow Mononuclear Cells	Injectable Fibrin	MI in rats- Chronic	+	*	*	+	*	*	[Ryu, 2005]
	poly-glycolide-*co*-caprolactone Patch	MI l in rats- Acute	+	+	-	+	+	+	[Piao, 2007]
Bone Marrow Mesenchymal Stem Cells	Type I Collagen-(GAG) patch	MI in rats- Acute	+	*	*	+	*	*	[Xiang, 2006]
	Type I Collagen patch	MI in rats- Acute	-	NA	NA	+	+	+	[Simpson, 2007]
	Sliced acellular pericardia patch & cell sheet	MI in rats- Chronic	+	+	+	+	*	*	[Wei, 2008]
	Sliced a cellular pericardia patch & folded cell sheet	MI in rats- Chronic	+	+	+	+	-	+	[Chen, 2008]
	Intra-myocardial injection of cell sheet fragments	MI in rats- Acute	+	+	+	+	+	+	[Wang, 2008]
	Collagen injection	MI in rats- Acute	+ (16%)	*	*	*	-	-	[Dai, 2009]
	Porcine SIS patch	MI in rabbits- Chronic	+	+	+	+	+	+	[Tan, 2009]
	Poly lactide-co-ε-coprolactone patch	MI in rats- Acute	+	+	*	*	+	+	[Jin, 2009]
Adipose tissue-Mesenchymal stem cells	Cell sheet monolayer	MI in rats - Chronic	+	+	+	+	+	+	[Miyahara, 2006]

* *LV, Left Ventricular; MI, myocardial infarction; GAG, glycosaminoglycans; SIS, small intestine submucosa; +, indicates found parameter; -, indicates not found parameter; *, indicates non-evaluated parameter; NA, indicates non-applicable.*

1.4 Ascorbic Acid

Ascorbic acid (Vitamin C) is an essential dietary constituent for humans. Its deficiency leads to scurvy, a disease characterized by bleeding gums, hemorrhage due to impaired collagen deposition and the consequent defective formation and repair of blood vessels [Hodges, 1971]. Ascorbic acid is ubiquitousl; it is an essential part of our diet, and can be easily administered in large doses as a therapeutic supplement in various formulations.

Ascorbic acid (AA) is in high concentration in tissues with high potential of ROS generation such as eyes, brain, liver, lungs, and the heart. It is an aqueous phase antioxidant concentrated in the cytosol that seems to play an important role in DNA protection from oxidative damage. This hydrophilic antioxidant scavenges toxic free radicals and other reactive oxygen species (ROS) efficiently [Arrigoni, 2002] . Ascorbate can terminate radical reactions by serving as a stable (electron + proton) donor in interactions with ROS, being converted into the radical ion semidehydroascorbate and subsequently into dehydroascorbate. These oxidized forms of ascorbate donor cause cellular damage, and can be converted back to ascorbate by cellular enzymes. Furthermore, attenuation of hypoxia-induced apoptosis after ascorbic acid treatment in vitro has been demonstrated in HL-1 cardiomyocytes [Vassilopoulos, 2005], and endothelial progenitor cells [Fiorito, 2008]. In hypoxic conditions in vitro hypoxia-inducible factor-1α (HIF-1α) promotes apoptosis in H9C2 cells (i.e. rat cardiomyoblasts of embryonic origin), and in cardiomyocytes [Malhotra, 2008, Vassilopoulos, 2005]. Moreover, it has been shown that ascorbic acid depletion interrupts HIF-1α proteosomal degradation, as it is a cofactor for proline hydroxylation [Telang, 2007].

Ascorbic acid intake enhances immunocompetence [Long, 1999]. Increased levels of AA have been associated with increased levels of immunoglobulins and increased

neutrophils function in mammals [Blair, 1985], as well as with a mitogenic-related release of immunoglobulins in human lymphocytes [Tanaka, 1994].

There is an ascorbic acid-dependant modulation of collagen, as it may directly enhance transcription of the procollagen gene. Collagen synthesis is a complex process that involves transcription of procollagen, translation followed by hydroxylation, processing of procollagen to collagen and formation of fibrils. One of the most well documented effects of ascorbic acid is collagen hydroxylation [Hitomi, 1996]. Ascorbic acid has a stimulatory effect on angiogenesis through increase of collagen type IV synthesis by endothelial cells [Telang, 2007]. It has been shown that human umbilical vein endothelial cell (HUVECs) type IV collagen production is enhanced when ascorbic acid is added in vitro. At physiological concentrations (up to 100 μmol/L), ascorbic acid induces tube formation by HUVECs cultured in extracellular matrix [Telang, 2007]. Furthermore, large doses of ascorbic acid induce superior mesenchymal tissue healing in rats. The later results derive from early angiogenesis induction and increased collagen synthesis [Omeroglu, 2008]. AA also has an effect on cell differentiation, as it has been shown to modulate expression of genes associated with myoblast differentiation [Nandan, 1990]. More importantly, ascorbic acid promotes in vitro differentiation of embryonic stem cells into cardiomyocytes [E, 2006, Wang, 2010], in a process associated with collagen synthesis [Sato, 2006].

In tissue engineering, AA has been used as a supplement in culture medium to enhance collagen production and cell proliferation within hydrogel templates containing bFGF [Yoshida, 2010]. Likewise, it has been suggested that AA-containing polyurethane scaffolds may be useful in bone tissue-engineering applications as these materials stimulate collagen type I production, cell proliferation, and alkaline phosphatase synthesis in vitro. [Zhang, 2003]. Futhermore, it has been proposed that the encapsulation of Magnesium l-ascorbic

acid 2-phosphate and α-tocopherol acetate (stable vitamin C and vitamin E derivatives) together with polyacrylonitrile nanofibers in the form of core-shell structure, has potential application as functional dressing for photoprotection [Wu, 2011]. However, to date the potential of ascorbic acid for cell therapy and tissue repair has not been exploited. Experimental studies to assess the effect of ascorbic acid on cell survival and to promote angiogenesis in 3-D compounds destined for myocardial restoration have yet to be conducted.

1.5 Towards a Novel Model for Graft Vascularization In vivo

1.5.1 Adipose Tissue and Angiogenesis

Adipose tissue is a highly vascularized tissue, since each adipocyte is surrounded by capillaries. Angiogenesis in adipose tissue provides oxygen, nutrients and growth factors, as well as inflammatory and mesenchymal stem cells that help to keep the tissue's homeostasis and adipocytes' function. Furthermore, adipocytes produce angiogenic factors (e.g. VEGFA and FGF), and adipokines (e.g. leptin, resistin, visfatin) that synergistically modulate both angiogenesis and survival mechanisms. [Cao, 2010]. Notably, the presence of inflammatory cells and pluripotent adipose-derived stromal cells further contribute to adipose tissue angiogenesis through pro-angiogenic growth factors production and stem cell-derived vascular differentiation. Human fat tissue has been used in ex-vivo angiogenesis assays, particularly to study the role of angiogenesis in obesity and associated disorders [Gealekman, 2008, Greenway, 2007]. Furthermore evidence indicates that spontaneous differentiation of adipose tissue-derived stem cells into functional cardiomyocyte-like cells without chemical induction with 5- azacytidine in vitro [Planat-Benard, 2004] and in vivo [Choi, 2010]. It has also been suggested that in spite of poor engraftment, intramyocardial delivery post-MI of freshly isolated ASC have a beneficial therapeutic

effect on heart function in rats through a potent pro-angiogenic effect [Schenke-Layland, 2009]

1.5.2 Perirenal Fat

The adipose capsule of the kidney -or perirenal fat- is an accumulation of extraperitoneal adipose tissue that completely surrounds the kidney, and its primary function is keeping the kidney in place. It has been shown that the amount of perirenal fat in males exceeds that in females. Furthermore, it seems that body mass index (BMI) is weakly correlated with the amount of perirenal fat, compared to subcutaneous fat distribution which undergoes BMI-related changes [Eisner, 2010]. This may have important implications for our proposed model, as perirenal fat might be a reliable source of adipose tissue regardless of BMI. Of note, clinical first-stage pro-angiogenic tissue implantation in the renal capsule may be performed endoscopically, on a day-surgery basis.

1.6 Hypotheses and Aims

The hypotheses for this thesis were formulated as follows:

I. Supplementation with ascorbic acid improves donor cell viability in vitro and in vivo, as well as angiogenesis and remodeling of thick myocardial artificial grafts (MAG), suitable for implantation and myocardial repair.

II. Epicardial implantation of an ascorbic acid- enriched myocardial artificial graft, which has been pre-vascularized in the recipients' own body, promotes restoration of the ischemic heart.

Based on these hypotheses, the following specific aims were identified:

1. To generate three-dimensional myocardial artificial grafts (MAG), and to evaluate dose-dependent effects of ascorbic acid on cell viability and phenotype in vitro.
2. To provide MAG with blood vessels of autologous origin, by developing a novel model (renal pouch model) for in vivo graft pre-vascularization in healthy rats.
3. To evaluate whether ascorbic acid enrichment has any effect on MAG's viability, angiogenesis and remodeling in vivo using the renal pouch model in healthy rats.
4. To prevent adverse remodeling and myocardial stiffening, promote angiogenesis and provide viability support concurrently, by implanting ascorbic acid- enriched and pre-vascularized myocardial artificial grafts into ischemic rat hearts.

An overview of the strategies and experimental design to achieve the proposed aims is illustrated in a flowchart in Figure 1.3.

1.7 Novelty and Significance

The findings from the current study are expected to contribute to the knowledge in two areas: tissue engineering and myocardial restoration. Here, we indentify ascorbic acid, a ubiquitous and essential substance, as a suitable supplement for cell and tissue transplant-based therapies.

Our approach provides a realistic perspective for the clinical setting: enhancement of cell survival in three-dimensional bioengineered tissues destined for myocardial repair both in vitro and in vivo, and a novel method to vascularize grafts for later autologous implantation. With our approach viability support (cell therapy and

antioxidant effects), structural support (prevention of remodeling) and revascularization (stimulation of angiogenesis) are all addressed.

Moreover, the utilization of biocompatible, inexpensive, FDA approved compounds, as well as the incorporation of autologous blood vessels within three-dimensional grafts make this strategy plausibly translatable to the clinical arena and potentially extendableto various donor cell types, as well as to other organs and regenerative interventions.

1.8 Organization of the Thesis

Chapter 1 provides a summarized background related to the epidemiology of ischemic heart disease and heart failure, as well as an overview of cardiac tissue engineering as a therapeutic approach for ischemic heart disease. Next, a more detailed literature review is presented, which includes the relevant concepts that motivated this research and lead to our hypotheses and the strategies proposed in this project.

Chapter 2 describes the materials and methods for all the assays, techniques and procedures used in this research, organized according to the project's hypotheses.

Chapter 3 displays the results derived from this research, organized in two parts. The first portion includes the data resulting from experimental work to test our first hypothesis (included in a published original paper [Martinez, 2010]). The second part contains the results from experiments carried out to test our second hypothesis (results currently under review in a peer-reviewed international scientific journal).

Chapter 4 contains the discussion, key findings summary and conclusions derived from this research, as well as the limitations of this project and recommendations for future directions.

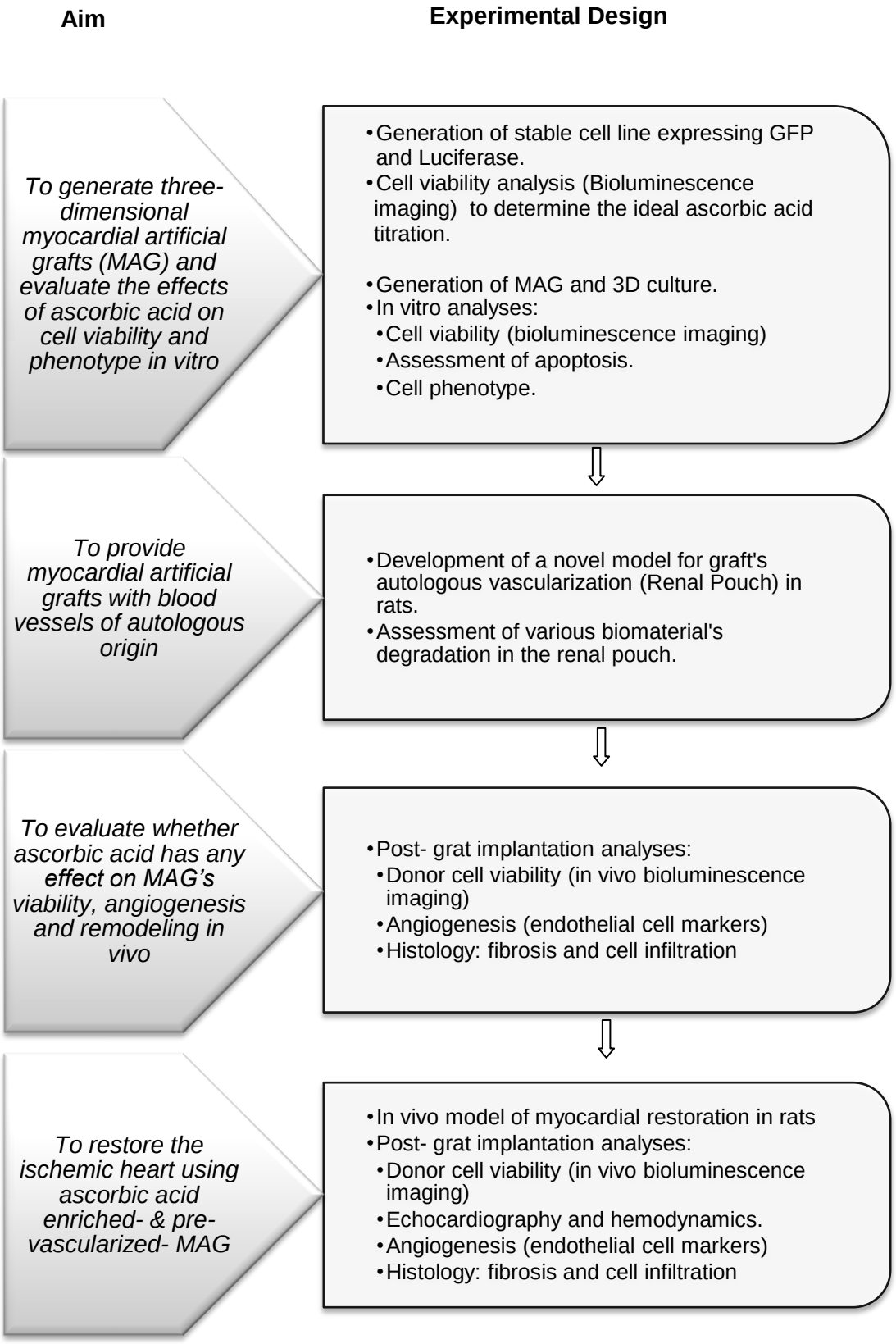

Figure 1.3 Aims and experimental design

2 Materials and Methods

2.1 Materials and Methods Hypothesis I

The experimental methods carried out for both in vitro and in vivo studies in order to test our first hypothesis (and to achieve the project aims 1 to 3) are summarized in Figure 2.1 and Figure 2.3.

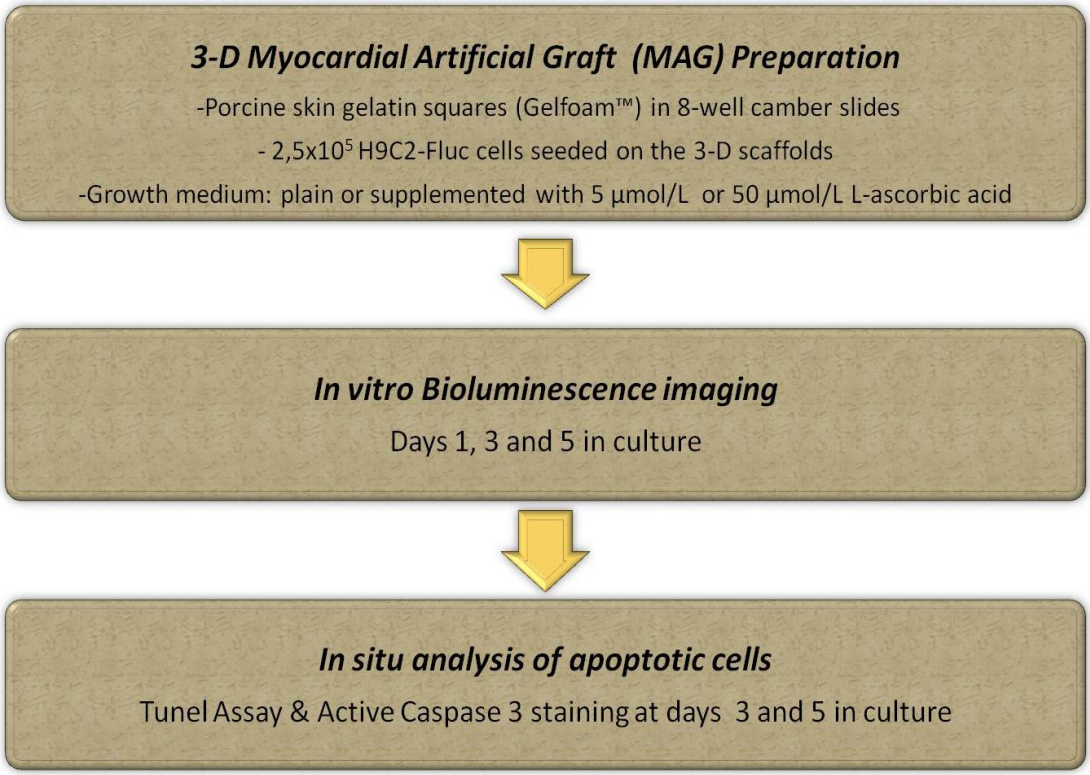

Figure 2.1 Flow chart indicating the methods to achieve Aim 1 (In vitro studies): To generate three-dimensional myocardial artificial grafts (MAG), and to evaluate dose-dependent effects of ascorbic acid on cell viability and phenotype in vitro.

2.1.1 Cell Culture

H9c2(2-1) cardiomyoblasts derived from embryonic rat hearts were obtained from the American Type Culture Collection (ATCC, Manassas, VA, USA) and maintained in DMEM supplemented with 10% fetal bovine serum, 100,000 U/L of penicillin, and

100 mg/L of streptomycin (Gibco), under 5% CO_2 at 37°C. Cells were passed on reaching 70% subconfluency to maintain the myoblast phenotype.

2.1.2 Generation of Fluorescent/ Bioluminescent Cell Lines

pWPT-GFP (kindly provided by Dr. D. Trono, EPFL, Switzerland) and pWPT-Fluc (modified from pWPT-GFP) second generation lentiviral vectors were used to infect H9C2 cells. pWPT-Fluc was cloned by removing GFP from pWPT-GFP and inserting the firefly luciferase (Fluc) gene PCRed from pGL3 (Promega). Lentiviral vectors were produced by transient transfection of 293T cells. $5x10^6$cells/plate were seeded in 10cm tissue culture plates 24 hr before transfection. The latter was performed using calcium phosphate precipitation method with 10µg pWPT-GFP or pWPT-Fluc vector, 7.5 µg helper plasmid pCMV8.91, and 2.5 µg of MD2G envelope plasmids (gifts from Dr. D Trono, University of Geneva, Geneva, Switzerland). Cell culture medium was replaced with fresh medium 14-16 hours after transfection. The supernatant was filtered through 0.45 µm filter, and the titre of supernatant on 293T cells was determined using flow cytometry. H9C2 cells were shown to be highly infectable (>90%) with unconcentrated lentiviral supernatant (unpublished data). H9C2 cells to be used in vivo were initially infected with supernatant containing pWPT-GFP, sorted for GFP positivity, and subsequently infected with pWPT-Fluc (H9C2-GFP-Fluc). Furthermore, cells destined for in vitro experiments were infected with pWPT-Fluc (H9C2-Fluc).

Transfection efficiency was assessed with optical bio- imaging using an ultrasensitive charged couple device camera that can capture bioluminescence and fluorescence (Xenogen IVIS® Lumina). $1x10^5$ and $2x10^5$ H9C2-Fluc-GFP cells were seeded in 6-well plates and 150 µg/ml of D-Luciferin (Caliper Life Sciences, Hopkinton, MA, USA) in pre-warmed cell culture medium was added to each well. In another experiment,

$1x10^5$ cells were seeded in 24 well plates (2-D culture) or in squares of a porous matrix (Gelfoam™) and covered with culture medium. Both, bioluminescence and fluorescence imaging were performed in the same 2-D and 3-D cultures to assess the correlation between luciferase-mediated and GFP-derived photon emission in H9C2-GFP-Fluc cells. The bioluminescence flux (photons per second) and fluorescence radiance emission were quantified with Living Imaging Software version 2.6 (Caliper Life Sciences).

2.1.3 Ascorbic Acid Titration

Prior to in vitro experiments, the concentrations of ascorbic acid with no cytotoxic effect on H9C2 cells were established, as it has also been previously described for other cell types [Telang, 2007, Vissers, 2007]. Three-dimensional cultures were established by seeding $1x10^5$ H9C2-Fluc cells in 100 μL of Collagen Type I (1μg/ml) in 96-well plates. The collagen was allowed to polymerize for 30 min and 3-D cultures were supplemented with 150 μL of medium containing 5, 50, 100 or 200 μmol/L L-ascorbic acid (Sigma, St. Louis, MO, USA). AA-enriched cell culture medium was changed twice a day. Cell viability was assessed with in vitro bioluminescence imaging (BLI) at days 3 and 7 in culture (see detailed BLI methods below). Experiments were carried out in triplicate.

2.1.4 3-D Graft Preparation for in vitro Studies

Sterile, porous sponges prepared from purified porcine skin gelatin (Gelfoam™, Pharmacia & Upjohn Company, Kalamazoo, MI, USA) were used as scaffold material to fabricate three-dimensional myocardial artificial grafts (MAG). Gelfoam™ squares (10 x 10 x 5 mm) were placed in 8-well chamber slides (Lab-Tek™II Chamber Slide™, NUNC A/S Roskilde, Denmark) under sterile conditions. Subsequently,

foams were hydrated with 100 μl growth medium supplemented with 5 μmol/L or 50 μmol/L L-ascorbic acid (Sigma, St. Louis, MO, USA). Scaffolds with just medium i.e. without ascorbic acid and/or without cells, were used as controls. A 100 μl medium solution containing 2,5x10^5 H9C2-Fluc cells was added on top of the 3-D scaffolds. Chamber slides were then placed in an incubator under 5% CO_2 at 37°C for 30 minutes to allow cell solution absorption into the sponge (Figure 2.2). Next, scaffolds were covered with 0.4 ml growth medium and placed back into the incubator. We changed the medium daily. Assays were conducted in quadruplet in five separate experiments.

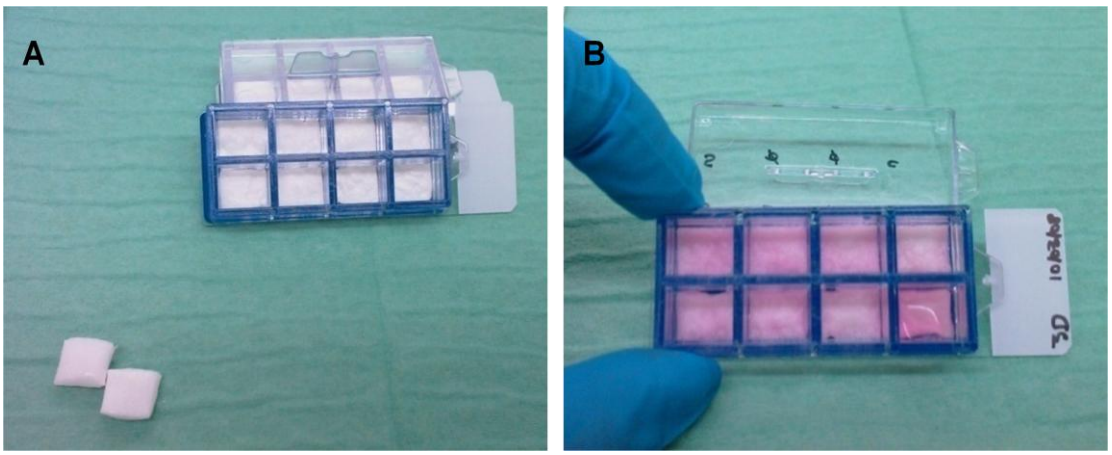

Figure 2.2 Myocardial artificial graft preparation. (A) Porcine gelatin porous scaffolds (30-700 μm pore size-) were cut in squares and placed in 8-well chamber slides (chamber size: 9x9 mm; area 0.82 cm2). (B) Scaffolds were re-hydrated with cell culture medium containing ascorbic acid prior to H9C2 cell seeding.

2.1.5 In vitro Bioluminescence imaging

Bioluminescence imaging was used to evaluate the effect of ascorbic acid on H9C2-Fluc cells in vitro survival when seeded in three-dimensional MAG after 1, 3 and 5 days in culture (n=20/ treatment/ time-point). For bioluminescence imaging, 150 μg/ml working solution of D-Luciferin (Caliper Life Sciences, Hopkinton, MA, USA) in

pre-warmed cell culture medium was added on each well and chamber slides were scanned five minutes later using a Xenogen IVIS® Lumina System (Caliper Life Sciences). Bioluminescence was quantified in units of photons per second total flux (p/s) using Living Imaging Software version 2.6 (Caliper Life Sciences).

2.1.6 TUNEL Assay and Immunohistochemical Staining for Active Caspase-3

Three-dimensional myocardial artificial grafts were fixed in 10% buffered formalin, embedded in OCT and stored at -80°C after in vitro experiments at days 3 and 5. *In situ* terminal deoxynucleotidyl transferase-mediated dUTP nick-end labeling (TUNEL) analysis was done using the ApopTag Red in Situ Apoptosis Detection Kit (Millipore Billerica, MA, USA) according to the manufacturer's instructions on five-micrometer cryosections. Sections from at least three different experiments were visualized using *a* Leica TCS SP5, DMI6000 confocal laser scanning microscope (Leica Microsystems, Wetzlar, Germany). The number of TUNEL positive cells was counted in ten different fields (400x), from three different grafts per condition. Next, to quantify apoptosis and exclude necrosis, ten-micrometer cryosections were stained with active Caspase 3 antibody (1:100, rabbit polyclonal antibody to active caspase 3, ab2302, Abcam, Cambridge, UK). Sections were counterstained with DAPI (Molecular Probes®, Invitrogen, Carlsbad, CA, USA) and z-stacks in 0.5 μm steps were obtained using confocal microscopy. A single image of maximum projection was obtained from the z-stacks by using Leica Application Suite Advanced Fluorescence (LAS-AF) quantification software (version 1.8.2 build 1465). Sections from at least three different experiments were analyzed. Cells were counted using Image J 1.42q (National Institutes of Health, USA). The percentage of TUNEL positive and active Caspase 3 positive cells was calculated as 100 X (number of positive cells counted/total number of nuclei counted).

2.1.7 Assessment of H9C2 Phenotype in 3-D Culture

Immunohistochemical assays were carried out to evaluate the effect of AA on H9C2 cardiomyoblast differentiation. Five-micron cryosections obtained from in vitro experiments at days 3 and 5 were stained with an antibody specific to α-cardiac and skeletal (sarcomeric) muscle actins (1:100, monoclonal mouse anti-sarcomeric actin, clone Alpha-Sr-1, DakoCytomatation, Glostrup, Denmark). Sections were then incubated with a secondary antibody Alexa Fluor®-568, counterstained with DAPI (Molecular Probes), and visualized with an Olympus BX61 fluorescence microscope equipped with a DP72 12.8 megapixel cooled digital camera (Olympus, Tokyo, Japan). Photomicrographs were processed using the DP2-BSW 2.2. (Build 6212) software (Olympus).

2.1.8 Animals and Renal Pouch Model

This study conforms to the *Guide for the Care and Use of Laboratory Animals* published by the US National Institutes of Health (NIH Publication No. 85-23, revised 1996). The experimental protocol was approved by the National University of Singapore-Institutional Animal Care and Use Committee (IACUC). Male SPF Wistar Rats (300-350 gr) were used for our experiments (Figure 2.3). All surgical procedures were performed using aseptic techniques.

Anesthesia was induced and maintained in animals with inhalational isoflurane (2%) and intraperitoneal (IP) injection of Ketamine:Xylazine (90 mg/kg :10mg/kg). Carprofen (5 mg/Kg, SC) was administered preoperatively for analgesia. A mid laparotomy was performed followed by displacement of the bowel and mild retraction of the kidney. Blunt preparation of the retroperitoneal fossa was done and a pouch was created between the perirenal (retrorenal) fat and the psoas muscle (Figure 2.4). Subsequently, the myocardial artificial graft was implanted into the retro-renal

pouch. Grafts containing cells were implanted in the right renal pouch, where as acellular controls were implanted in the contralateral pouch. We did not use suture material in the implantation process. Finally, the bowel was repositioned and the abdomen was closed in two layers. Animals were allowed to recover in a small-animal ICU. Carprofen (5 mg/Kg/day, SC) was administered postoperatively for analgesia.

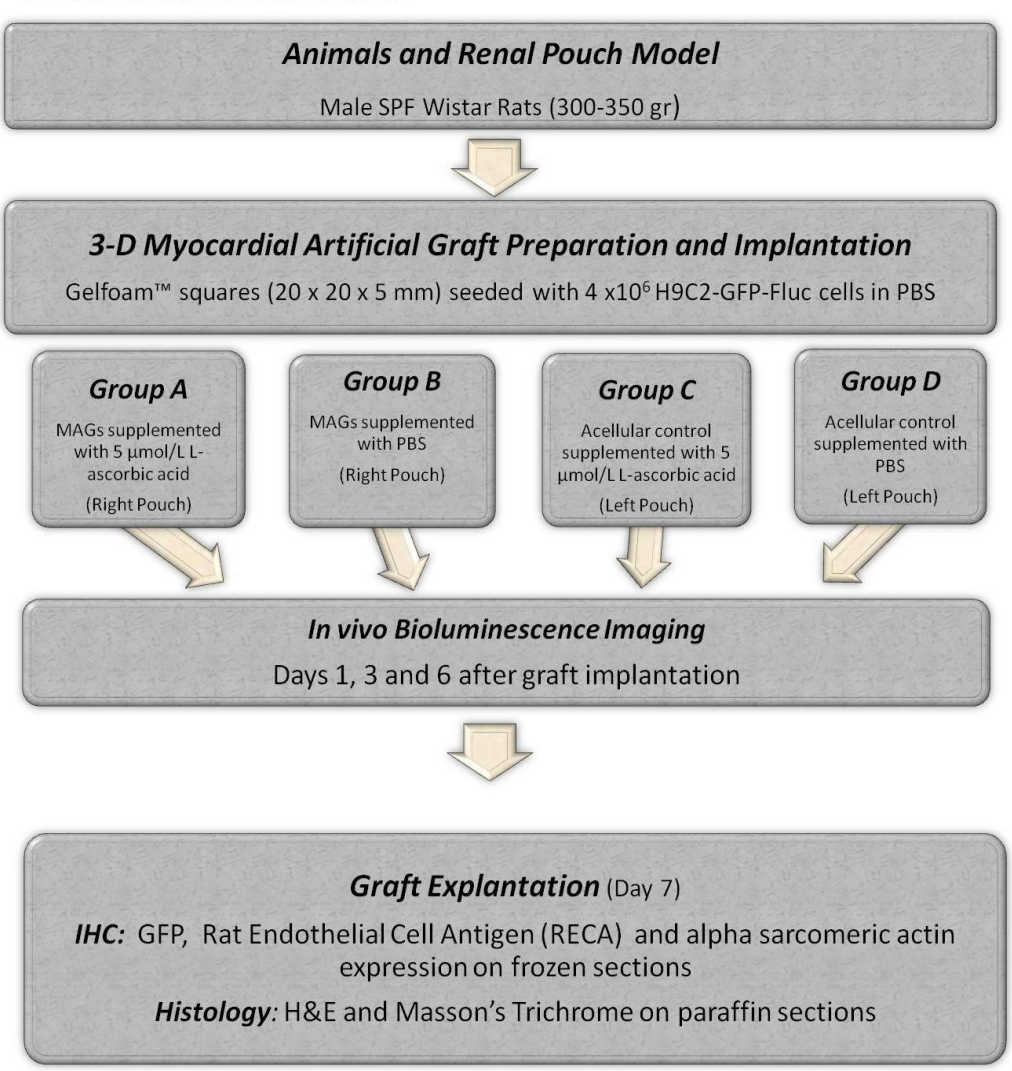

Figure 2.3 Flowchart indicating the methods followed to achieve Aims 2 & 3 (In vivo studies): To provide myocardial artificial grafts (MAG) with blood vessels of autologous origin, by developing a novel model for in vivo graft pre-vascularization in healthy rats, and to evaluate whether ascorbic acid enrichment has any effect on MAG's viability, angiogenesis and remodeling in vivo using the renal pouch model.

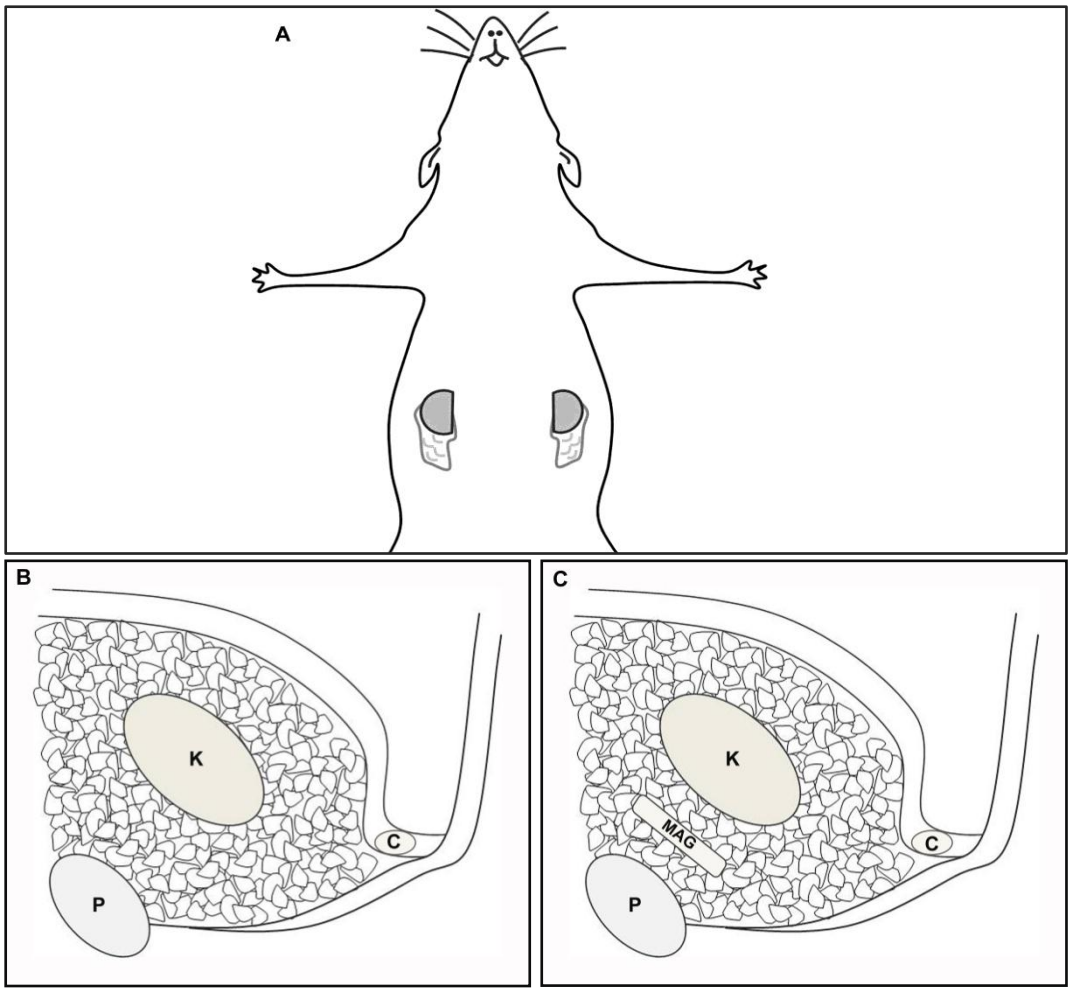

Figure 2.4 Perirenal fat and renal pouch model. (A) Illustrates the location of the kidneys and perirenal fat in the rat. (B) Cross-section illustrating the normal anatomy of the extraperitoneal perirenal space occupied by adipose tissue. K, kidney; P, psoas muscle; C, descending colon. (C) MAG implanted in the perirenal fat. A pouch is created in the perirenal fat between the psoas muscle and the kidney (retrorenally), followed by implantation of the myocardial artificial graft (MAG) for in vivo vascularization.

2.1.9 3-D Graft Preparation for in vivo Studies

In our preliminary studies, eight rats were used to test several 3-dimensional matrices and to identify the one displaying the least degradation and low inflammatory reaction after 10 days of implantation using the renal pouch model. Four different collagenous foam-scaffolds from diverse origin (i.e. Equine collagen and human fibrinogen (Tachotop®, Nycomed, Zurich, Switzerland); bovine collagen (Lyostypt®, B. Braun Melsungen AG, Melsungen, Germany); native equine collagen (TissuFleece E®, Baxter, Vienna, Austria); porcine skin gelatin (Gelfoam™), were

implanted in the renal pouch without cells (). H9C2-GFP-Fluc cells were washed three times in cold PBS and centrifuged. Gelfoam™ squares (20 x 20 x 5 mm) were placed in 12-well plates and covered with 4 x10^6 H9C2-GFP-Fluc cells in 250 µl PBS under sterile conditions. Based on our in vitro studies, we chose 5 µmol/L L-Ascorbic acid in PBS enrichment for the ascorbic acid animal group (Group A, n=10). Plain MAG without ascorbic acid (PBS and cells) were used as control group (Group B, n=10). Acellular grafts containing just PBS (Group C, n=10) or PBS-5 µmol/L ascorbic acid (Group D, n=10) were used as negative controls and implanted in the left renal pouch.

2.1.10 In vivo Bioluminescence Imaging:

We performed optical in vivo BLI with the Xenogen-IVIS® Lumina *in vivo* imaging system as previously described [Hauck, 2008, Kutschka, 2006a, Shinde, 2006]. Briefly, rats were anesthetized with isoflurane 2% and D-luciferin was administered IP at a dose of 150 mg per kilogram of body weight. They were placed in the chamber in supine position and peak luciferase activity was detected by imaging animals for 40 minutes with two-minute acquisition separated by two-minute intervals [Hauck, 2008]. The same rats were scanned repeatedly on post-implantation days 1, 3 and 6. Regions of interest (ROIs) which identify the location the most intense signal were created using Living Imaging Software version 2.6. Bioluminescence was quantified in units of photons per second total flux (p/s) [Cao, 2006, Shinde, 2006].

2.1.11 Immunohistochemistry- Assessment of GFP and RECA Expression:

At seven days post-implantation, MAG were explanted and fixed in 10% formalin. The grafts were subsequently OCT-embedded and stored at -80°C.

Immunohistochemical staining was performed in five-micrometer cryosections using the primary antibody RECA-1, a ubiquitous marker of rat endothelial cells (1:50 monoclonal mouse anti-RECA-1; HyCult biotechnologt b.v, The Netherlands). Sections were then incubated with secondary antibodies Alexa Fluor®-647 and Anti GFP-Alexa Fluor®-488, and nuclei were stained with DAPI (Molecular Probes).

Images were acquired using a Leica TCS SP5, DMI6000 confocal laser scanning microscope (Leica Microsystems, Wetzlar, Germany), times 40 and 20 magnification. They were subsequently processed using Leica Application Suite Advanced Fluorescence (LAS-AF) quantification software (version 1.8.2 build 1465).

The mean pixel intensity, a semi-quantitative analysis of fluorescence was used to evaluate GFP and RECA expression within the explanted 3-D grafts. Predefined settings for laser power and detector gain were used for all experiments.

2.1.12 Histological Analysis:

We performed Masson's Trichrome and hematoxylin-eosin (H&E) staining on five-micrometer sections of formalin-fixed and paraffin-embedded explanted MAG. Histological assessment was performed by an experienced pathologist in a blinded fashion. To assess angiogenesis within the explanted graft, the number of blood vessels per high power field (hpf) 400x was quantified. The degree of cell infiltration and fibrosis was evaluated as the percentage of area of the scaffold infiltrated by cellular reaction and collagen deposition covering the total cellular reaction using a manual semi-quantitative method. Ten random fields were chosen in each section for all the quantifications.

2.1.13 Statistical Analysis

Data are presented as mean ± SD. To test for statistically significant differences, we used two-way ANOVA and the unpaired Student's *t* test when appropriate. Differences were considered significant if $p<0.05$. Regression plots were used to describe the relationship between bioluminescence and cell number in vitro; r^2 values are reported to assess the quality of the linear regression model. All the statistical analyses were performed using GraphPad Prism® software version 5.01 for Windows (GraphPad Software, San Diego, CA, USA).

2.2 Materials and Methods Hypothesis II

The experimental methods carried out for in vivo studies to test our second hypothesis and that are related to the project aim 4, are summarized in a flow chart in Figure 2.5.

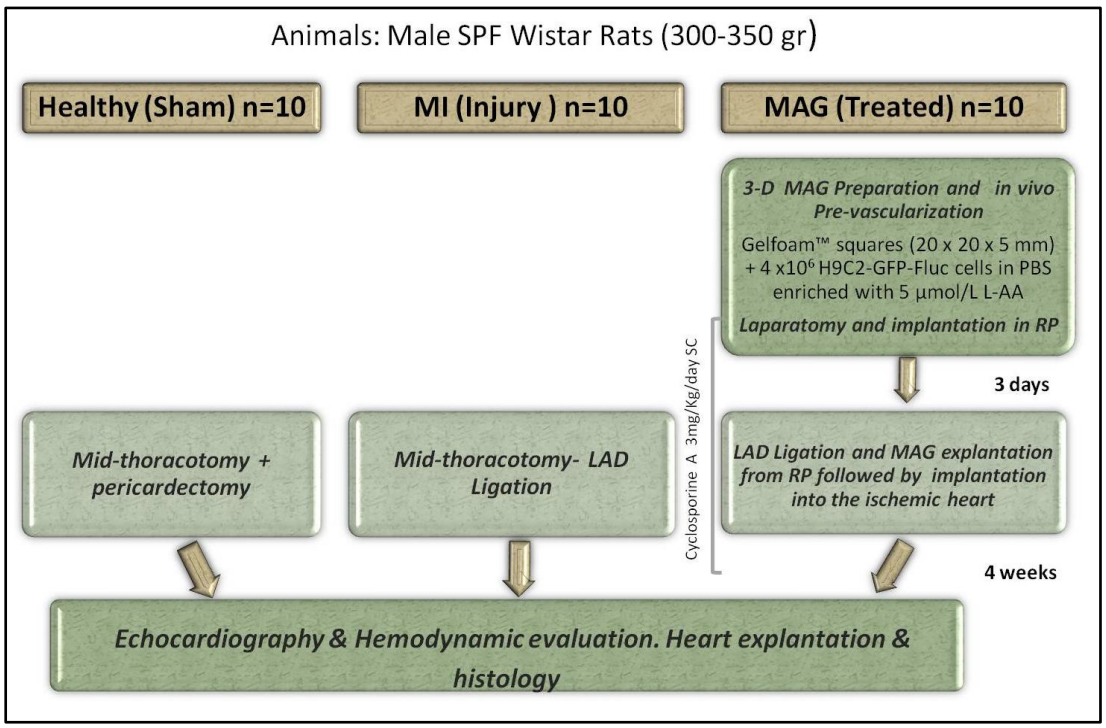

Figure 2.5 Flow chart indicating the experimental design and methods to Aim 4: Myocardial restoration in an acute rat model of myocardial infarction.

2.2.1 Cell Culture

H9c2(2-1) cardiomyoblasts derived from embryonic rat hearts were cultured as described elsewhere. Fluorescent and bioluminescent cells lines were generated as previously described (see methods to hypothesis I).

2.2.2 3-D Myocardial Artificial Graft (MAG) Preparation

We have chosen porcine skin gelatin (Gelfoam™) as scaffold material for our study, due to its porosity and biocompatibility. Ascorbic Acid-enriched MAG were prepared as previously described. Briefly, 4 $x10^6$ H9C2-GFP-Fluc cells were harvested, washed three times in cold PBS, centrifuged and resuspended in 250 μl PBS containing 5 μmol/L L-Ascorbic acid (Sigma, St. Louis, MO, USA). The 250 μl cell-AA suspension was added to Gelfoam™ squares (1.0 x 1.0 x 5 mm) placed in 8-well plates chamber slides (Lab-Tek™II Chamber Slide™, NUNC A/S Roskilde, Denmark) under sterile conditions. Cell solution absorption into the sponge, and cell attachment were allowed for 3 hr under 5% CO_2 at 37°C prior to in vivo implantation.

2.2.3 Animals

Male SPF Wistar Rats (300-350 gr) were used for our experiments. All surgical procedures were performed using aseptic techniques.

2.2.4 MAG Pre-vascularization

Anesthesia was induced and maintained in animals with inhalational isoflurane (2%) and intraperitoneal (IP) injection of ketamine:xylazine (90 mg/kg :10mg/kg). Carprofen (5 mg/kg, SC) was administered preoperatively for analgesia. A renal pouch for graft pre-vascularization was created. In brief, following laparatomy, a pouch was disected in the right retrorenal fat. Next, the MAG was implanted into the

pouch and pre-vascularized for three days. Animals were allowed to recover in a small-animal ICU. Carprofen (5 mg/Kg/bid, SC), Ceftazoline (15 mg/Kg/bid, SC) were administered postoperatively for the next 3 days. Animals received cyclosporine A (3 mg/Kg /day, SC) for immunosuppression until the end of the study (4 weeks after the restorative therapy).

2.2.5 Myocardial Infarction Model and MAG Angiogenic Restorative Therapy

Animals were anesthetized as decribed above and intubated for continuous ventilation with oxygen and 2% isoflurane using a rodent ventilator (Inspira ASV, Harvard Apparatus, Inc Holliston, Massachusetts, USA). Hearts were exposed through mid-throacotomy, and after gentle pericardectomy, left anterior descending coronary artery (LAD) ligation was performed by placing a 7-0 polypropylene suture stitch from the left border of the pulmonary conus to the right border of the left atrial appendage. Acute evidence of ischemia was assessed by direct observation of myocardial blanching and ECG changes. In the MAG group (n=6), a mid laparatomy was performed concomitantly and the pre-vascularized MAG was explanted from the renal pouch and implanted into the area of myocardial ischemia. The patch was attached to the recipient heart 30 minutes after MI using fibrin glue (Tisseel, Baxter Healthcare Corporation, Deerfield, IL) (Figure 2.6). In the MI (injury) group (n=6), animals did not receive any treatment following LAD ligation, whereas the healthy (sham operated) group (n=7) only underwent mid-thoracotomy and pericardectomy. After the restorative procedure, the chest was closed in 3 layers and animals were allowed to recover in a small-animal ICU. Carprofen (5 mg/Kg/bid, SC), Ceftazoline (15 mg/Kg/bid, SC) were administered postoperatively for the next 7 days.

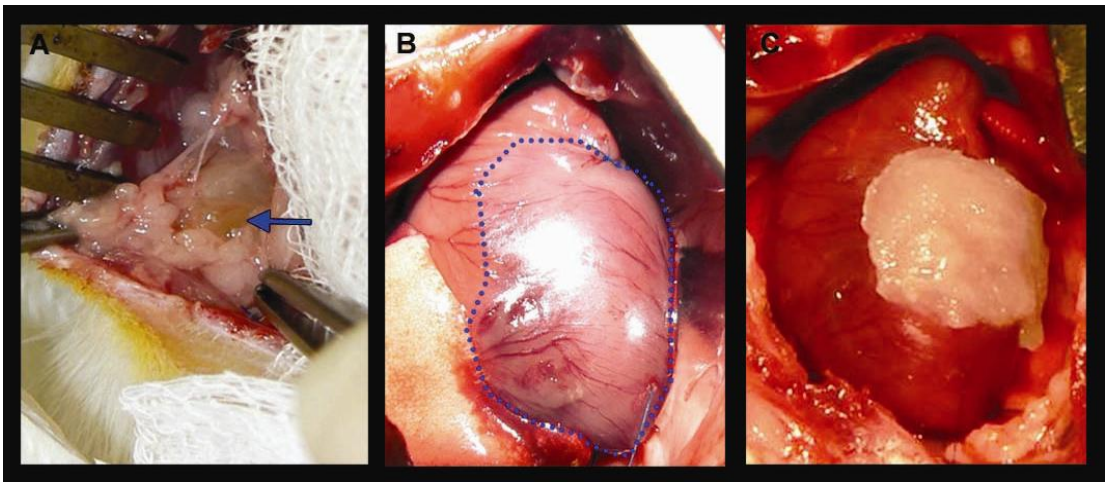

Figure 2.6 Pre-vascularized myocardial artificial graft (MAG) implantation. (A) MAG was explanted from the renal pouch 3 days after autologous in vivo pre-vascularization. Blue arrow indicates the MAG within the pre-renal fat. (B) Following left anterior descending coronary artery ligation and myocardial ischemia. The discontinuous line in (B) delimits the area of ischemia. (C) The pre-vascularized MAG was implanted epicardially into the heart of the same animal.

2.2.6 In vivo Bioluminescence Imaging

To monitor in vivo H9C2 cell survival in the implanted MAG, we performed optical in vivo bioluminescence imaging (BLI) using a Xenogen-IVIS® Lumina *in vivo* imaging system (Caliper Life Sciences, Hopkinton, MA, USA) as previously described. [Hauck, 2008, Kutschka, 2006a, Martinez, 2010, Shinde, 2006] Briefly, rats were anesthetized with isoflurane 2% and D-luciferin (Caliper Life Sciences) was administered IP at a dose of 150 mg per kilogram of body weight. Animals were placed in the chamber in supine position and peak luciferase activity was detected by imaging the rats' chest for 90 minutes with two-minute acquisition separated by 5-minutes interval. All rats from the treatment group were prospectively scanned on post- MAG implantation days 1, 7 and 14. Regions of interest (ROIs) which correspond to the location of the most intense signal were created using Living Imaging Software version 3.1. Bioluminescence was quantified in units of photons per second total flux (p/s) [Cao, 2006, Shinde, 2006].

2.2.7 Echocardiography

Echocardiography was performed at 4 weeks postoperatively for all groups by a blinded investigator (LHL) using the Vivid 7 Dimension ultrasound system (General Electric VingMed, Horton, Norway) equipped with a broadband 10S transducer. Following anesthesia with ketamine:xylazine (90 mg/kg :10mg/kg) injected IP, two-dimensional echocardiographic images of the LV at the papillary muscle level were recorded at a transducer frequency of 10 MHz, and used to guide M-mode recordings. Offline measurements of LV dimensions and areas were made from 3 consecutive cardiac cycles using EchoPac software (version 6, General Electric Vingmed, Horten, Norway). LV volumes were calculated using a modified Teichholz formula: π x D^3/6a, where D=diameter of the ventricle in short axis view; a=ellipticity factor. An ellipticity factor of 1/3 was used as described elsewhere [Weytjens, 2006]. Ejection fraction (%) was calculated as LV end-diastolic volume – LV end-systolic volume/LV end-diastolic volume.

2.2.8 Hemodynamic Measurements

We performed LV pressure and volume measurements 4 weeks postoperatively. Rats were anesthetized and intubated for ventilation with 3% isoflurane/97% oxygen. Following sternotomy, a 2 mm transient time flow probe was placed in the ascending aorta for cardiac output measurement (Transonic Systems Inc, Ithaca, NY). Next, the apex of the LV was cannulated with a pressure transducer catheter (Millar Micro-Tip® model SPC-721, Millar, Inc, TX, USA) (Figure 2.7). Pressure and aortic flow wave forms were recorded with the Powerlab 8/30 data acquisition system (ADInstruments Pty Ltd, Castle Hill, NSW, Australia). Data were analyzed using Lab Chart Pro version 7.0 software (ADInstruments).

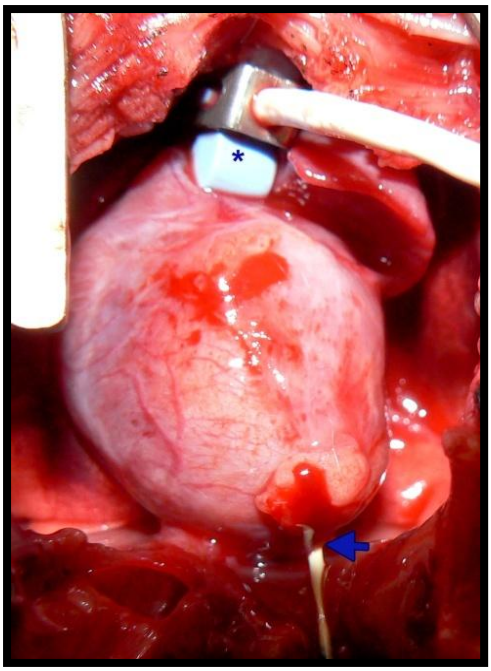

Figure 2.7 Hemodynamics measurement set-up in an infarcted heart four weeks after LAD ligation. Asterisk indicates the location of the time flow probe placed around the ascending aorta. Arrow pointing at the intra-ventricular pressure transducer catheter inserted into the left ventricle from the apex.

2.2.9 Histology and Immunofluorescence

Two animals underwent bilateral real pouch MAG implantation for graft histology after 3 days of in vivo vascularization. Animals were anestethized, and direct labeling of the blood vessels by cardiac perfusion with 1,1'-dioctadecyl-3,3,3',3'-tetramethylindocarbocyanine perchlorate (DiI) was done [Li, 2008]. MAG were then explanted from the pouch (n=4), and fixed in 10% buffered formalin. Half of the graft was embedded in paraffin and rest was OCT-embedded and stored at -80°C.

Immediately after hemodynamic assessment, hearts were excised and cut into two equal transverse slices and fixed in 10% buffered formalin. The upper slice was embedded in paraffin, whereas the lower slice was cryoprotected in sucrose 20% at 4°C overnight, and subsequently OCT-embedded and stored at -80°C.

We performed Masson's Trichrome and hematoxylin-eosin (H&E) staining on five-micrometer paraffin sections from all the hearts included in this study. Semi-quantitative histological assessment was performed by an experienced pathologist in a blinded fashion. Inflammatory cell infiltration and fibrosis were evaluated in the following LV areas: (A) infarction, (B) peri-infarct border zone, and (C) graft area for the MAG group. Comparable anatomic areas (to those in A and B) were assessed in healthy hearts. Fibrosis was evaluated as the percentage of area of the left ventricle covered by collagen deposition. Ten random fields were chosen in each section for all the quantifications.

To assess angiogenesis, two consecutive 5 μm heart sections were stained using a blood vessel staining kit (Millipore Corp., Bedford, Massachusetts, USA) in which von Willebrand factor (vWF) was used as an endothelial cell marker (Rabbit anti-vWF polyclonal antibody, Millipore). Blood vessels per high power field (hpf) 400x were quantified in ten random fields per section in all the experimental groups using Image J 1.42q software (National Institutes of Health, USA).

Neovascularization within the graft was assessed in MAG twenty-micrometer cryosections through the detection of DiI+ blood vessels. Immunohistochemical staining was performed in two consecutive five-micrometer cryosections from each heart using a ubiquitous marker of rat endothelial cells (1:50 monoclonal mouse anti-RECA-1; HyCult biotechnologt b.v). Sections were then incubated with secondary antibodies Alexa Fluor®-594 and Anti GFP-Alexa Fluor®-488, and nuclei were stained with DAPI (Molecular Probes®, Invitrogen, Carlsbad, CA). Images were acquired using a *Leica TCS SP5***,** DMI6000 confocal laser scanning microscope (Leica Microsystems, Wetzlar, Germany), times 40 and 20 magnification. They were

subsequently processed using Leica Application Suite Advanced Fluorescence (*LAS-AF*) quantification software *(*version 1.8.2 *build 1465).*

2.2.10 Statistical Analysis

Sample calculation: Based on power calculation from our previous studies using gelfoam and H9C2 cell grafts for myocardial restoration [Kutschka, 2006a], 7 rats per group will afford statistical power to differentiate response between treated and untreated groups (G-Power 3.1.2 software). In total, 30 rats will be used for this study, including extra rats to offset losses due to mortality (30% based in pilot studies).

Statistics: Data are presented as mean ± SEM. To test for statistically significant differences, we used two-way ANOVA and the unpaired Student's *t* test when appropriate. Differences were considered significant when $p<0.05$. All statistical analyses were performed using GraphPad Prism® software version 5.01 for Windows (GraphPad Software, San Diego, CA).

3 Results

3.1 Results Experimental Approach to Hypothesis I

3.1.1 Generation of Bioluminescent/Fluorescent Cell Lines

Strong bioluminescence activity and good correlation of cell photon emission to cell number (number of cells seeded in 2-D culture) was found in H9C2-GFP-Fluc cells (r^2= 0.96) (Figure 3.1). Likewise, evaluation of both bioluminescence and fluorescence using the IVIS® Lumina bioimaging system indicated that there is a linear relationship between bioluminescence signals and fluorescence in 2-D (r^2= 1.0) and 3-D (r^2= 0.92) culture (Figure 3.2). The latter slight variation in 3-D culture is likely to be related to increased fluorescence signals derived from the scaffold material (collagen's auto-fluorescence). Hence, we chose to use bioluminescence imaging to assess cell survival in vitro and in vivo, and GFP immunostaining to detect donor cells in histological sections (Figure 3.3).

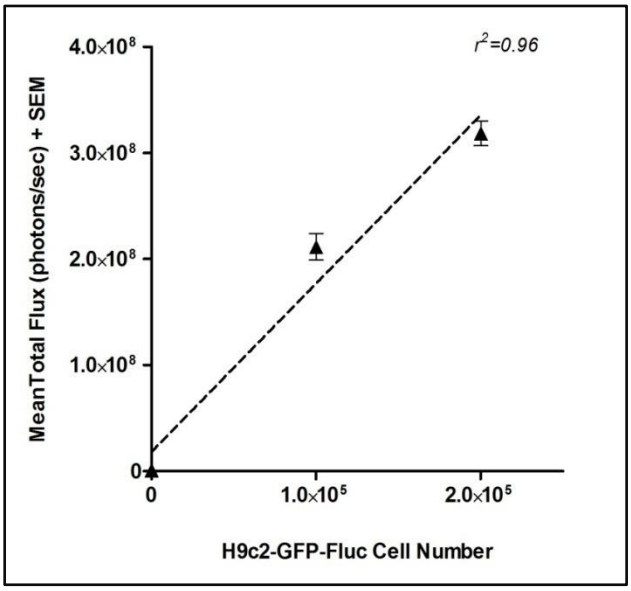

Figure 3.1 H9C2 cells Luciferase transfection efficiency. Correlation between mean bioluminescence (mean total photon flux) and cell number in 2-D culture.

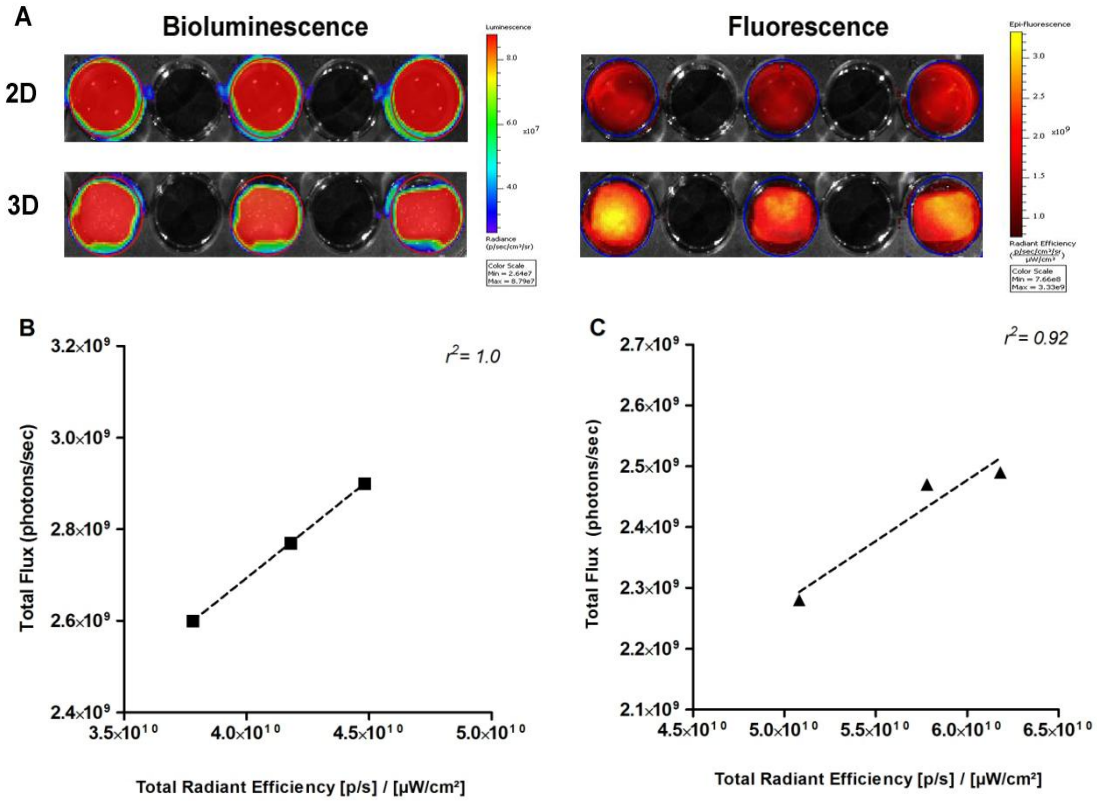

Figure 3.2 Bioimaging (bioluminescence and fluorescence) in two-dimensional and three-dimensional cell culture. (A) 1x10^5 H9C2-GFP-FLuc cells were seeded on each well for 2-D cultures and on a porous collagen matrix for 3-D culture. A slight increase of fluorescence radiance was detected in 3-D cultures. (B) There is a perfect linear correlation between the amount of photons released per second (Total Flux) and the fluorescence emitted by GFP (Total Radiant Efficiency) in two-dimensional culture. (C) A good correlation between bioluminescence and fluorescence three-dimensional was also observed.

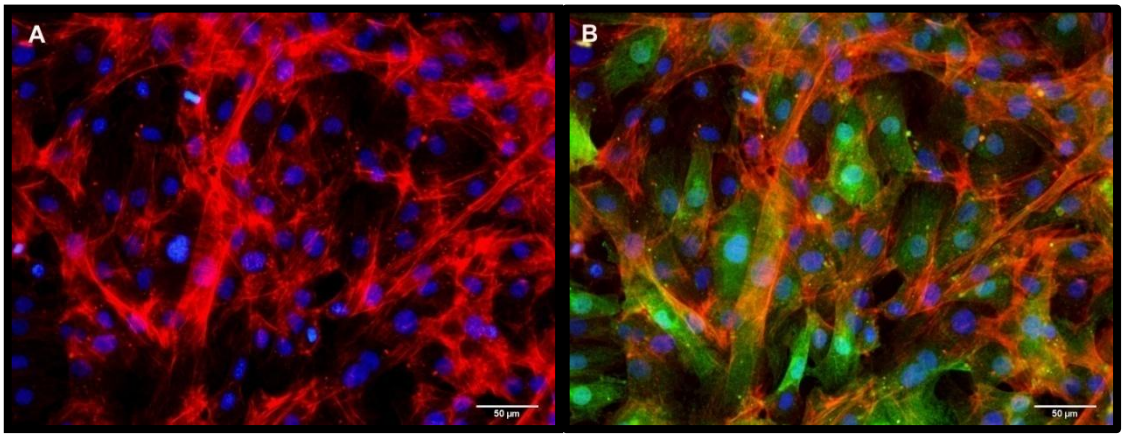

Figure 3.3 H9C2-GFP-Fluc cells. Immunofluorescence images showing H9C2-GFP-Fluc cardiomyoblasts expressing (A) F-actin (in red) and (B) F-actin and GFP (in green). Nuclei appear in blue. Scale bar equals 50 µm.

3.1.2 Ascorbic Acid Titration

Ascorbic acid titration assays in collagen 3-D cultures, indicated that any dosage equal or above 100 μmol/L AA does not have any protective effect on H9C2 rat cardiomyoblasts (Figure 3.4). A significant decrease in cell photon emission was observed at day 7 compared to day 3 in cultures supplemented with 100μmol/ L AA ($P<0.05$) and 200 μmol/L AA ($P<0.001$), as well as in cultures that did not receive any ascorbic acid (-AA, $P<0.001$) in the culture medium. No significant difference in cell bioluminescence was found between 3D cultures supplemented with 5 and 50 μmol/L AA at day 7. On the other hand, a significant increase in cell signals by day 7 was observed in 3-D cultures enriched with 5 μmol/L AA, when compared to the other culture conditions, Consequently, we chose to continue using 5 and 50 μmol/L ascorbic acid in any further in vitro studies. Similar AA physiological concentrations (up to 50 μmol/L) have also been previously reported as safe in other cell types [Telang, 2007, Vissers, 2007].

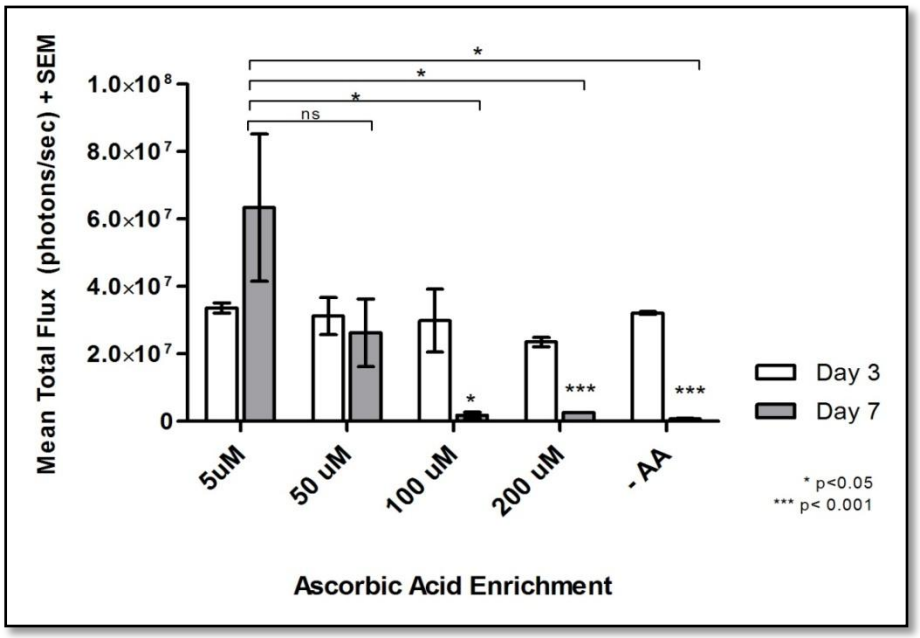

Figure 3.4 Bioluminescence imaging evaluating cell viability in 3-D collagen cultures after supplementation of cell culture medium with various concentrations of ascorbic acid (n=6). –AA, indicates that cell culture medium without ascorbic acid was added. SEM, standard error of the mean.

3.1.3 ECM-based Scaffold Degradation in the Renal Pouch

We carried out preliminary studies to assess the degradation of several FDA-approved ECM foams following implantation of 1cm^2 scaffolds (without cells) in the perirenal fat of Wistar rats for 7 days (Table 3.1) . The porcine gelatin foam was recovered almost intact after 10 days of implantation and did not trigger fibrosis or foreign body reaction in the renal pouch. Hence, Gelfoam was chosen as scaffold material for cell-based animal experiments in the present study.

Table 3.1 Degradation of collagen-based foams in the renal pouch.

Matrix (Foam)	Components	Size upon implantation in RP (cm^2)	Size upon retrieval (cm^2)
TachoComb® n=4	Horse collagen Human fibrinogen Bovine thrombin Bovine aprotinin	1.0	0.54±0.096 *
Lyostyp® n=4	Bovine collagen	1.0	0.37±0.71*
Tissue Fleece E® n=4	Equine Collagen	1.0	0.0*
Gelfoam® n=4	Porcine Gelatin	1.0	0.95±0.02 ns

* p<0.0001; ns: not significant

3.1.4 In vitro Bioluminescence Imaging/ Effect of Ascorbic Acid on 3-D H9C2 Cell Graft Survival in vitro

BLI showed that there was a significant increase in cell bioluminescent baseline signals from day 1 to day 5 in grafts supplemented with both 5 µmol/L and 50 µmol/L

ascorbic acid (55.23±0.45%, P<0.001 and 49.83±0.45%, P<0.01 respectively) (Figure 3.5 A-D). H9C2-Fluc cells seeded within the three-dimensional MAG receiving 5 µmol/L ascorbic acid-supplemented medium showed significantly larger bioluminescent signals after 3 days ($2.1x10^8 \pm 9.5x10^7$ p/s vs. $1.5x10^8 \pm 7.4x10^7$p/s, P<0.05 versus control) and 5 days in culture ($2.3x10^8 \pm 7.9x10^7$vs. $1.7x10^8 \pm 4.8x10^7$, P<0.05 versus control). Likewise, 50 µmol/L ascorbic acid-supplemented grafts displayed significantly increased cell signals at day 3 when compared to control grafts receiving plain culture medium ($2.0x10^8 \pm 8.0x10^7$, P<0.05 versus control) (Figure 3.5 D). There were no large differences in photon emission between the two dosages of ascorbic acid.

Histological cell counts (DAPI $^+$cells) indicated that the amount of DAPI$^+$ cells per hpf (x400) in the 5 µmol/L ascorbic acid –enriched grafts was significantly higher than in the plain grafts after 3 days in culture (53±21.4 vs. 30±7.18, P<0.05). Likewise, mean cell number was higher in grafts that received 50 µmol/L AA after 5 days in static culture when compared to untreated MAG (41.4±14.3 vs. 19.6±6.9, P<0.05). There were differences in cell density between the ascorbic acid-treated grafts. A good correlation of luciferase activity per graft to mean cell number (DAPI $^+$ cells/ graft) was found after 3 days (r^2= 0.90) and 5 days (r^2= 0.97) in culture (Figure 3.5 E and F).

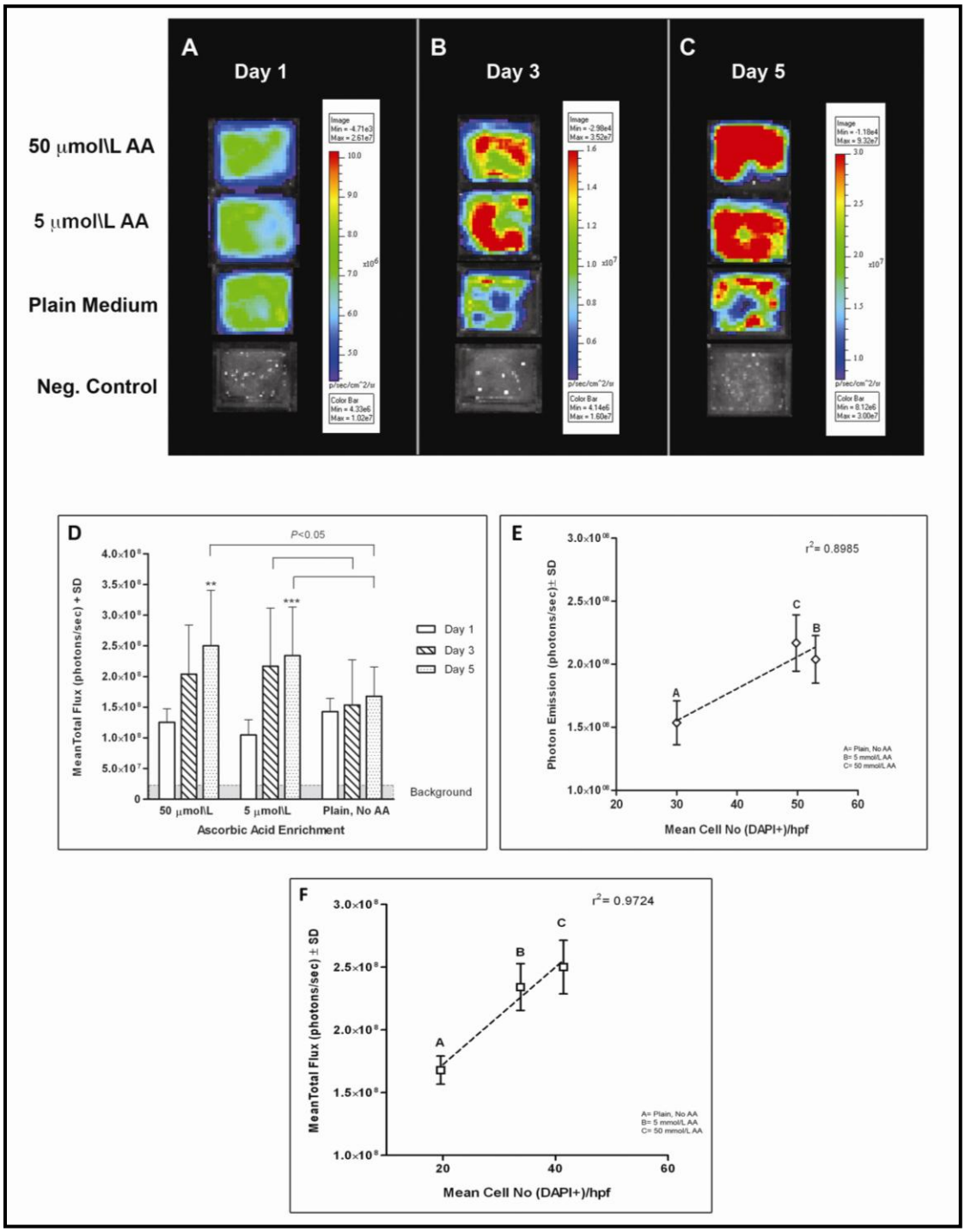

Figure 3.5 In vitro Bioluminescence imaging of 3-D MAG. BLI of AA-enriched and plain MAG after (A) 1 day, (B) after 3 days in culture, and (C) after 5 days in culture; n=20. (D) MAG receiving 50 and 5 μmol/L AA-supplemented medium showed significantly larger bioluminescent signals after 5 days in culture ($p<0.05$ vs. control). 5 μmol/L AA-enriched MAG also displayed higher photon emission at day 3 in culture ($p<0.05$ vs. control). An increase in cell bioluminescent baseline signals from day 1 to 5 was found in grafts supplemented with both 5 μmol/L AA (***$p<0.001$) and 50 μmol/L AA (**$p<0.01$). Correlation between mean bioluminescence (mean total photon flux) and histological mean cell number after (E) 3 days and (F) 5 days in culture. 3-D, three-dimensional; AA, ascorbic acid; BLI, bioluminescence imaging; hpf, high-power field (400x); MAG, myocardial artificial grafts; SD, standard deviation.

3.1.5 The Effect of Ascorbic Acid on Cell Apoptosis in 3-D MAG in vitro

TUNEL assay and active Caspase 3 staining were used to assess the effect of ascorbic acid on H9C2-luc cells apoptosis when cultured in thick three-dimensional myocardial artificial grafts (MAG) (Figure 3.6 A-F). The percentage of $TUNEL^+$ cells per hpf (400x) in plain grafts increased significantly from day 3 in culture (23.5±12.6%) to day 5 (61.9±30.1%, $P<0.001$). The percentage of $TUNEL^+$ cells was significantly inferior in the 5 µmol/L and 50 µmol/L MAG at day 5 in culture (4.8±8.6%, $P<0.001$ and 8.3±9.2%, $P<0.001$ respectively) when compared with plain control grafts (61.9±30.1%) (Figure 3.6 G). Given that TUNEL assay tags apoptotic and necrotic cells, we used active Caspase 3 staining as a more specific method to identify apoptotic cells. The percentage of active Caspase 3^+ cells was considerably higher in plain grafts after 3 (41.6±11.2%) and 5 (44.8±20.0%) days in culture when compare to both dosages of ascorbic acid (Figure 3.6 A-F and H). The 5 µmol/L AA grafts had 16.5 ±6.17% ($P<0.01$) apoptotic cells at day 3, and 15.7 ±6.8% ($P<0.001$) at day 5. Likewise, the 50 µmol/L AA MAG had 11±5.7% ($P<0.01$) of apoptotic cells at day 3 and 18.8±5.9% ($P<0.01$) at day 5 in culture.

3.1.6 Ascorbic Acid Effect on H9C2 Cells Phenotype in vitro

After 3 days in culture, H9C2 cardiomyoblasts were attached to the scaffold material and formed a primitive syncytium in all groups (Figure 3.7 A, C and E). Cells fused and formed elongated myotube-like structures that were evident in the ascorbic acid-treated grafts (Figure 3.7 C and E). Immunohistochemical assays revealed that α-sarcomeric actin was expressed by untreated and ascorbic acid-enriched cells after 3 and 5 days in 3-D culture. However, the ascorbic acid-treated groups displayed organized sarcomeric patterns at days 3 and 5 in culture, whereas z-lines were not apparent in the untreated cells after 5 days in culture (Figure 3.7 A- F).

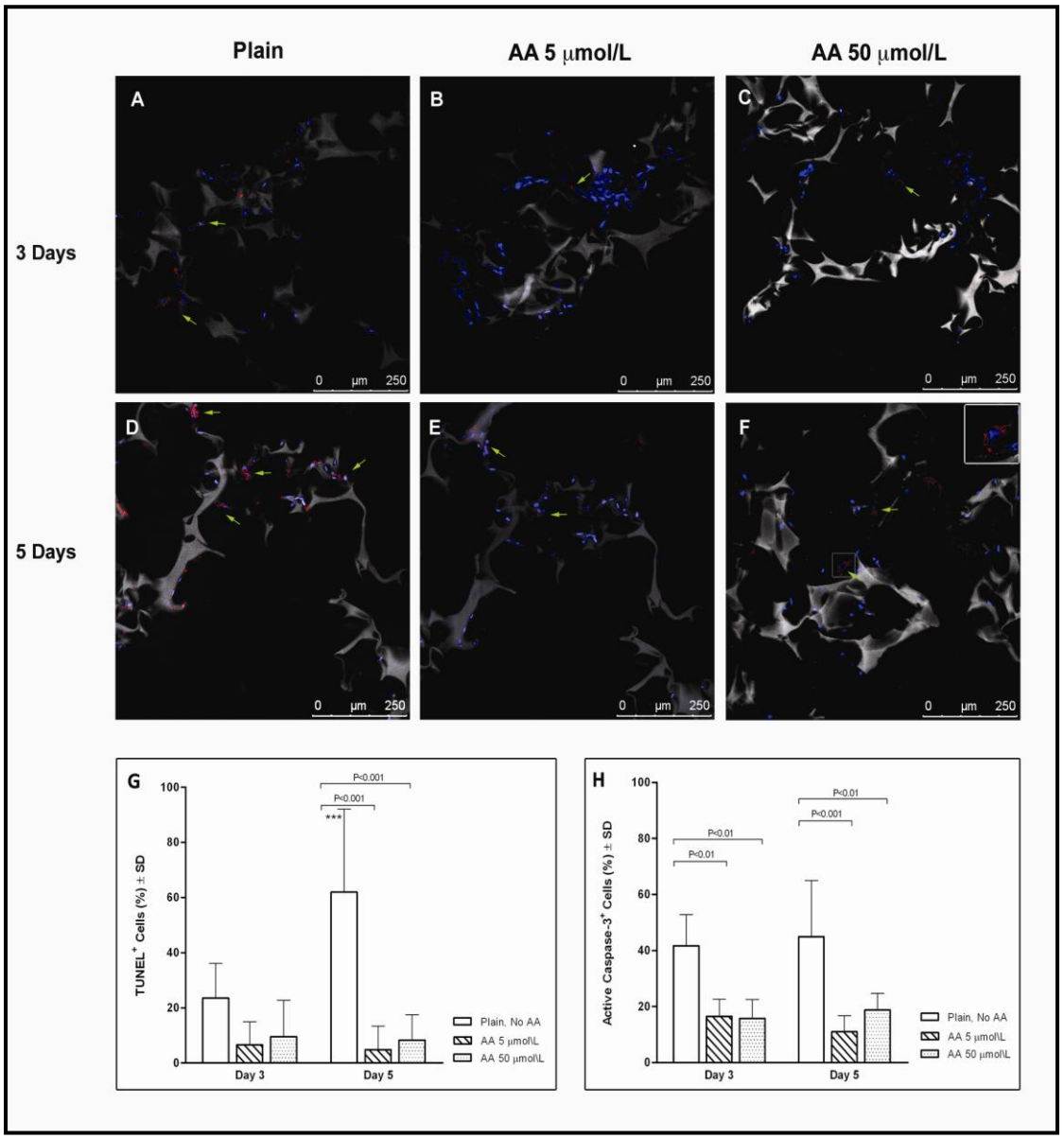

Figure 3.6 Apoptosis assessment in three-dimensional myocardial artificial grafts. Confocal micrographs of active Caspase 3 staining (Red) performed after 3 and days in culture in A, Plain MAG,; B, 5 µmol/L AA MAG and C, 50 µmol/L AA MAG. Active Caspase-3 staining after 5 days in culture in D, Plain MAG; E, 5 µmol/L AA MAG and F, 50 µmol/L AA MAG. The insert is a higher magnification showing cytoplasmic active Caspase 3 expression. G, In the plain MAG, TUNEL assay showed an increase in the percentage of TUNEL positive cells from day 3 to day 5 in culture (****P*<0.001, n=9). H, The percentage of apoptotic cells (active Caspase-3^{+}; n=5) was significantly inferior at days 3 and 5 in the 5 µmol/L AA (*P*<0.01 and *P*<0.001, respectively) and 50 µmol/L AA MAG (*P*<0.01). Nuclei were counterstained with DAPI (Blue). Scaffold autofluorescence appears in grey. Scale bars indicate 25µm. MAG, myocardial artificial grafts; AA, ascorbic acid.

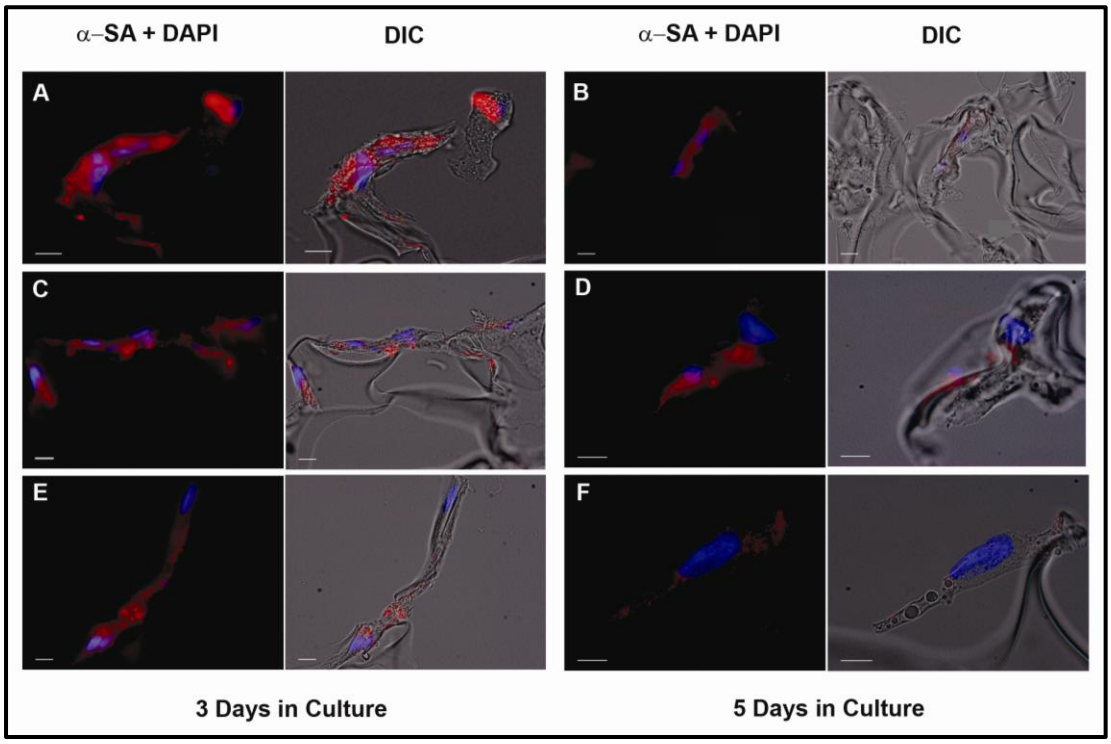

Figure 3.7 Ascorbic acid effect on H9C2 cardiomyoblasts phenotype in 3-D culture. Alpha-sarcomeric actin staining (Red) performed after 3 days in culture in A, Plain MAG; B, 5 µmol/L AA MAG and C, 50 µmol/L AA; and after 5 days in culture in D, Plain MAG; E, 5 µmol/L AA MAG and F, 50 µmol/L AA. Nuclei were counterstained with DAPI (Blue). Right side panels depict DIC images that were merged to the fluorescence micrographs to identify cell morphology and distribution in the scaffold. Scale bars indicate 10µ. α–SA, alpha-sarcomeric actin; DIC, differential interference contrast.

3.1.7 In vivo Bioluminescence Imaging

Bioluminescent signals progressively decreased from day 1 to 6 in both the plain and ascorbic acid enriched MAG (Groups A and B) (Figure 3.8 A and B). However, photon emission fell dramatically in plain MAG (Group B) from day 1 to 6 post-implantation (Figure 3.8 A). Cell photon emission by day 6 plunged by 74±0.9% of the baseline in the plain MAG, while the ascorbic acid-enriched grafts signals decreased by just 36.42±1.81% ($P<0.0001$). There was no significant difference in the mean photon emission among groups at days 1 and 3 post graft implantation. However, the ascorbic acid MAG (Group A) displayed significantly higher cell signals at day 6 (6.1x106±1.7x105 p/s vs. 1.8x106±2.8x105 p/s, $P<0.05$) (Figure 3.8 C).

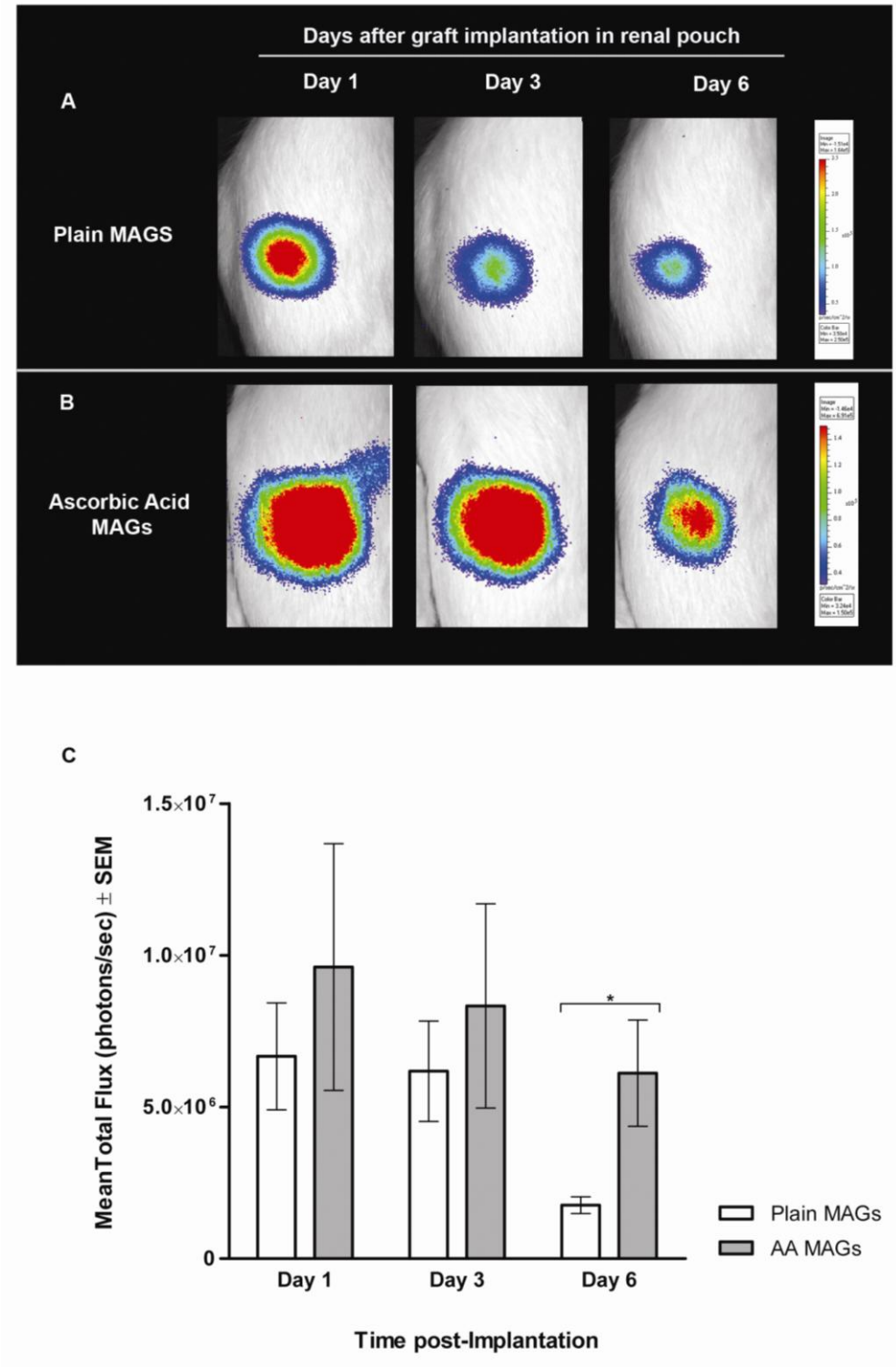

Figure 3.8 In vivo bioluminescence imaging after 1, 3 and 5 days of graft implantation in the renal pouch. (A) Plain MAG (n=9). (B) Ascorbic acid-enriched MAG (n=9). (C) The ascorbic acid-enriched MAG displayed significantly higher cell photon emission at day 6 after graft implantation (*P<0.05). MAG, myocardial artificial grafts; AA, ascorbic acid.

3.1.8 Renal Pouch Model

None of the rats died before the scheduled euthanasia. There were no visible signs of infection, inflammation, adhesions or foreign body reaction in any group after one week of myocardial artificial graft implantation in the renal pouch. Explanted grafts containing cells (Groups A and B) displayed preserved size and shape. In contrast, the negative control grafts (Groups C and D) were slightly smaller in size after one week of implantation, which could be due to scaffold's degradation. All the implanted grafts were surrounded by a thin layer of connective tissue adhered to the pre-renal fat. Numerous blood vessels were visible by the naked eye in both plain (Figure 3.9 A) and ascorbic acid- enriched MAG (Figure 3.9 C), whilst fewer vascular networks could be seen in negative control acellular grafts (Figure 3.9 B and D).

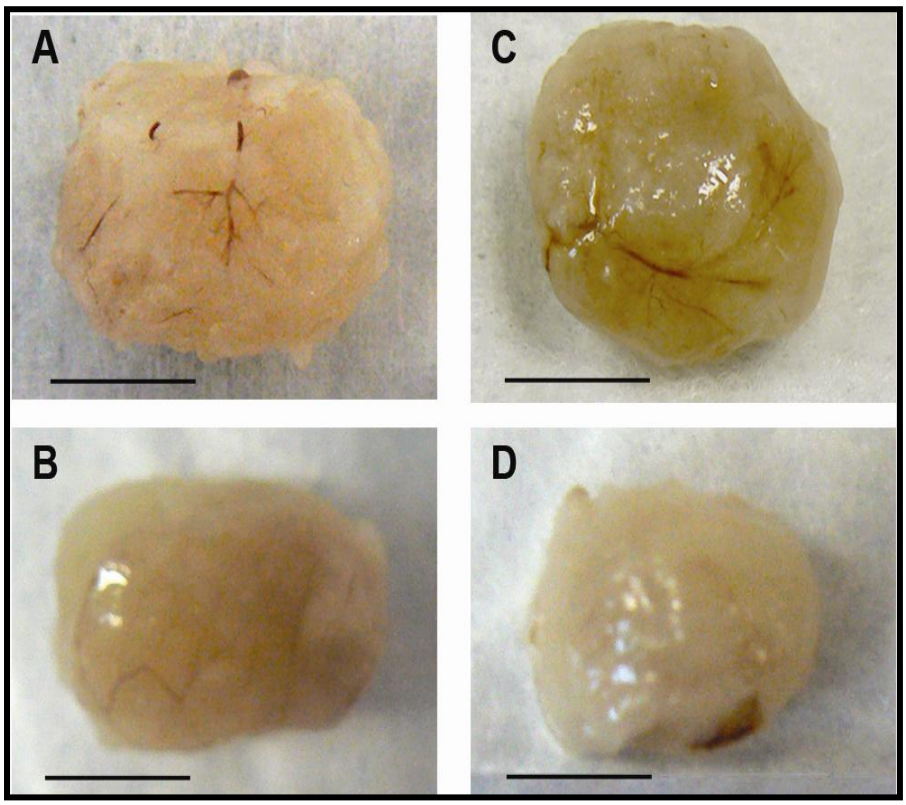

Figure 3.9 Explanted MAG from the renal pouch. Abundant blood vessels infiltrating the (A) plain and (C) ascorbic acid-enriched MAG explanted from the right renal pouch. Fewer blood vessels could be observed by the naked eye in the (B) plain negative (acellular) control and (D) ascorbic acid negative (acellular) control, explanted from the left renal pouch. Bar equals 10 □m. MAG, myocardial artificial grafts.

3.1.9 Immunohistochemistry- Assessment of GFP and RECA Expression:

Fluorescence pixel intensity analysis of the confocal micrographs revealed that the amount of GFP positive cells (donor cells) was significantly greater in the group A (ascorbic acid- enriched MAG) when compared to the plain grafts from group B (2.09±1.42 vs. 0.94 ±0.24, $P<0.01$) (Figure 3.10 E).

Abundant vascular networks infiltrating the MAG could be observed under the confocal microscope (Figure 3.10 A and B); angiogenesis was particularly abundant in the ascorbic acid group (Figure 3.10 B and D). Furthermore, blood vessels infiltration observed in group A (ascorbic acid) was not limited to the outmost regions of the graft, as vessels in close contact with the gelatin scaffold were found towards the graft's core (Figure 3.10 D). Accordingly, pixel intensity analysis showed that expression of the rat endothelial cell antibody (RECA) was significantly higher in the explanted grafts from group A (ascorbic acid) than those from group B (plain) (4.28±1.98 vs. 1.46±1.21, $P<0.05$). Fluorescence intensity quantification of $DAPI^+$ cells did not reveal any difference among groups (Figure 3.10 E).

3.1.10 Histology

Histology analysis showed a higher amount of blood vessels per hpf (400x) in the ascorbic acid-MAG (Group A) compared to plain MAG (Group B) (3.65±0.5 vs. 2.75 ±0.5, $P<0.05$) (Figure 3.11 A, B and E). These results are in agreement with the analysis of endothelial cell markers following confocal microscopy. In both groups, peripheral angiogenesis was higher. However, a few capillaries could also be detected at the graft's core. Ingrowth of vessels was also observed in the periphery of the acellular negative controls (Figure 3.11 C and D), but no capillaries were detected towards the core. There was no difference in the number of blood vessels found in the negative control groups (Figure 3.11 E).

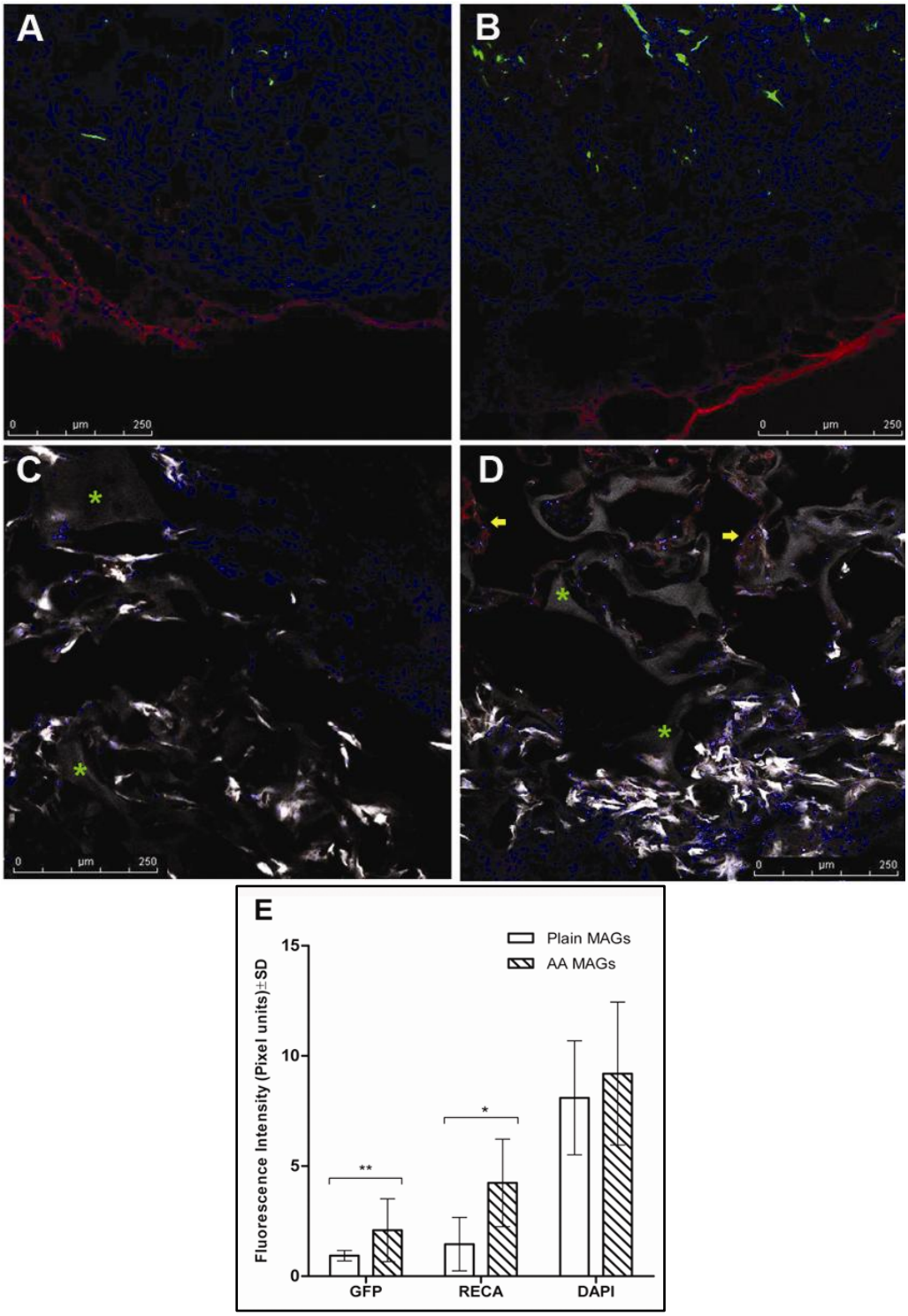

Figure 3.10 GFP and rat endothelial cell antibody (RECA) expression in explanted MAG from the renal pouch. (A, C) Plain MAG. (B, D) AA-enriched MAG. Confocal micrographs show H9C2-Fluc-GFP cells in green; RECA+ cells in red (blood vessels), and nuclei stained with DAPI in blue. Vascular networks infiltrating the grafts could be observed in both (A) plain and (B) AA-enriched MAG. The amount of GFP+ and RECA+ cells is more evident in the AA group. (C, D) Distribution of donor (GFP+) cells and blood vessels in the scaffold. GFP+ cells can be seen in white and nuclei in blue. Asterisks indicate the scaffold structure. Arrows point to blood vessels. (E) Semiquantitative fluorescence pixel intensity analysis showed that the number of GFP-positive cells was greater in the AA-enriched MAG (**P<0.01). Likewise, expression of RECA was higher in the explanted grafts from the AA group (*P<0.05). GFP, green fluorescent protein.

There was no significant difference in collagen deposition among groups. The mean collagen deposition score (% of area covered by collagen of the total cellular reaction) was mild (0-25%) for both ascorbic acid- enriched and plain MAG, as well as for negative controls (Table 3.2 and Figure 3.11 A-D). Cell infiltration was mild in all groups, eosinophils being the most abundant cell type found within the grafts. Occasional lymphocytes and neutrophils were observed in all the graft sections. Likewise, mild foreign body reaction was observed in all the groups. Macrophages and giant cell reaction were observed in all groups. Just one of the explanted grafts from the negative control (group D) displayed moderate necrosis, 26-50% collagen deposition and abundant cell infiltration by neutrophils.

Table 3.2 Histological semi-quantitative scoring of explanted myocardial artificial grafts.†

Parameter	Group A AA- MAG	Group B Plain MAG	Group C AA- control	Group D Plain control
Cellular reaction (%)	0-25	0-25 $^{\alpha}$	0-25	0-25 $^{\alpha}$
No of Eosinophils / hpf	2.3±0.9	2.0±1.0	1.5±0.0	1.5±0.0
Collagen deposition (%)	0-25	0-25	0-25	0-25

† *Cellular reaction was defined as the percentage of scaffold area covered by cells, and collagen deposition reflects the percentage of collagen covered of the total cellular reaction.* $^{\alpha}$ *Indicates minimal cellular reaction. MAG, myocardial artificial grafts; AA, ascorbic acid; hpf, high power field.*

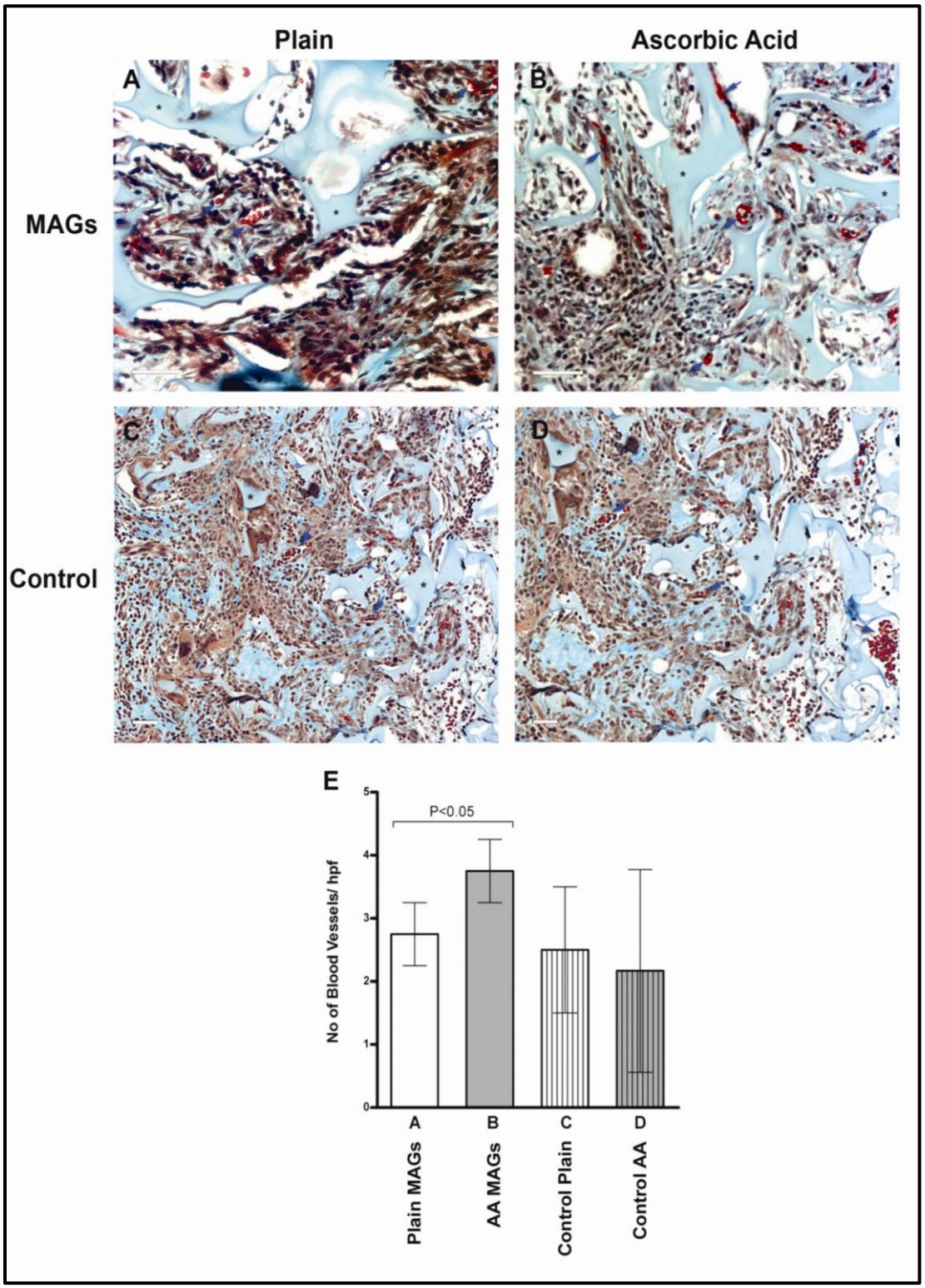

Figure 3.11 Masson's trichrome staining micrographs of explanted MAG from the renal pouch. (A) plain MAG, (B) AA-enriched MAG, (C) plain negative (acellular) control, and (E) AA negative (acellular) control. Mild collagen deposition was observed in all groups. Scaffold material is stained in blue and pointed out with asterisks, to differentiate it from extracellular matrix deposition. Arrows indicate blood vessels within the grafts. (D) Histological analysis of the explanted MAG showed fewer amounts of blood vessels per high power field (400x) in the plain MAG when compared with the AA-enriched grafts (P<0.05). Scale bars indicate 50 µm.

3.2 Results Experimental Approach to Hypothesis II

3.2.1 Animal Model

A total of 30 rats were included in this study. Of 22 rats that underwent LAD ligation, 5 died in the first 24 hr after LAD ligation, two from the MAG group and three from the MI group (22% postoperative mortality after MI). One of 8 healthy sham rats died after surgery. There were no surgical complications or mortality during laparatomy and MAG implantation in the renal pouch. Two animals had to be excluded from the study 2 weeks after MAG epicardial implantation due to extensive skin necrosis at the Cyclosporine-A injection site. One rat died after 3 weeks of LAD ligation (MI group) and at 4 weeks after LV injury, two rats died during anesthesia for echocardiography (one from the MI group and one from the MAG group). Overall, 19 rats completed the study (6 in the MAG group, 6 in the MI group and 7 in the healthy (sham operated) group.

3.2.2 Donor Cell Survival

In vivo bioluminescence imaging (BLI) showed a significant decrease in grafted cell photon emission from day 1 to day 7 post- epicardial patch implantation by 84% of baseline ($1.43x10^7 \pm 3.1x10^6$ p/s, and $2.29\ x10^6 \pm 5.87x10^5$ p/s, $P<0.0001$). No cell signals were detected after two weeks of MAG implantation (Figure 3.12).

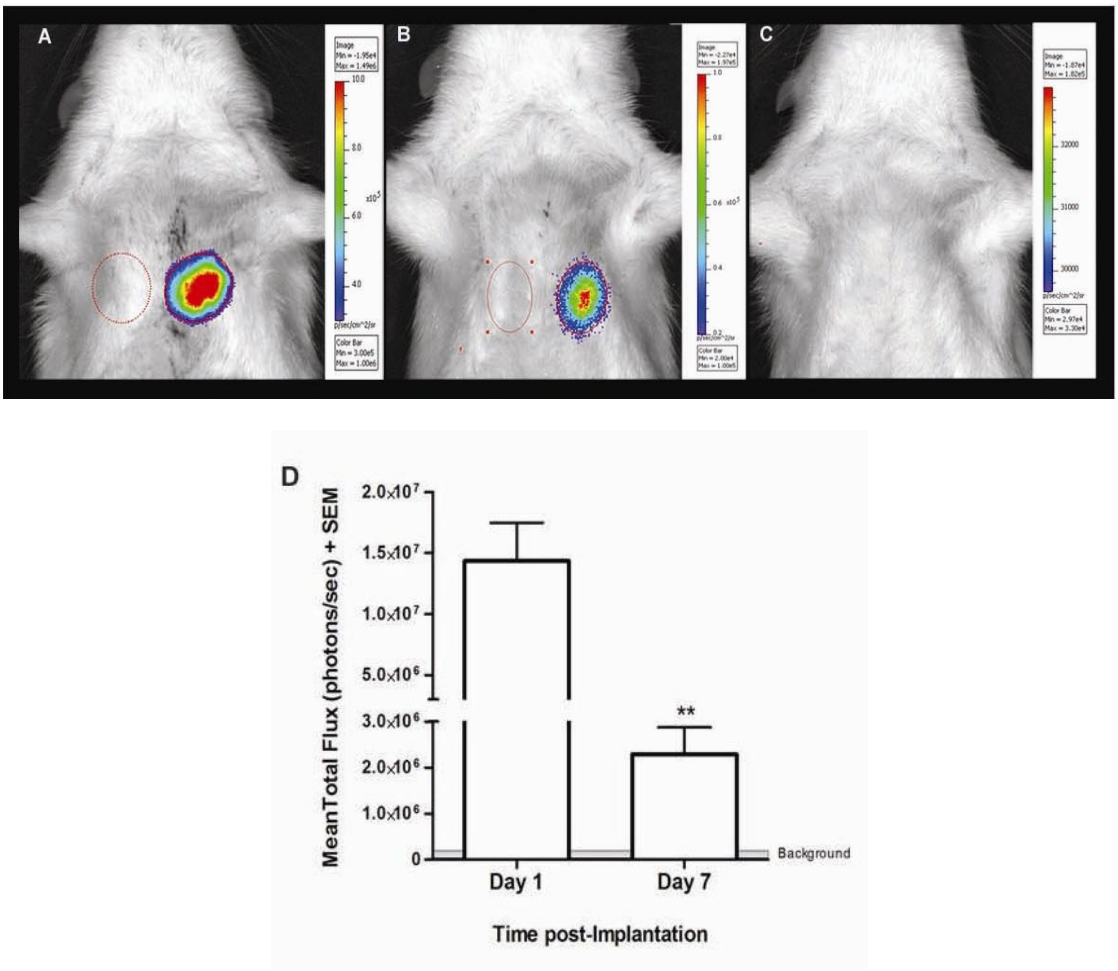

Figure 3.12 In vivo donor cell survival in ascorbic acid-enriched pre-vascularized MAG after epicardial implantation on the ischemic heart. In vivo bioluminescence imaging after (A) 3, (B) 7 and (C) 14 days of graft implantation into the ischemic heart of MAG-treated rats. (D) There was a significant reduction in cell photon emission after the first week of graft implantation (**P<0.0001). MAG, myocardial artificial grafts.

3.2.3 Left Ventricular Function and Remodeling Assessment by Echocardiography

Echocardiography four weeks after surgery revealed that MAG treatment attenuated LV remodeling (LV end-systolic volume 0.31 ± 0.13 vs. 0.81 ± 0.01 ml, P<0.05; LV end-diastolic volume 0.79 ± 0.33 vs. 1.83 ± 0.26 ml, P<0.076), and preserved LV wall thickness (0.21 ± 0.03 vs. 0.09 ± 0.005 cm, P<0.05) compared to MI. There were no significant differences in LV remodeling and function parameters between healthy and MAG rats. The percent change in LV cross-sectional area between diastole and

systole (FAC) was 33.50 ± 2.02% in MI, 42.80 ± 5.36% in MAG-treated, and 57.0 ± 9.29% in healthy animals (P<0.05, MI vs. healthy). Furthermore, LV ejection fraction (EF) was 54.2 ±7.3 % in MI, 62.8±8.8% in MAG-treated, and 83.0 ± 4.6% in healthy animals (P<0.05, MI vs. healthy) (Table 3.3 and Figure 3.13).

Table 3.3 Echocardiographic assessment of myocardial remodeling and function in healthy sham operated, myocardial infarction (MI), and myocardial artificial graft (MAG) rats. ‡

	Healthy n=4	**MI n=5**	**MAG n=5**
IVSd (cm)	0.18 ± 0.01	0.09 ± 0.01 *a, b	0.21 ± 0.03
LVIDd (cm)	0.73 ± 0.01	1.05 ± 0.05 *a, b	0.75 ± 0.10
LVPWd (cm)	0.17± 0.01	0.17 ± 0.02	0.18 ± 0.02
IVSs (cm)	0.30 ±0.01	0.14 ± 0.05 a	0.28 ± 0.04
LVIDs (cm)	0.40 ± 0.05	0.81 ± 0.01 *a, b	0.52 ± 0.09
LVPWs (cm)	0.31 ± 0.04	0.26 ± 0.02	0.28 ± 0.05
FS (%)	45.63 ± 5.38	23.14 ± 4.14 a	30.87 ± 7.30
LVEDV (ml)	0.60 ± 0.03	1.83 ± 0.26 *a	0.79 ± 0.33
LVESV (ml)	0.11 ± 0.03	0.81 ± 0.01 **a, b	0.31 ± 0.13
LVAd (cm^2)	4.30 ± 0.10	8.60 ± 0.28 *a	6.48 ± 3.83
LVAs (cm^2)	2.15 ± 0.35	5.75 ± 0.64 a	3.84 ± 2.39
FAC (%)	57.0 ± 9.29	33.50 ± 2.02 a	42.80 ± 5.36
EF (%)	83.0 ± 4.6	54.2 ±7.3 a	62.8±8.8

‡*IVSd, interventricular septal thickness-diastole, LVIDd, left ventricular internal dimension-diastole; LVPWd, left ventricular posterior wall dimension-diastole; IVSs, interventricular septal thickness-systole; LVIDs, left ventricular internal dimension-systole; LVPWs, left ventricular posterior wall dimension-systole, FS, fractional shortening; LVEDV, left ventricular end-diastolic volume; LVESV, left ventricular end-systolic volume; LVAd, left ventricular area-diastole; LVAs, left ventricular area-systole; FAC,fractional area change; EF, ejection fraction. Statistical significance is indicated as follows: a P<0.05 vs. healthy;*a P<0.01 vs. healthy; **a P<0.001 vs. healthy; b P<0.05 vs. MAG; *b P<0.01 vs. MAG.*

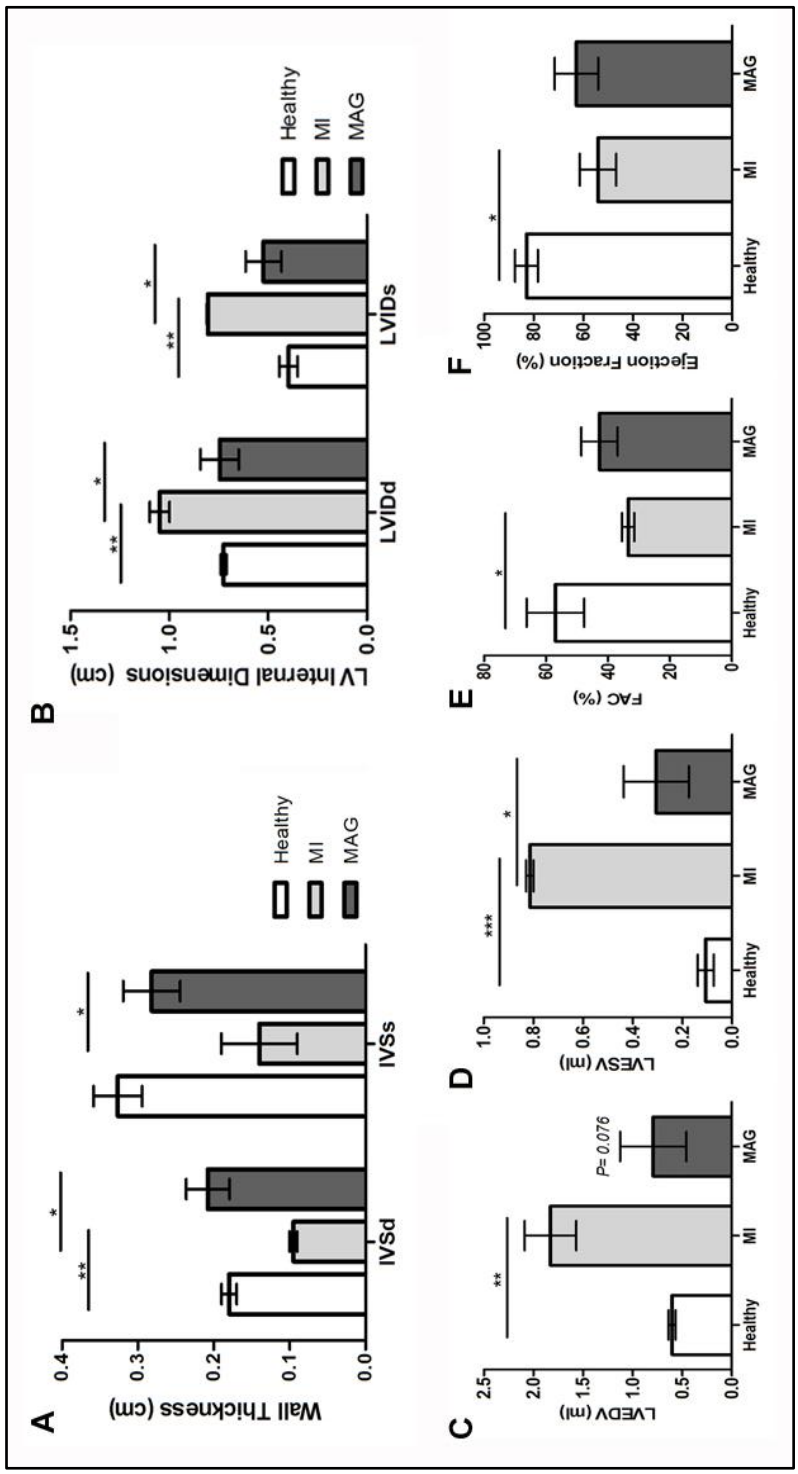

Figure 3.13 Effect of myocardial artificial graft (MAG) treatment on left ventricular remodeling and function. Echocardiographic evaluation four weeks after left anterior descending coronary artery ligation in MI (myocardial infarction) and MAG-treated rats, and after thoracotomy in sham/healthy rats . (A) Left ventricular (LV) wall thickness/ interventricular septum dimensions in diastole and systole (IVDd and IVDs), (B) LV internal dimensions in diastole and systole (LVIDd and LVIDs), (C) LV end-diastolic volume (LVEDV), (D) LV end-systolic volume (LVESV), (E) LV fractional area change, and (F) LV ejection fraction. Statistical significance is indicated as: * P<0.05; **P<0.01; ***P<0.001.

3.2.4 Hemodynamics

We performed invasive hemodynamic analyses four weeks after LAD ligation (MAG and MI groups) or thoracotomy (healthy group) (Table 3.4). Infarcted (MI) rats had decreased contractility and heart rate (*P*<0.0001 vs. both healthy and MAG). LV end-diastolic pressure (LVEDP) was increased both in MI and MAG groups (6.3 ± 0.3 and 5.1 ± 0.2 mmHg, respectively) compared to healthy animals (3.1 ± 0.1 mmHg; *P*<0.0001). However, this was lower in MAG-treated rats compared to MI (*P*<0.01). MAG rats had higher cardiac output than MI animals (51.59 ± 6.5 vs. 25.06 ± 4.24 ml·min^{-1}, *P*<0.01), and comparable to healthy animals (47.08 ± 1.9 ml·min^{-1}, P=0.46).

Table 3.4 Hemodynamics assessment of myocardial function in healthy sham operated, myocardial infarction (MI), and myocardial artificial graft (MAG) groups. §

	Healthy (n=7)	**MI (n=6)**	**MAG (n=6)**
Body Weight (gr)	419.7 ± 15.9	421.5 ± 8.6	430.2 ± 10.6
Heart Rate (bpm)	188.0 ± 7.5	147.7 ± 11.1 **a, **b	193.6 ± 12.5
Maximum LV Pressure (mmHg)	75.6 ± 4.3	83.7 ± 7.3	81.8 ± .7
LVEDP (mmHg)	3.1 ± 0.1	6.3 ± 0.3 ***a, *b	5.1 ± 0.2 ***a
Mean LV Pressure	21.2 ± 1.3	19.6 ± 1.1	23.58 ± 2.0
Cycle Duration (s)	0.33 ± 0.01	0.43 ± 0.04 a, b	0.32 ± 0.02
Maximum positive dP/dt (mmHg/s)	3,484.1 ± 344.5	3,613.1 ± 423.2	3,703.7 ± 267.4
Contractility Index (1/s)	93.6 ± 3.0	78.9 ± 3.0 a	89.9 ± 6.5
Maximum negative dP/dt (mmHg/s)	-2,573.8 ± 146.1	-2,309.6 ± 263.5 a, b	-2,732.2 ± 282.3
IRP (mmHg/s)	-1,599.7 ± 163.0	-1,598.8± 194.9	-1,658.7 ± 83.9
Tau (s)	0.02 ± 0.002	0.03 ± 0.01	0.02 ± 0.002
Stroke Volume (ml·beat^{-1})	0.25 ± 0.01	0.17 ± 0.02 *a, b	0.26 ± 0.02
Cardiac output (ml·min^{-1})	47.08 ± 1.9	25.06 ± 4.24 **a, **b	51.59 ± 6.49

*§ bpm, beats per minute; s, seconds; LVEDP, left ventricular end-diastolic pressure; IRP, isovolumetric relaxation period. Statistical significance is indicated as follows: a P<0.05 vs. healthy; *a P<0.01 vs. healthy; **a P<0.001 vs. healthy; ***a P<0.0001 vs. healthy; b P<0.05 vs. MAG;*b P<0.01 vs. MAG; **b P<0.001 vs. MAG.*

3.2.5 MAG Prevascularization in the Renal Pouch

After 3 days in the renal pouch, grafts preserved their size and shape and were covered by a thin layer of connective tissue (Figure 3.14 A). H&E staining showed donor H9C2 cardiomyoblasts forming syncytia, as well as neo-blood vessels within the graft (Figure 3.14 B). Effective MAG neo-vascularization after 3 days in the renal pouch was evidenced, as host's DiI^{+} blood vessels were found throughout the graft (Figure 3.14 C and D).

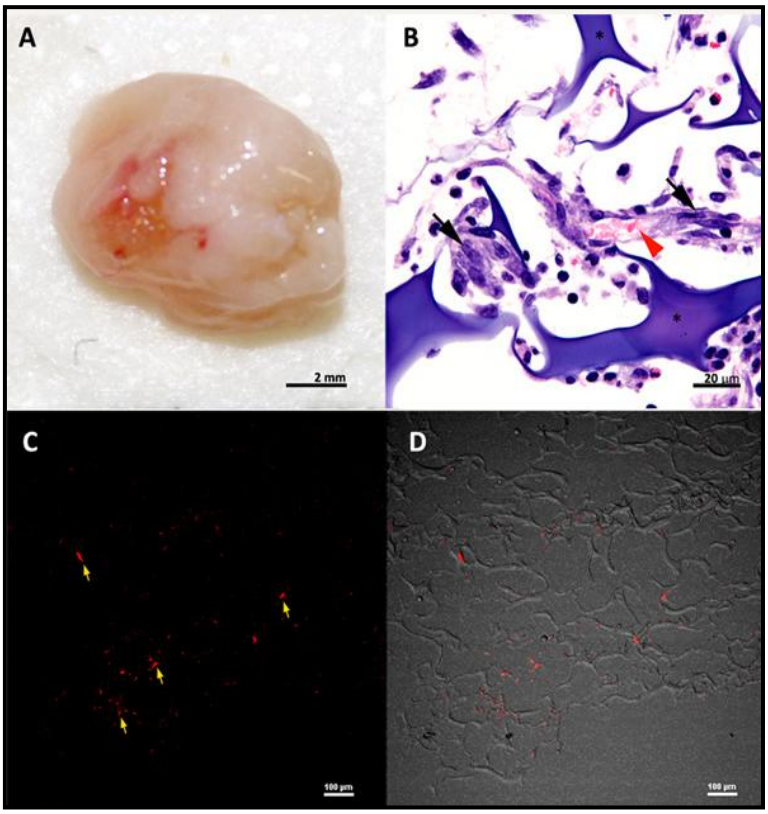

Figure 3.14 Prevascularized Myocardial Artificial Graft (MAG). (A) Explanted MAG after 3 days in the renal pouch. (B) H&E staining (200x) shows donor H9C2 cells forming syncytia (black arrows), and neo-blood vessels containing red blood cells (red arrowhead) within the graft. (C) Confocal, and (D) merged confocal and bright field images (100x) of explanted MAG after direct labeling of the blood vessels by cardiac perfusion with 1,1'-dioctadecyl-3,3,3',3'-tetramethylindocarbocyanine perchlorate (DiI). Yellow arrows indicate DiI+ blood vessels (in red) infiltrating the macroporous gelatin graft.

3.2.6 Left Ventricular Morphology and Histology

Consistent with the echocardiographic evaluation, MAG-treated hearts displayed more preserved LV dimensions in comparison to MI hearts 1 month after LAD ligation (Figure 3.15 A-C). Alignment of the implanted graft was observed along the epicardium, which may have contributed to the preservation of LV wall thickness (Figure 3.15 C). The geometrical improvements seen in MAG-treated rats were associated with a 25% reduction in fibrosis in the infarct and peri-infarct border zone compared with MI control hearts (Figure 3.15 D-F and Table 3.5).

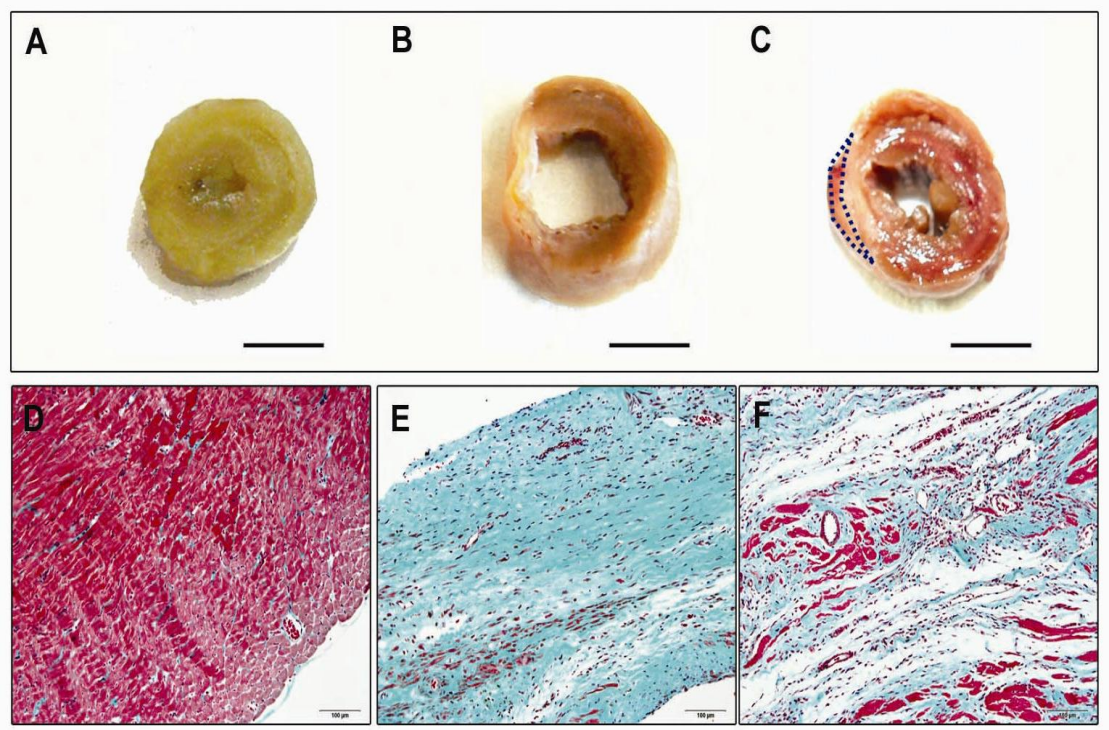

Figure 3.15 (A-C) Morphology of explanted hearts. Mid-ventricular cross-section of (A) healthy (B) myocardial infarction (MI), and (C) myocardial artificial graft (MAG)-treated hearts. Engrafted MAG, indicated by blue dotted line, remained firmly attached and aligned to the left ventricular scar area. (D-F) Masson's thrichrome staining micrographs of explanted hearts in (D) healthy, (E) MI and (F) MAG-treated animals. Reduced collagen deposition, as well as islets with cardiomyocytes were observed in the scar area of MAG-treated hearts. Scale bar indicates 5 mm in (A-C), and 20 μm in (D-F).

Table 3.5 Histological semi-quantitative fibrosis scoring of explanted hearts from healthy sham operated, myocardial infarction (MI), and myocardial artificial graft (MAG) rats. [**]

	Healthy	**MI**	**MAG**
	n=7	**n=6**	**n=6**
LV fibrosis (%)	0	>50%	26-50
LV infarct border zone fibrosis (%)	NA	0-25%	0

There was significant neutrophil recruitment to the graft area in MAG-treated rats relative to the LV scar area in the same animals and in MI rats, as well as to sham operation/healthy rats ($P< 0.001$). Similarly, the amount of mast cells observed in the graft area was greater compared to the infarcted LV of the same MAG-treated animals ($P< 0.05$), and to the LV of infarcted (MI) and healthy rats ($P< 0.001$). On the other hand, lymphocyte concentration in the LV infarcted area was significantly decreased in the MAG-treated group compared to MI ($P< 0.001$). Plasma cells were not observed in any experimental group (Table 3.6).

H&E staining revealed that the implanted patch engrafted to the scarred myocardium of treated hearts (Figure 3.16 A-C). Newly formed vessels were found both within the implanted graft and in the LV (scar area) of the MAG group (Figure 3.16 C). The LV wall in MAG-treated hearts was thicker compared to MI hearts due in part to the presence of the epicardial patch.

[**] *LV, left ventriclular; NA, not applicable*

Abundant RECA^{+} blood vessel networks infiltrating the scarred myocardium of MAG-treated hearts were also observed under confocal microscopy (Figure 3.17). Angiogenesis assessment using an endothelial marker (von Willebrand factor) (Figure 3.18 A-C), revealed a 7-fold increase in blood vessel density in the scar area of MAG-treated compared to MI hearts (15.28 ± 1.1 vs. 2.06 ± 0.3 blood vessels/hpf, *P*<0.0001, Figure 3.18 D).

Table 3.6 Left ventricular (LV) inflammatory cell infiltration[††]

	Healthy n=7	**MI n=6**	**MAG n=6**	
Area Assessed / hpf	**LV**	**LV Scar**	**LV Scar**	**Graft**
Neutrophils	0	1.28±0.38	0	4.64±0.75 ***a,b,c
Lymphocytes	0	6.61±1.84 ***b; **d	1.79±0.18	3.64±0.7 ***a
Macrophages	0	0	1.29±0.75	1.57±0.78
Mast Cells	0	1.67±0.25	0	4.07±0.90 ***a,c; *b
Plasma Cells	0	0	0	0

[††] *Evaluation of inflammatory cell infiltration in H&E stained sections reflects the number of cells counted in the assessed area/high power field (hpf). Significance is indicated as *P<0.05 and ***P<0.001, vs. (a) LV of healthy animals; (b) LV infarct (scar) area in myocardial infarction (MI) group; (c) LV scar area in myocardial artificial graft (MAG)-treated rats; and (d) graft area in the MAG-treated group.*

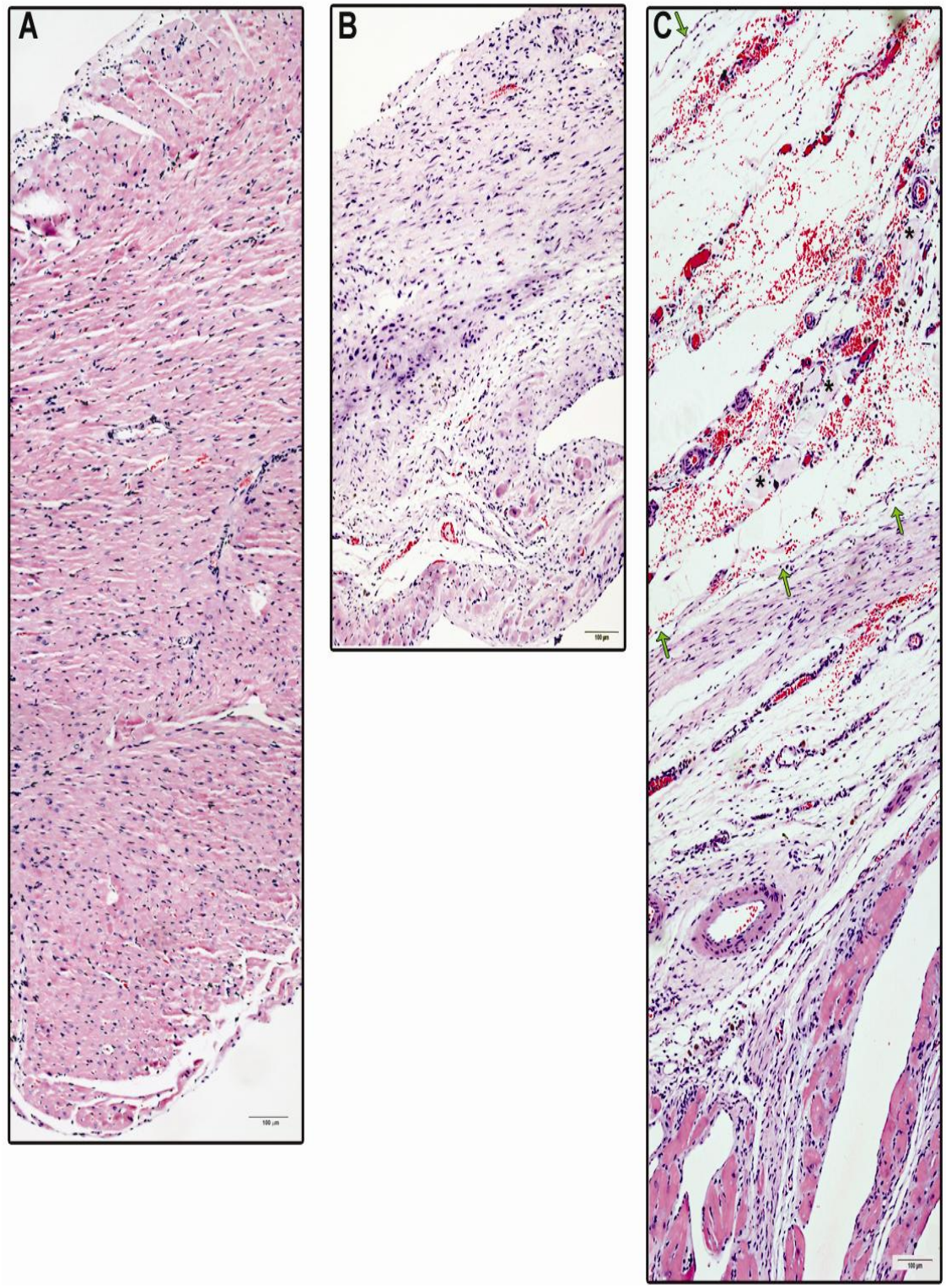

Figure 3.16 Reconstruction of the left ventricular wall using H&E staining micrographs (200x) in (A) healthy sham operated, (B) myocardial infarction (MI); and (C) myocardial artificial graft (MAG)-treated explanted hearts. The implanted patch engrafted to the epicardium and newly formed blood vessels were found within the implanted graft and in the left ventricle (scar area) of MAG-treated rats. Green arrows are delimiting the epicardial graft, and remnants of scaffold material are pointed out by asterisks in (C). Scale bar indicates 100 μm.

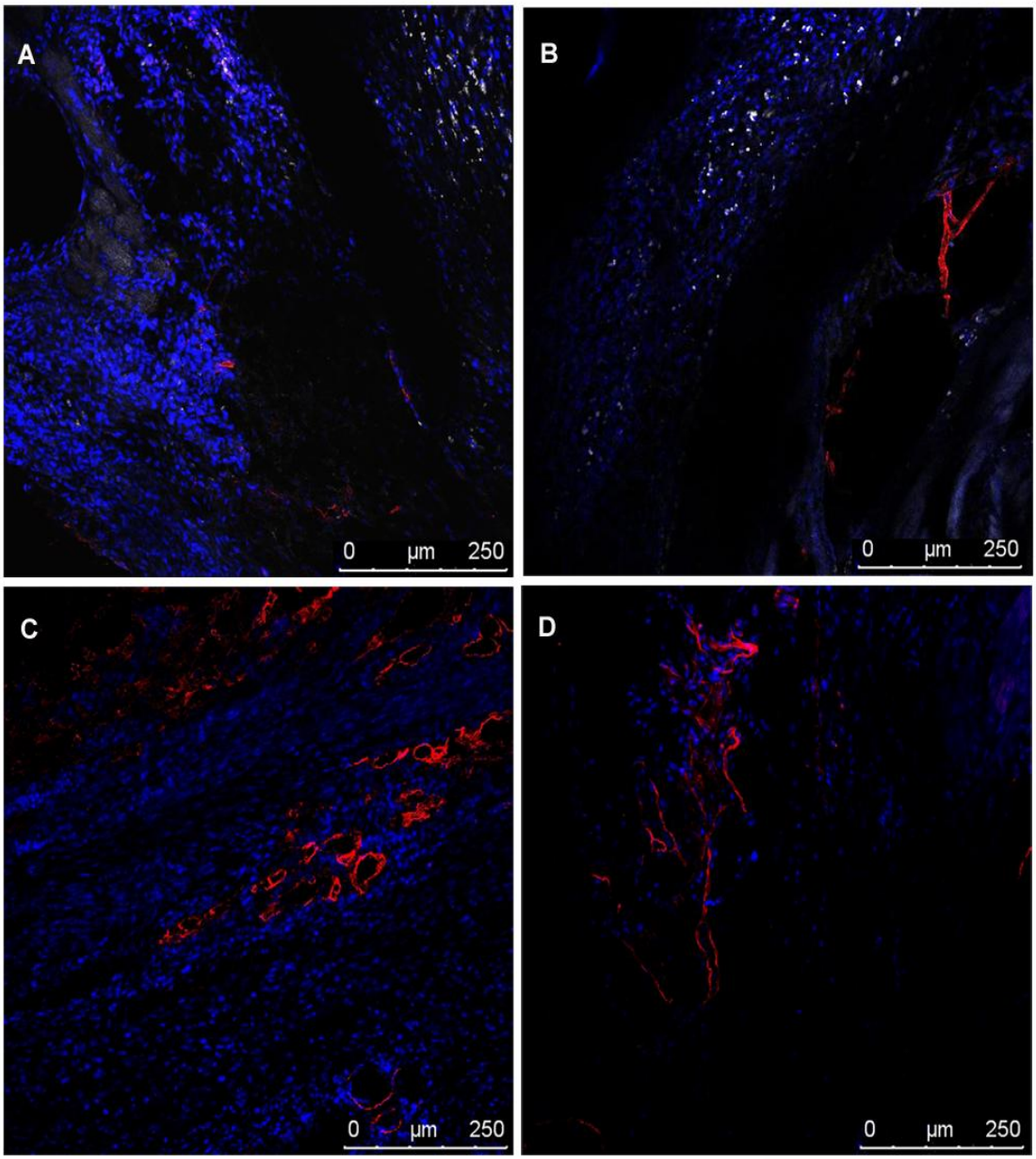

Figure 3.17 Left ventricular endothelial cell antibody (RECA) expression. Confocal micrographs of (A-B) infarcted, and (C-D) MAG (myocardial artificial graft)-treated hearts. $RECA^{+}$ cells are labeled in red (blood vessels) and DAPI-labeled nuclei appear in blue. Vascular networks infiltrating the scarred myocardium could be observed in the MAG-treated animals, 4 weeks after epicardial patch implantation. GFP^{+} donor cells were not observed in any of the treated hearts. Scale bar indicates 250 μm.

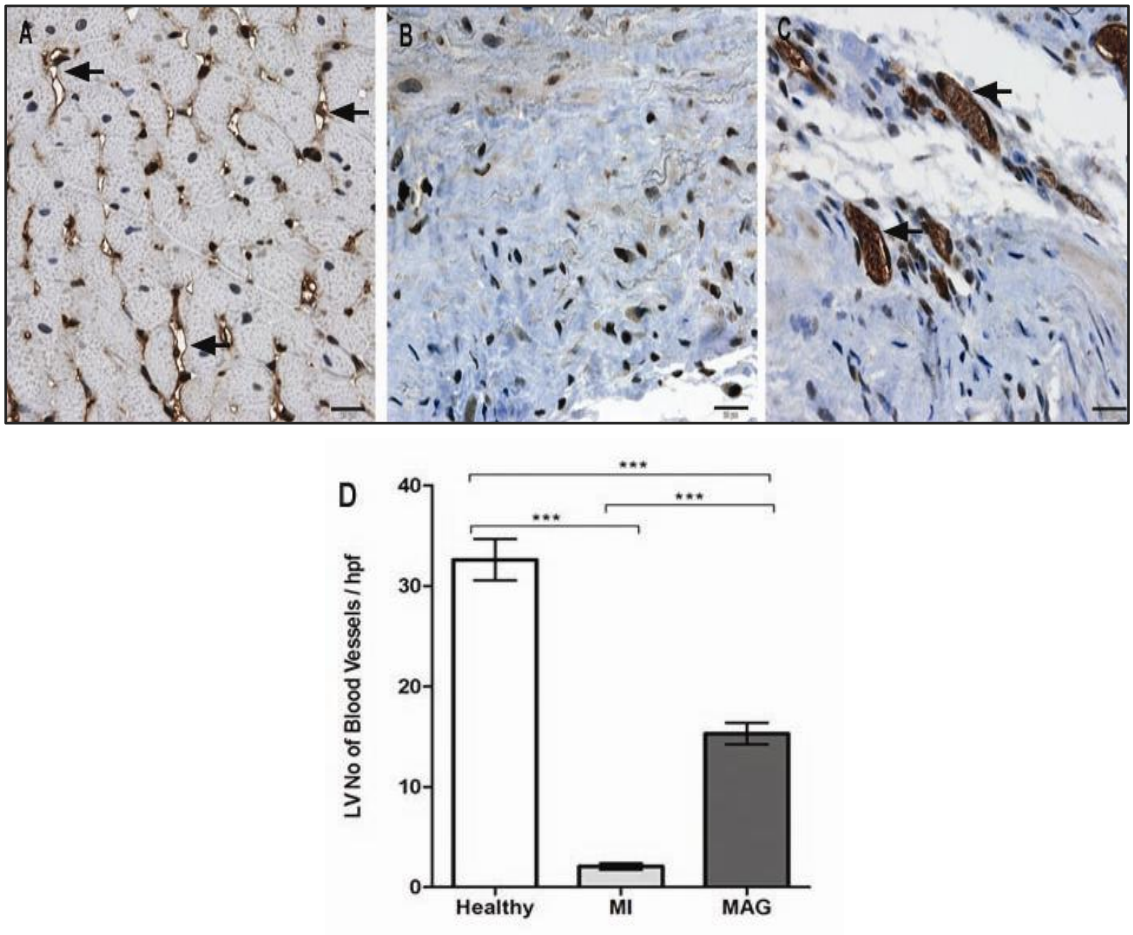

Figure 3.18 Left ventricular blood vessels density. von Willebrand factor staining of heart paraffin sections (in dark brown) from (A) healthy (n=7), (B) myocardial infarction (MI, n=6) and (C) myocardial artificial graft (MAG)-treated rats (n=6). (D) There was a 7-fold increase of blood vessels per high power field (x400) in the left ventricle of MAG-treated hearts compared to MI hearts. Black arrows indicate blood vessels. (***P<0.001). Scale bar indicates 20 µm.

4 Discussion

4.1 Ascorbic Acid Improves Embryonic Cardiomyoblast Cell Survival & Promotes Vascularization in Potential Myocardial Grafts in vivo

The main findings in the present study are fourfold: first, ascorbic acid enhances thick bioengineered myocardial tissue survival in vitro through inhibition of cell apoptosis; second, the graft's viability and angiogenic potential in vivo are superior with ascorbic acid enrichment; third, we introduced an in vivo model for myocardial graft pre-vascularization that provides the graft with blood vessels of autologous origin before implantation in the targeted organ; and finally, the post-ischemic angiogenic therapy explored in this study using ascorbic acid-enriched- pre-vascularized- myocardial artificial grafts attenuated left ventricular remodeling and preserved left ventricular function in a rat model of myocardial infarction.

4.1.1 Effect of Ascorbic Acid on H9C2 Cell Survival within Myocardial Artificial Grafts in vitro

Stem cell- and bioartificial tissue- based therapies for the heart remain supplementary measures. The unique architecture and limited regenerative potential of the heart muscle restrict the capacity of random injections and implants to restore myocardium efficiently and permanently. The progress of such methods from random and supplementary to first-line therapeutic options will largely depend upon improvement on various levels: first, therapies have to be less traumatic and, second, the effect has to be stronger and more durable by enhancing graft viability and functionality in vivo. It is critical to sustain donor cell survival within bioengineered myocardial grafts through in vitro establishment of vascular networks for successful cardiac repair. Cell death constitutes a major limitation in cell and tissue implantation

in the frame of restorative therapies. Some reports indicate that more than 70% of cells die during the first two days after injection into the myocardium [Muller-Ehmsen, 2002], whilst others point out a cell loss of ~ 55% just 10 minutes following implantation into the heart [Suzuki, 2004]. Furthermore, there is evidence that, in spite of capillary formation in vivo, donor cell survival after myocardial 3-D graft implantation is still at risk [Leor, 2000].

We improved graft viability using ascorbic acid, a biocompatible, FDA approved and inexpensive compound that could be beneficial for the tissue engineering and the cell therapy field in general. The addition of ascorbic acid to the graft constitutes an uncomplicated method to counteract fulminant events which occur during acute ischemia and remodeling within the area of myocardial lesion. Such events are cytokine and radical oxygen species liberation, accumulation of purine derivates (danger signals), inflammation and apoptosis. Ascorbic acid is a ubiquitous and essential substance with practically no side-effects even in high doses, and can easily be integrated in a regenerative therapy protocol. Ascorbic acid participates in a variety of physiological functions in living organisms. In humans, its deficiency causes defective healing and disturbed blood vessel formation due to impaired collagen deposition [Hodges, 1971, Telang, 2007]. Besides its role in angiogenesis, ascorbic acid reduces hypoxia-induced apoptosis in vitro [Vassilopoulos, 2005, Vissers, 2007]. Accordingly, we hypothesized that ascorbic acid could be used to reduce cell death in myocardial grafts both in vitro and in vivo.

We used bioluminescence imaging to assess H9C2-luc cell survival within thick three-dimensional myocardial artificial grafts (MAG) in vitro. The high sensitivity of BLI to monitor viable cells [Chen, 2009, Jenkins, 2003] was effectively demonstrated in our in vitro model, as we found a robust correlation between luciferase activity and histological cell counts. We did not find significant difference in cell photon emission among groups after one day in culture, suggesting homogeneous delivery of cells

within the grafts. However, an increase in cell photon emission was observed within 5 days in culture, indicating that cell survival and proliferation were enhanced [Cao, 2006] when 3-D myocardial artificial tissues are supplemented with ascorbic acid.

4.1.2 Effect of Ascorbic Acid on Cell Apoptosis within Myocardial Artificial Grafts in vitro

Our data suggest that ascorbic acid enhance cell viability within bioengineered tissues in vitro in spite of the harsh conditions in culture (i.e. static 3-D culture, hypoxia and limited growth medium volume). Apoptosis is an active process associated with both the acute and chronic phases of myocardial infarction in response to oxidative insults [Kang, 2003]. The role of hypoxia on apoptosis via mitochondrial pathway activation of downstream effector caspases has already been demonstrated [McClintock, 2002]. It has been shown that in hypoxic conditions, hypoxia inhibitor alpha (HIF-1a) promotes apoptosis in H9C2 cells and cardiomyocytes [Graham, 2004, Malhotra, 2008, Vassilopoulos, 2005]. There is also evidence that depletion of ascorbic acid interrupts HIF-1a proteosomal degradation, leading to increased expression of the latter [Telang, 2007].

Our in vitro experiments showed that graft viability improved via reduction of cell apoptosis, particularly when medium is supplemented with both 5 μmol\L and 50 μmol\L ascorbic acid. Furthermore, the amount of cells within the ascorbic-acid grafts is preserved over time in static culture conditions, whereas it significantly decreases in the plain MAG. These data correlate with our in vitro BLI results. Thus, our findings suggest that ascorbic acid has a protective effect on donor cells when cultured in thick three-dimensional bioartificial constructs. The precise mechanism of such effect was not explored in this study. However, the enhancement in cell viability observed in the antioxidant-supplemented groups could be attributed to ascorbic

acid-driven ROS scavenging that preserves the integrity of the mitochondria, and stabilization of the key regulator of hypoxia (HIF-1α) [Malhotra, 2008, Telang, 2007, Vassilopoulos, 2005]. We do not have direct proof that ascorbic acid was in its active form during our study. However, previous studies have demonstrated that the oxidized form of ascorbic acid -dehydroascorbic acid, (DHAA)- is neuroprotective in ischemia models [Huang, 2001, Kim, 2008], and it also prevents apoptosis and oxidative damage in macrophages [Asmis, 1998], lymphoid, myeloid and mesothelial cells [Gogou, 2007], among others [Martino, 2009]. DHAA is transported by the glucose transporters Glut1 into the mitochondria, and not the reduced form (ascorbic acid) [Kc, 2005]. Subsequently, DHAA is reduced back to ascorbic acid by protein disulfide isomerases. Thus, we assume that even if ascorbic acid was oxidized during our experiments, there was a protective effect that could have been initiated by dehydroascorbic acid, which is ultimately reduced back to ascorbate in the mitochondria.

Our preliminary in vitro titration studies suggested that any dosage equal or above 100µmol/L AA have a cytotoxic effect on cardiomyoblasts. In vivo, it has been reported that ascorbic acid induces apoptosis of myeloid and lymphoid cells at concentrations above serum level (50µmol/L) [Puskas, 2000]. The ascorbic acid dosages utilized in our in vitro studies have also been previously reported as safe physiological dosage in other cell types [Kc, 2005, Vassilopoulos, 2005]. Hence, we chose the lowest possible physiological dose (5 µmol/L) for our in vivo studies according to this rationale, and due to the observation that after a 10 fold increase of ascorbic acid dose there were no differences in cell survival in vitro.

4.1.3 Ascorbic acid effect on H9C2 Cells Phenotype within Myocardial Artificial Grafts in vitro

Besides cytoprotection, ascorbic acid seems to have an effect on cell differentiation. It has been shown that 100 µmol/L AA enhances differentiation of embryonic stem cell into cardiomyocytes in vitro [Takahashi, 2003], as well as ex-vivo differentiation of adult bone marrow stem cells into cardiomyocytes-like cells [Shim, 2004]. In our study, immunohistochemical assessment of MAG after 3 and 5 days in culture revealed that ascorbic acid induced morphological myogenic characteristics including elongation and cell fusion [Leong, 2007]. Expression of α–sarcomeric actin was observed among all groups at day 3, yet more organized 'z-line like' patterns were observed in the ascorbic acid-enriched grafts both at days 3 and 5 in culture. These results suggest that ascorbic acid may have an effect on H9C2 cardiomyoblasts differentiation. However, this interesting observation should be further addressed in future studies.

4.1.4 Renal Pouch model and effect of ascorbic acid on myocardial artificial grafts in vivo

To evaluate the ascorbic acid effect on a bioartificial graft in vivo we developed a simple and reproducible renal pouch model. In order to assess donor H9C2-Luc-GFP cell survival within the graft, we performed noninvasive imaging at days 1, 3 and 6 post-implantation with a bioluminescence charge-coupled device (CCD) camera. We observed that one week after graft implantation in a renal pouch for in vivo pre-vascularization, H9C2 cardiomyoblast survival decreases substantially. The latter was reflected by reduction of cell photon emission by nearly 75% of baseline in Group B (plain MAG). This observation is consistent with previously reported data from studies where bioluminescence imaging was used to assess myocardial graft

survival in vivo in a heterotopic model of myocardial restoration in immunosuppressed rats [Kutschka, 2006a]. The authors have shown that H9C2 cardiomyoblasts injected in thin (3x3x1 mm) gelfoam grafts undergo massive cell death within 5 days after implantation into the ischemic myocardium. Early cardiomyoblast survival within the implanted grafts could only be improved by addition of collagen and growth factors [Kutschka, 2006a] or by cell transduction with the anti-apoptotic hBcl-2 gene [Kutschka, 2006b]. In addition, premature H9C2 cell death has been also documented after injection in healthy myocardium [Wu, 2003]. Here, we observed that by day 6 post-implantation cell survival was significantly enhanced within the implanted myocardial artificial tissues via ascorbic acid enrichment (Group A). This indicates donor H9C2-GFP-Fluc cell survival and proliferation in the host in the ascorbic acid-enriched MAG during the first days post graft implantation. Yet, confirmation of a proliferative effect of ascorbic acid on H9C2 cells needs to be further addressed in future studies. Our results are of interest for cell transplantation models given the fact that we used an allogeneic model in immunocompetent rats.

A limiting factor on cell or bioartificial tissue engraftment and survival is immune or inflammatory reaction. In past work we had demonstrated that the density of equine collagen scaffolds decreases by 30% after two weeks of implantation in skeletal muscle and triggers a heavy host cell infiltration. Our previous and current studies also demonstrate a bioluminescence signal drop over the first week indicating decrease in cell survival [Mueller-Stahl, 2008]. The latter apparently occurs regardless the administration of immunosuppresant (i.e. cyclosporine) or not. It seems that the most sensitive and specific time-window to capture in vivo photon emission in MAG –and also the most accurate- is the first week post-implantation in the renal pouch. In spite of this short time frame, it was sensitive enough in our hands to display the difference in bioluminescence signals in the ascorbic acid

enriched MAG. Cell viability after implantation has been demonstrated to be compromised in a time-dependent manner, even in models where one or two immunosuppresive agents have been used [Kutschka, 2006a, Mueller-Stahl, 2008]. Furthermore, in our previous study donor cells could be detected using a cell tracker up to day 21 after graft implantation in immunosupressed rats [Mueller-Stahl, 2008] . This demonstrates that in current models, the fate of grafted tissue is limited by immunologic barriers even when immunosupression is used.

It is likely that the restorative effect of implanted bioartificial grafts is achieved via neovascularization/paracrine effects [Frangogiannis, 2008, Leor, 2000] which in turn attenuate the infarct expansion, rather than by cardiomyocyte regeneration, cell differentiation, or functional graft integration into the host's myocardium. Evidence has shown that most bioengineered tissues for myocardial restoration have mainly focused on multicellular allogeneic approaches to achieve neovascularization within bioengineered grafts [Caspi, 2007, Narmoneva, 2004, Sekine, 2008, Sekiya, 2006, Tan, 2009, Zimmermann, 2009]. With our study, we introduce a strategy to promote a natural pattern of angiogenic sprouting and graft vascularization in the graft recipient itself.

A prominent novelty of the present study is the introduction of the pouch model for in vivo graft pre-vascularization that has proven to be an easy and efficient way to supply bioengineered myocardial tissues with blood vessels of autologous origin. Using neonatal rat cardiomyocytes cast in an equine collagen type I mesh, we have recently shown that graft survival after implantation is determined by host immune responses and degree of angiogenesis [Mueller-Stahl, 2008]. In such model, vascularization could only be seen in the superficial layer of the graft after 14-21 days of implantation. Interestingly, the vascular density was significantly lower when the rats received immunosuppressive therapy. Here we present a model with superior

and faster angiogenic potential. Moreover, we demonstrate that the neovascularization process is enhanced in ascorbic acid-enriched grafts.

4.2 Post-Ischemic Angiogenic Therapy Using In Vivo Pre-Vascularized Ascorbic Acid-Enriched Myocardial Artificial Grafts Improves Heart Function in a Rat Model

Cardiac tissue engineering holds the potential to become a therapeutic option for cardiac repair after MI. Pre-clinical studies suggest that various cell types have the capacity to somewhat restore infarcted myocardium [Bursac, 2009, Toma, 2002, Zimmermann, 2009]. Regardless of the cell type used, myocardial grafts seem to have a positive effect on LV dysfunction, myocardial remodeling and neovascularization via paracrine mechanisms [Kinnaird, 2004, Lionetti, Nakanishi, 2008, Zimmermann, 2009]. However, donor-cell derived paracrine effects on the injured myocardium are not sufficient to support mature vascularization within thick bioengineered grafts, and in the injured heart. Hence, the incorporation of blood vessels within three-dimensional myocardial grafts, as well as the stimulation of in-situ angiogenesis in the ischemic area may play a key role for successful cardiac regeneration. Though the formation of capillaries within ex vivo generated cardiac muscle derived from human embryonic stem cells has been documented [Caspi, 2007], and it has been shown that when transplanted in vivo the human vessels within the graft can become functional and contribute to tissue perfusion [Lesman, 2010b]. However, this approach has not been evaluated yet in pre-clinical studies aiming at post-ischemic myocardial repair. Also, the utilization of human embryonic stem cell-derived cardiomyocytes could be a limitation for immediate clinical application as further studies are required to ensure their safety. data from work involving in vitro generation of human endothelial cell-derived capillary networks

within biodegradable polymer matrices indicate that these in vitro bioengineered blood vessels may become leaky after transplantation [Nor, 2001].

Our previous work showed that supplementation with ascorbic acid improves survival of bioengineered myocardial tissue in vitro via inhibition of cell apoptosis, and enhances donor cell viability, as well as the graft's angiogenic potential in vivo [Martinez, 2010]. Since angiogenesis remains a challenge in cardiac tissue engineering, we tested herein the hypothesis that AA-enriched MAG which have been pre-vascularized in the recipients' own body will promote restoration of the ischemic heart.

Here, we used a model of ischemic LV injury and remodeling in rats, without necessarily satisfying the definition of heart failure. The post-ischemic angiogenic therapy explored in this study decreased LV remodeling and preserved LV function. It is likely that the restorative effect of the implanted MAG was achieved via donor cell-induced early paracrine effects (attenuation of infarct expansion and remodeling), LV structural support, as well as through the robust angiogenic response induced in ischemic rat hearts. The degree of neovascularization obtained in this study is greater than that resulting from previously reported cardiac tissue engineering strategies where only a two-fold increase in blood vessels density was found in the scar zone of infarcted hearts treated with omentum-generated pre-vascularized grafts [Dvir, 2009]. This superior outcome could be due both to the angiogenic effect of AA [Fiorito, 2008, Martinez, 2010, Omeroglu, 2008, Telang, 2007], and to blood vessels of autologous origin from the pre-vascularized graft. Neovessels embedded in the patch may have served as an immediate source of endothelial cells and pro-angiogenic growth factors, as well as a template for new sprouts to "infiltrate" the ischemic myocardium.

4.2.1 Allogeneic Donor Cell Survival in the Implanted Patch

Although reduction of hypoxia-induced apoptosis in vitro has been demonstrated following supplementation with AA in several cell types including rat H9C2 cardiomyoblasts, [Fiorito, 2008, Martinez, 2010, Vassilopoulos, 2005] sustained donor cell survival could not be achieved in our study as evidenced by significantly reduced cell photon emission signals one week after epicardial patch implantation (i.e. 10 days after implantation in the renal pouch). This observation is in agreement with other reports indicating that after graft implantation, early allogeneic donor cell death occurs regardless of the administration of immunosuppressant [Mueller-Stahl, 2008, Pereira, 1990]. The fate of the cells embedded in the implanted patch is limited by the harsh hypoxic environment in the ischemic myocardium which is not conducive to cell survival, and also by immunological barriers. In our previous study, in vivo donor cell survival was enhanced by MAG supplementation with 5 μmol/L AA. However, this effect did not extend beyond 1 week post-implantation in the renal pouch of immunocompetent allogeneic rats [Martinez, 2010]. On the other hand, in the present study it seems that donor cell viability could be maintained for the period of graft pre-vascularization (3 days), to then show a steep decrease (80%) during the first week after epicardial implantation in the ischemic heart. There is evidence of the existence of a cyclosporine A-resistant pathway of T cell activation [Pereira, 1990], and lymphocytes may be activated by macrophages during the post-ischemic wound healing process. The latter might explain why biodegradation and mild foreign body reaction occurred despite immunosuppressive therapy [Mueller-Stahl, 2008]. Since the natural protein-derived (gelatin) scaffold sponges used in this study do not elicit a significant foreign body reaction (FBR) [Rohanizadeh, 2008], the immunogenic reaction observed in the graft area of the MAG group could have been triggered by the allogeneic donor cells. While inflammatory cell infiltration could have compromised donor cell survival, it may have boosted neovascularization in the

ischemic myocardium. Animal studies indicate that the presence of macrophages and neutrophils is sufficient to produce angiogenesis. Likewise, the infiltration of mast cells in the graft area of the MAG-treated animals could have played a critical role in neovascularization [Kim, 2010]. In response to inflammatory cytokines, mast cells -as well as macrophages- secrete IL-8, a chemokine known for its pro-angiogenic effect [Koch, 1992].

4.2.2 Effect of Ascorbic Acid-enriched and Pre-vascularized- MAG on Heart Function

Growing evidence suggests that regardless of early cell donor death, cardiac tissue engineering strategies have a positive effect on heart function. The latter may be attributable to paracrine effects and cardioprotection that lead to neovascularization, containment of remodeling and limitation of non-ischemic infarct expansion, rather than *de novo* cardiomyogenic differentiation of donor cells. As shown herein, MAG treatment immediately after MI attenuated LV remodeling and preserved LV wall thickness. Furthermore, our approach limited LV contractile dysfunction, since percentage FAC, LV ejection fraction and cardiac output were comparable between MAG-treated and healthy animals. Since the heart rate of MI animals is lower than in healthy or MAG animals, this might limit definitive conclusions derived from comparisons for cardiac output and stroke volume, as cardiac output is the product of stroke volume and heart rate. However, it seems that MAG treatment may have prevented relative bradycardia, a complication that may accompany inferior wall infarction [Trappe, 2010].

In a previous study, our group evaluated the effect of porcine gelatin matrix implantation (Gelfoam scaffold without cells) on the infarcted myocardium using a rat heterotopic heart transplant model in which restored hearts were transplanted into the abdomen of syngeneic recipients [Kutschka, 2006b]. Functional evaluation four

weeks after the restorative procedure indicated that transplantation of infarcted control hearts with Gelfoam patches without cells had no beneficial effects on heart function, since it led to significantly lower FS and LVEF compared to heterotopic normal control hearts and infarcted hearts treated with gelfoam grafts seeded with rat cardiomyoblasts overexpressing the BCL2 gene.

Various strategies aiming either at inducing angiogenesis within cardiac grafts or pre-vascularizing them prior to implantation into the ischemic heart have emerged during the last decade [Caspi, 2007, Dvir, 2009, Morritt, 2007, Shao, 2008, Ueyama, 2004]. As expected, the effects on heart function and remodeling obtained after the pre-clinical application of such constructs have been similar to the findings observed in the present study. However, some of the previously reported studies on graft pre-vascularization may have limitations for immediate clinical application due to the utilization of ex vivo allogeneic models or the incorporation of non-FDA approved materials [Caspi, 2007, Dvir, 2009]. Though we cannot consider the progress in the field of production of functional heart muscle anything more than nascent at the present time, here we introduce a model for graft vascularization that may have the potential to be translated into clinical interventions.

Further preclinical studies exploring the effects of AA supplementation and in-vivo vascularization on cardiac grafts containing autologous adult stem cells or cardiac stem cells, as well as their application in chronic models of heart failure are warranted.

4.3 Summary of Key Findings

- Ascorbic Acid enhances donor cell survival within thick three-dimensional bioengineered myocardial grafts cultured under static conditions. Graft viability is improved via reduction of cell apoptosis.

- Supplementation with ascorbic acid induces the expression of cardiac markers in H9C2 cells (rat cardiomyoblasts) cultured in three-dimensional constructs.

- A novel model for myocardial graft pre-vascularization in vivo was introduced, which provides grafts destined for myocardial repair with blood vessels of autologous origin, devoid of side effects.

- Ascorbic acid enrichment promotes neovascularization of potential myocardial artificial grafts in vivo.

- Epicardial implantation of AA-enriched- pre-vascularized- grafts induced a robust angiogenic response in ischemic rat hearts, attenuated left ventricular remodeling (preservation of LV internal dimensions and wall thickness), and limited LV contractile dysfunction.

4.4 Conclusions

In conclusion, the current research introduces a model that is a powerful one to vascularize engineered implants in vivo. The possible explanation for the superior ascorbic acid-enriched graft viability in our allogeneic pre-clinical model might be both the anti-apoptotic and pro-angiogenic effects exerted by ascorbic acid. These findings render ascorbic acid a considerable supplement for cell and tissue transplant-based therapies. Yet, to confirm the wide translational potential of our approach further studies should be done to evaluate the effect of ascorbic acid in 3-D bioartificial myocardial grafts containing human adult stem cells or differentiated cells, as well as in bioengineered tissues destined to regenerate other organs (i.e. bone, cartilage, skin, etc).

Furthermore, the importance of angiogenic therapy to prevent post-ischemic heart failure has been demonstrated in this study. Regardless of the cell approach used to regenerate the myocardium, establishing and maintaining a vascular network is crucial to achieve any improvement in cardiac function within the ischemic area.

On the other hand, our findings suggest that AA-enriched-pre-vascularized MAG constitute a superior source of blood vessels for three-dimensional bioartificial grafts destined for myocardial regeneration. Here we present a tissue engineering-based therapy to prevent adverse remodeling. Furthermore, with our approach, viability support (cell therapy and antioxidant effects), and myocardial revascularization (stimulation of angiogenesis) have been addressed in an acute model of myocardial repair.

In addition, the utilization of biocompatible, inexpensive, FDA approved compounds, as well as MAG vascularization with blood vessels of autologous origin, makes this strategy plausibly translatable and applicable to various donor cell types (ideally, adult stem cells of autologous origin to avoid immune rejection), other organs and regenerative interventions.

We have made progress towards clinical translation of cardiac tissue engineering by providing autologous vascularization to cardiac patches without requiring the utilization and harvest of a major blood vessel. Of note, all first-stage pro-angiogenic tissue implantation could be performed through a minimally invasive laparoscopic procedure, on a day-surgery basis in the clinical setting.

4.5 Challenges and Recommendations

A limitation of our study is the utilization of an allogeneic cell type with poor translational potential (i.e. embryonic cells of rodent origin). Hence, in our currently

ongoing studies we are using human bone marrow-derived mesenchymal stem cells and human umbilical cord mesenchymal stem cells which have the potential to be applied in the clinical arena.

In our myocardial restoration experiments of the present study we did not have negative controls such as acellular patches or MAG without prevascularization. Yet, previous studies carried out by our group suggested that epicardial implantation of Gelfoam alone or Gelfoam seeded with H9C2 cells did not improve cardiac function in an acute model of myocardial restoration in rats. Improvements in cardiac performance were only observed with the addition of growth factors within the graft, or after transduction of H9C2 cells with the human BCL2 transgene [Kutschka, 2006a, Kutschka, 2006b]. Furthermore, echocardiography assessments performed in the myocardial repair experiments of this study were done in a reduced number of animals. Thus, this smaller sample size may not be statistically robust (particularly in the healthy group), and might lead to type I and type II errors. However, our hemodynamics and histology analyses were carried out in all the rats included in this study.

Some aspects besides incorporation of vascularization and control of immune or inflammatory responses need yet to be addressed towards application of engineered myocardial grafts as a therapeutic approach in the clinical setting. Perhaps efforts at myocardial regeneration via tissue engineering do not essentially require implantation of grafts representing partially differentiated “cardiac tissue” that will ultimately not engraft to the left ventricle, increasing thereby the risk of arrhythmias [Smith, 2008]. It has become increasingly evident that cell delivery is not the only –or even the best- tool for myocardial repair, and that cardiac patches should also be used to provide structural support to the ventricular wall while delivering the necessary proteome, cytokines and genes that will stimulate efficiently the heart’s intrinsic regenerative potential.

Finally, emerging tissue engineering-based approaches have yet to be proven as offering advantage over and above existing treatments without unacceptable additional risk to the patient. Our strategy could face some challenges towards its clinical application, as our pre-clinical model involves acute post-MI epicardial patch implantation. The latter is unlikely in the clinical setting due to a high risk of complications and mortality when acute surgery is performed in patients with evolving MI. Ideally, tissue-engineered based interventions should be applied in sub-acute and chronic situations. On the other hand, MAG prevascularization in the renal pouch might have risks associated with any surgical procedure (e.g. infection, bleeding). Yet, these events can be avoided with adequate antibiotic prophylaxis and minimally invasive surgery performed by expert hands.

References

Al Sabti, H. "Therapeutic angiogenesis in cardiovascular disease." *J Cardiothorac Surg* 2, (2007): 49.

Amir, G., Miller, L., Shachar, M., Feinberg, M. S., Holbova, R., Cohen, S., and Leor, J. "Evaluation of a peritoneal-generated cardiac patch in a rat model of heterotopic heart transplantation." *Cell Transplant* 18, no. 3 (2009): 275-82.

Arrigoni, O., and De Tullio, M. C. "Ascorbic acid: much more than just an antioxidant." *Biochim Biophys Acta* 1569, no. 1-3 (2002): 1-9.

Arroll, B., Doughty, R., and Andersen, V. "Investigation and management of congestive heart failure." *BMJ* 341, (2010): c3657.

Asmis, R., and Wintergerst, E. S. "Dehydroascorbic acid prevents apoptosis induced by oxidized low-density lipoprotein in human monocyte-derived macrophages." *Eur J Biochem* 255, no. 1 (1998): 147-55.

Barandon, L., Couffinhal, T., Dufourcq, P., Alzieu, P., Daret, D., Deville, C., and Duplaa, C. "Repair of myocardial infarction by epicardial deposition of bone-marrow-cell-coated muscle patch in a murine model." *Ann Thorac Surg* 78, no. 4 (2004): 1409-17.

Beltrami, A. P., Barlucchi, L., Torella, D., Baker, M., Limana, F., Chimenti, S., Kasahara, H., Rota, M., Musso, E., Urbanek, K., Leri, A., Kajstura, J., Nadal-Ginard, B., and Anversa, P. "Adult cardiac stem cells are multipotent and support myocardial regeneration." *Cell* 114, no. 6 (2003): 763-76.

Bennett, L. E., Keck, B. M., Daily, O. P., Novick, R. J., and Hosenpud, J. D. "Worldwide thoracic organ transplantation: a report from the UNOS/ISHLT International Registry for Thoracic Organ Transplantation." *Clin Transpl* (2000): 31-44.

Birla, R. K., Borschel, G. H., Dennis, R. G., and Brown, D. L. "Myocardial engineering in vivo: formation and characterization of contractile, vascularized three-dimensional cardiac tissue." *Tissue Eng* 11, no. 5-6 (2005): 803-13.

Birla, R. K., Dhawan, V., Dow, D. E., Huang, Y. C., and Brown, D. L. "Cardiac cells implanted into a cylindrical, vascularized chamber in vivo: pressure generation and morphology." *Biotechnol Lett* 31, no. 2 (2009): 191-201.

Blair, R., and Newsome, F. "Involvement of water-soluble vitamins in diseases of swine." *J Anim Sci* 60, no. 6 (1985): 1508-17.

Boilson, B. A., Raichlin, E., Park, S. J., and Kushwaha, S. S. "Device therapy and cardiac transplantation for end-stage heart failure." *Curr Probl Cardiol* 35, no. 1 (2010): 8-64.

Brutsaert, D. L. "Cardiac endothelial-myocardial signaling: its role in cardiac growth, contractile performance, and rhythmicity." *Physiol Rev* 83, no. 1 (2003): 59-115.

Buckberg, G. D. "Basic science review: the helix and the heart." *J Thorac Cardiovasc Surg* 124, no. 5 (2002): 863-83.

Buckberg, G. D. "Form versus disease: optimizing geometry during ventricular restoration." *Eur J Cardiothorac Surg* 29 Suppl 1, (2006a): S238-44.

Buckberg, G. D. "Rethinking the cardiac helix--a structure/function journey: overview." *Eur J Cardiothorac Surg* 29 Suppl 1, (2006b): S2-3.

Bursac, N. "Cardiac tissue engineering using stem cells." *IEEE Eng Med Biol Mag* 28, no. 2 (2009): 80, 82, 84-6, 88-9.

Bursac, N., Papadaki, M., Cohen, R. J., Schoen, F. J., Eisenberg, S. R., Carrier, R., Vunjak-Novakovic, G., and Freed, L. E. "Cardiac muscle tissue engineering: toward an in vitro model for electrophysiological studies." *Am J Physiol* 277, no. 2 Pt 2 (1999): H433-44.

Cao, F., Lin, S., Xie, X., Ray, P., Patel, M., Zhang, X., Drukker, M., Dylla, S. J., Connolly, A. J., Chen, X., Weissman, I. L., Gambhir, S. S., and Wu, J. C. "In vivo visualization of embryonic stem cell survival, proliferation, and migration after cardiac delivery." *Circulation* 113, no. 7 (2006): 1005-14.

Cao, Y. "Adipose tissue angiogenesis as a therapeutic target for obesity and metabolic diseases." *Nat Rev Drug Discov* 9, no. 2 (2010): 107-15.

Carmeliet, P., Ng, Y. S., Nuyens, D., Theilmeier, G., Brusselmans, K., Cornelissen, I., Ehler, E., Kakkar, V. V., Stalmans, I., Mattot, V., Perriard, J. C., Dewerchin, M., Flameng, W., Nagy, A., Lupu, F., Moons, L., Collen, D., D'Amore, P. A., and Shima, D. T. "Impaired myocardial angiogenesis and ischemic cardiomyopathy in mice lacking the vascular endothelial growth factor isoforms VEGF164 and VEGF188." *Nat Med* 5, no. 5 (1999): 495-502.

Caspi, O., Lesman, A., Basevitch, Y., Gepstein, A., Arbel, G., Habib, I. H., Gepstein, L., and Levenberg, S. "Tissue engineering of vascularized cardiac muscle from human embryonic stem cells." *Circ Res* 100, no. 2 (2007): 263-72.

CDC. "Centers for Disease Control and Prevention, National Center for Health Statistics. Compressed Mortality File 1999-2006. CDC WONDER On-line Database, compiled from Compressed Mortality File 1999-2006 Series 20 No. 2L, 2009." http://wonder.cdc.gov/cmf-icd10.html Access date: Aug 5, 2010

Chachques, J. C., Trainini, J. C., Lago, N., Cortes-Morichetti, M., Schussler, O., and Carpentier, A. "Myocardial Assistance by Grafting a New Bioartificial Upgraded Myocardium (MAGNUM trial): clinical feasibility study." *Ann Thorac Surg* 85, no. 3 (2008): 901-8.

Chen, C. H., Wei, H. J., Lin, W. W., Chiu, I., Hwang, S. M., Wang, C. C., Lee, W. Y., Chang, Y., and Sung, H. W. "Porous tissue grafts sandwiched with multilayered mesenchymal stromal cell sheets induce tissue regeneration for cardiac repair." *Cardiovasc Res* 80, no. 1 (2008): 88-95.

Chen, I. Y., Greve, J. M., Gheysens, O., Willmann, J. K., Rodriguez-Porcel, M., Chu, P., Sheikh, A. Y., Faranesh, A. Z., Paulmurugan, R., Yang, P. C., Wu, J. C., and Gambhir, S. S. "Comparison of optical bioluminescence reporter gene and superparamagnetic iron oxide MR contrast agent as cell markers for noninvasive imaging of cardiac cell transplantation." *Mol Imaging Biol* 11, no. 3 (2009): 178-87.

Choi, Y. S., Matsuda, K., Dusting, G. J., Morrison, W. A., and Dilley, R. J. "Engineering cardiac tissue in vivo from human adipose-derived stem cells." *Biomaterials* 31, no. 8 (2010): 2236-42.

Dai, W., Hale, S. L., Kay, G. L., Jyrala, A. J., and Kloner, R. A. "Delivering stem cells to the heart in a collagen matrix reduces relocation of cells to other organs as assessed by nanoparticle technology." *Regen Med* 4, no. 3 (2009): 387-95.

Dawson, A., Davies, J. I., and Struthers, A. D. "The role of aldosterone in heart failure and the clinical benefits of aldosterone blockade." *Expert Rev Cardiovasc Ther* 2, no. 1 (2004): 29-36.

Dobert, N., Britten, M., Assmus, B., Berner, U., Menzel, C., Lehmann, R., Hamscho, N., Schachinger, V., Dimmeler, S., Zeiher, A. M., and Grunwald, F. "Transplantation of progenitor cells after reperfused acute myocardial infarction: evaluation of perfusion and myocardial viability with FDG-PET and thallium SPECT." *Eur J Nucl Med Mol Imaging* 31, no. 8 (2004): 1146-51.

Dvir, T., Kedem, A., Ruvinov, E., Levy, O., Freeman, I., Landa, N., Holbova, R., Feinberg, M. S., Dror, S., Etzion, Y., Leor, J., and Cohen, S. "Prevascularization of cardiac patch on the omentum improves its therapeutic outcome." *Proc Natl Acad Sci U S A* 106, no. 35 (2009): 14990-5.

E, L. L., Zhao, Y. S., Guo, X. M., Wang, C. Y., Jiang, H., Li, J., Duan, C. M., and Song, Y. "Enrichment of cardiomyocytes derived from mouse embryonic stem cells." *J Heart Lung Transplant* 25, no. 6 (2006): 664-74.

Eisner, B. H., Zargooshi, J., Berger, A. D., Cooperberg, M. R., Doyle, S. M., Sheth, S., and Stoller, M. L. "Gender differences in subcutaneous and perirenal fat distribution." *Surg Radiol Anat* (2010).

Falkenstein, E., Christ, M., Feuring, M., and Wehling, M. "Specific nongenomic actions of aldosterone." *Kidney Int* 57, no. 4 (2000): 1390-4.

Fiorito, C., Rienzo, M., Crimi, E., Rossiello, R., Balestrieri, M. L., Casamassimi, A., Muto, F., Grimaldi, V., Giovane, A., Farzati, B., Mancini, F. P., and Napoli, C. "Antioxidants increase number of progenitor endothelial cells through multiple gene expression pathways." *Free Radic Res* 42, no. 8 (2008): 754-62.

Frangogiannis, N. G. "The immune system and cardiac repair." *Pharmacol Res* 58, no. 2 (2008): 88-111.

Fukuda, K. "Regeneration of cardiomyocytes from bone marrow: Use of mesenchymal stem cell for cardiovascular tissue engineering." *Cytotechnology* 41, no. 2-3 (2003): 165-75.

Fukuhara, S., Tomita, S., Nakatani, T., Fujisato, T., Ohtsu, Y., Ishida, M., Yutani, C., and Kitamura, S. "Bone marrow cell-seeded biodegradable polymeric scaffold enhances angiogenesis and improves function of the infarcted heart." *Circ J* 69, no. 7 (2005): 850-7.

Gealekman, O., Burkart, A., Chouinard, M., Nicoloro, S. M., Straubhaar, J., and Corvera, S. "Enhanced angiogenesis in obesity and in response to PPARgamma activators through adipocyte VEGF and ANGPTL4 production." *Am J Physiol Endocrinol Metab* 295, no. 5 (2008): E1056-64.

Gnecchi, M., He, H., Liang, O. D., Melo, L. G., Morello, F., Mu, H., Noiseux, N., Zhang, L., Pratt, R. E., Ingwall, J. S., and Dzau, V. J. "Paracrine action accounts for marked protection of ischemic heart by Akt-modified mesenchymal stem cells." *Nat Med* 11, no. 4 (2005): 367-8.

Gogou, E., Hatzoglou, C., Chamos, V., Zarogiannis, S., Gourgoulianis, K. I., and Molyvdas, P. A. "The contribution of ascorbic acid and dehydroascorbic acid to the protective role of pleura during inflammatory reactions." *Med Hypotheses* 68, no. 4 (2007): 860-3.

Goldberg, L. R. "Heart failure." *Ann Intern Med* 152, no. 11 (2010): ITC61-15; quiz ITC616.

Graham, R. M., Frazier, D. P., Thompson, J. W., Haliko, S., Li, H., Wasserlauf, B. J., Spiga, M. G., Bishopric, N. H., and Webster, K. A. "A unique pathway of cardiac myocyte death caused by hypoxia-acidosis." *J Exp Biol* 207, no. Pt 18 (2004): 3189-200.

Greenway, F. L., Liu, Z., Yu, Y., Caruso, M. K., Roberts, A. T., Lyons, J., Schwimer, J. E., Gupta, A. K., Bellanger, D. E., Guillot, T. S., and Woltering, E. A. "An assay to measure angiogenesis in human fat tissue." *Obes Surg* 17, no. 4 (2007): 510-5.

Hauck, E. S., Zou, S., Scarfo, K., Nantz, M. H., and Hecker, J. G. "Whole animal in vivo imaging after transient, nonviral gene delivery to the rat central nervous system." *Mol Ther* 16, no. 11 (2008): 1857-64.

Hilfiker-Kleiner, Denise, Landmesser, Ulf, and Drexler, Helmut. "Molecular Mechanisms in Heart Failure: Focus on Cardiac Hypertrophy, Inflammation, Angiogenesis, and Apoptosis." *J Am Coll Cardiol* 48, no. 9_Suppl_A (2006): A56-66.

Hitomi, Kiyotaka, and Tuskagoshi, Norihiro. "Ascorbic acid and gene expression." In *Subcellular Biochemistry, Volume 25: Ascorbic Acid: Biochemistry and Biomedical Cell Biology* edited by J. R. Harris, p. 41-49. New York: Springer, 1996.

Hodges, R. E., Hood, J., Canham, J. E., Sauberlich, H. E., and Baker, E. M. "Clinical manifestations of ascorbic acid deficiency in man." *Am J Clin Nutr* 24, no. 4 (1971): 432-43.

Hosenpud, J. D., Bennett, L. E., Keck, B. M., Boucek, M. M., and Novick, R. J. "The Registry of the International Society for Heart and Lung Transplantation: seventeenth official report-2000." *J Heart Lung Transplant* 19, no. 10 (2000): 909-31.

Hosenpud, J. D., Mauck, K. A., and Hogan, K. B. "Cardiac allograft vasculopathy: IgM antibody responses to donor-specific vascular endothelium." *Transplantation* 63, no. 11 (1997): 1602-6.

Huang, J., Agus, D. B., Winfree, C. J., Kiss, S., Mack, W. J., McTaggart, R. A., Choudhri, T. F., Kim, L. J., Mocco, J., Pinsky, D. J., Fox, W. D., Israel, R. J., Boyd, T. A., Golde, D. W., and Connolly, E. S., Jr. "Dehydroascorbic acid, a blood-brain barrier transportable form of vitamin C, mediates potent cerebroprotection in experimental stroke." *Proc Natl Acad Sci U S A* 98, no. 20 (2001): 11720-4.

Hunt, S. A. "Current status of cardiac transplantation." *JAMA* 280, no. 19 (1998): 1692-8.

Jackson, G., Gibbs, C. R., Davies, M. K., and Lip, G. Y. "ABC of heart failure. Pathophysiology." *BMJ* 320, no. 7228 (2000): 167-70.

Jarvis, M. D., Rademaker, M. T., Ellmers, L. J., Currie, M. J., McKenzie, J. L., Palmer, B. R., Frampton, C. M., Richards, A. M., and Cameron, V. A. "Comparison of infarct-derived and control ovine cardiac myofibroblasts in culture: response to cytokines and natriuretic peptide receptor expression profiles." *Am J Physiol Heart Circ Physiol* 291, no. 4 (2006): H1952-8.

Jenkins, D. E., Oei, Y., Hornig, Y. S., Yu, S. F., Dusich, J., Purchio, T., and Contag, P. R. "Bioluminescent imaging (BLI) to improve and refine traditional murine models of tumor growth and metastasis." *Clin Exp Metastasis* 20, no. 8 (2003): 733-44.

Jin, J., Jeong, S. I., Shin, Y. M., Lim, K. S., Shin, H., Lee, Y. M., Koh, H. C., and Kim, K. S. "Transplantation of mesenchymal stem cells within a poly(lactide-co-epsilon-caprolactone) scaffold improves cardiac function in a rat myocardial infarction model." *Eur J Heart Fail* 11, no. 2 (2009): 147-53.

Jneid, H., Moukarbel, G. V., Dawson, B., Hajjar, R. J., and Francis, G. S. "Combining neuroendocrine inhibitors in heart failure: reflections on safety and efficacy." *Am J Med* 120, no. 12 (2007): 1090 e1-8.

Kang, P. M., and Izumo, S. "Apoptosis in heart: basic mechanisms and implications in cardiovascular diseases." *Trends Mol Med* 9, no. 4 (2003): 177-82.

Kannel, W. B. "Incidence and epidemiology of heart failure." *Heart Fail Rev* 5, no. 2 (2000): 167-73.

Kc, S., Carcamo, J. M., and Golde, D. W. "Vitamin C enters mitochondria via facilitative glucose transporter 1 (Glut1) and confers mitochondrial protection against oxidative injury." *FASEB J* 19, no. 12 (2005): 1657-67.

Kellar, R. S., Landeen, L. K., Shepherd, B. R., Naughton, G. K., Ratcliffe, A., and Williams, S. K. "Scaffold-based three-dimensional human fibroblast culture provides a structural matrix that supports angiogenesis in infarcted heart tissue." *Circulation* 104, no. 17 (2001): 2063-8.

Kim, E. J., Won, R., Sohn, J. H., Chung, M. A., Nam, T. S., Lee, H. J., and Lee, B. H. "Anti-oxidant effect of ascorbic and dehydroascorbic acids in hippocampal slice culture." *Biochem Biophys Res Commun* 366, no. 1 (2008): 8-14.

Kim, G. Y., Lee, J. W., Ryu, H. C., Wei, J. D., Seong, C. M., and Kim, J. H. "Proinflammatory cytokine IL-1beta stimulates IL-8 synthesis in mast cells via a leukotriene B4 receptor 2-linked pathway, contributing to angiogenesis." *J Immunol* 184, no. 7 (2010): 3946-54.

Kinnaird, T., Stabile, E., Burnett, M. S., Lee, C. W., Barr, S., Fuchs, S., and Epstein, S. E. "Marrow-derived stromal cells express genes encoding a broad spectrum of arteriogenic cytokines and promote in vitro and in vivo

arteriogenesis through paracrine mechanisms." *Circ Res* 94, no. 5 (2004): 678-85.

Koch, A. E., Polverini, P. J., Kunkel, S. L., Harlow, L. A., DiPietro, L. A., Elner, V. M., Elner, S. G., and Strieter, R. M. "Interleukin-8 as a macrophage-derived mediator of angiogenesis." *Science* 258, no. 5089 (1992): 1798-801.

Koerner, M. M., Durand, J. B., Lafuente, J. A., Noon, G. P., and Torre-Amione, G. "Cardiac transplantation: the final therapeutic option for the treatment of heart failure." *Curr Opin Cardiol* 15, no. 3 (2000): 178-82.

Kofidis, T., de Bruin, J. L., Yamane, T., Balsam, L. B., Lebl, D. R., Swijnenburg, R. J., Tanaka, M., Weissman, I. L., and Robbins, R. C. "Insulin-like growth factor promotes engraftment, differentiation, and functional improvement after transfer of embryonic stem cells for myocardial restoration." *Stem Cells* 22, no. 7 (2004): 1239-45.

Kofidis, T., Lebl, D. R., Martinez, E. C., Hoyt, G., Tanaka, M., and Robbins, R. C. "Novel injectable bioartificial tissue facilitates targeted, less invasive, large-scale tissue restoration on the beating heart after myocardial injury." *Circulation* 112, no. 9 Suppl (2005): I173-7.

Krown, K. A., Page, M. T., Nguyen, C., Zechner, D., Gutierrez, V., Comstock, K. L., Glembotski, C. C., Quintana, P. J., and Sabbadini, R. A. "Tumor necrosis factor alpha-induced apoptosis in cardiac myocytes. Involvement of the sphingolipid signaling cascade in cardiac cell death." *J Clin Invest* 98, no. 12 (1996): 2854-65.

Kutschka, I., Chen, I. Y., Kofidis, T., Arai, T., von Degenfeld, G., Sheikh, A. Y., Hendry, S. L., Pearl, J., Hoyt, G., Sista, R., Yang, P. C., Blau, H. M., Gambhir, S. S., and Robbins, R. C. "Collagen matrices enhance survival of transplanted cardiomyoblasts and contribute to functional improvement of ischemic rat hearts." *Circulation* 114, no. 1 Suppl (2006a): I167-73.

Kutschka, I., Kofidis, T., Chen, I. Y., von Degenfeld, G., Zwierzchoniewska, M., Hoyt, G., Arai, T., Lebl, D. R., Hendry, S. L., Sheikh, A. Y., Cooke, D. T., Connolly, A., Blau, H. M., Gambhir, S. S., and Robbins, R. C. "Adenoviral human BCL-2 transgene expression attenuates early donor cell death after cardiomyoblast transplantation into ischemic rat hearts." *Circulation* 114, no. 1 Suppl (2006b): I174-80.

Langer, R., and Vacanti, J. P. "Tissue engineering." *Science* 260, no. 5110 (1993): 920-6.

Leong, C. W., Wong, C. H., Lao, S. C., Leong, E. C., Lao, I. F., Law, P. T., Fung, K. P., Tsang, K. S., Waye, M. M., Tsui, S. K., Wang, Y. T., and Lee, S. M. "Effect of resveratrol on proliferation and differentiation of embryonic cardiomyoblasts." *Biochem Biophys Res Commun* 360, no. 1 (2007): 173-80.

Leor, J., Aboulafia-Etzion, S., Dar, A., Shapiro, L., Barbash, I. M., Battler, A., Granot, Y., and Cohen, S. "Bioengineered cardiac grafts: A new approach to repair the infarcted myocardium?" *Circulation* 102, no. 19 Suppl 3 (2000): III56-61.

Leor, J., Amsalem, Y., and Cohen, S. "Cells, scaffolds, and molecules for myocardial tissue engineering." *Pharmacol Ther* 105, no. 2 (2005): 151-63.

Lesman, A., Gepstein, L., and Levenberg, S. "Vascularization shaping the heart." *Ann N Y Acad Sci* 1188, (2010a): 46-51.

Lesman, A., Habib, M., Caspi, O., Gepstein, A., Arbel, G., Levenberg, S., and Gepstein, L. "Transplantation of a tissue-engineered human vascularized cardiac muscle." *Tissue Eng Part A* 16, no. 1 (2010b): 115-25.

Li, Y., Song, Y., Zhao, L., Gaidosh, G., Laties, A. M., and Wen, R. "Direct labeling and visualization of blood vessels with lipophilic carbocyanine dye DiI." *Nat Protoc* 3, no. 11 (2008): 1703-8.

Lietz, K., and Miller, L. W. "Will left-ventricular assist device therapy replace heart transplantation in the foreseeable future?" *Curr Opin Cardiol* 20, no. 2 (2005): 132-7.

Lin, Y. J., Lai, M. D., Lei, H. Y., and Wing, L. Y. "Neutrophils and macrophages promote angiogenesis in the early stage of endometriosis in a mouse model." *Endocrinology* 147, no. 3 (2006): 1278-86.

Lionetti, V., Bianchi, G., Recchia, F. A., and Ventura, C. "Control of autocrine and paracrine myocardial signals: an emerging therapeutic strategy in heart failure." *Heart Fail Rev*.

Lloyd-Jones, D., Adams, R. J., Brown, T. M., Carnethon, M., Dai, S., De Simone, G., Ferguson, T. B., Ford, E., Furie, K., Gillespie, C., Go, A., Greenlund, K., Haase, N., Hailpern, S., Ho, P. M., Howard, V., Kissela, B., Kittner, S., Lackland, D., Lisabeth, L., Marelli, A., McDermott, M. M., Meigs, J., Mozaffarian, D., Mussolino, M., Nichol, G., Roger, V. L., Rosamond, W., Sacco, R., Sorlie, P., Stafford, R., Thom, T., Wasserthiel-Smoller, S., Wong, N. D., and Wylie-Rosett, J. "Heart disease and stroke statistics--2010 update: a report from the American Heart Association." *Circulation* 121, no. 7 (2010): e46-e215.

Long, K. Z., and Santos, J. I. "Vitamins and the regulation of the immune response." *Pediatr Infect Dis J* 18, no. 3 (1999): 283-90.

Malhotra, R., Tyson, D. W., Rosevear, H. M., and Brosius, F. C., 3rd. "Hypoxia-inducible factor-1alpha is a critical mediator of hypoxia induced apoptosis in cardiac H9c2 and kidney epithelial HK-2 cells." *BMC Cardiovasc Disord* 8, (2008): 9.

Mancini, D., and Lietz, K. "Selection of cardiac transplantation candidates in 2010." *Circulation* 122, no. 2 (2010): 173-83.

Mann, D. L. "Recent insights into the role of tumor necrosis factor in the failing heart." *Heart Fail Rev* 6, no. 2 (2001): 71-80.

Mann, D. L., Bogaev, R., and Buckberg, G. D. "Cardiac remodelling and myocardial recovery: lost in translation?" *Eur J Heart Fail* 12, no. 8 (2010): 789-96.

Margulies, K. B. "Reversal mechanisms of left ventricular remodeling: lessons from left ventricular assist device experiments." *J Card Fail* 8, no. 6 Suppl (2002): S500-5.

Martinez, E. C., and Kofidis, T. "Adult Stem Cells for Cardiac Tissue Engineering." *J Mol Cell Cardiol* 50, no. 2 (2011): 312-9.

Martinez, E. C., and Kofidis, T. "Myocardial tissue engineering: the quest for the ideal myocardial substitute." *Expert Rev Cardiovasc Ther* 7, no. 8 (2009): 921-8.

Martinez, E. C., Wang, J., Gan, S. U., Singh, R., Lee, C. N., and Kofidis, T. "Ascorbic acid improves embryonic cardiomyoblast cell survival and promotes vascularization in potential myocardial grafts in vivo." *Tissue Eng Part A* 16, no. 4 (2010): 1349-61.

Martino, L., Novelli, M., Masini, M., Chimenti, D., Piaggi, S., Masiello, P., and De Tata, V. "Dehydroascorbate protection against dioxin-induced toxicity in the beta-cell line INS-1E." *Toxicol Lett* 189, no. 1 (2009): 27-34.

McClintock, D. S., Santore, M. T., Lee, V. Y., Brunelle, J., Budinger, G. R., Zong, W. X., Thompson, C. B., Hay, N., and Chandel, N. S. "Bcl-2 family members and functional electron transport chain regulate oxygen deprivation-induced cell death." *Mol Cell Biol* 22, no. 1 (2002): 94-104.

Menasche, P. "Cardiac cell therapy: Lessons from clinical trials." *J Mol Cell Cardiol* (2010).

Menasche, P. "Skeletal myoblast for cell therapy." *Coron Artery Dis* 16, no. 2 (2005): 105-10.

Messina, E., De Angelis, L., Frati, G., Morrone, S., Chimenti, S., Fiordaliso, F., Salio, M., Battaglia, M., Latronico, M. V., Coletta, M., Vivarelli, E., Frati, L., Cossu,

G., and Giacomello, A. "Isolation and expansion of adult cardiac stem cells from human and murine heart." *Circ Res* 95, no. 9 (2004): 911-21.

Meyer, G. P., Wollert, K. C., Lotz, J., Pirr, J., Rager, U., Lippolt, P., Hahn, A., Fichtner, S., Schaefer, A., Arseniev, L., Ganser, A., and Drexler, H. "Intracoronary bone marrow cell transfer after myocardial infarction: 5-year follow-up from the randomized-controlled BOOST trial." *Eur Heart J* 30, no. 24 (2009): 2978-84.

Miller, L. W., and Missov, E. D. "Epidemiology of heart failure." *Cardiol Clin* 19, no. 4 (2001): 547-55.

Miyahara, Y., Nagaya, N., Kataoka, M., Yanagawa, B., Tanaka, K., Hao, H., Ishino, K., Ishida, H., Shimizu, T., Kangawa, K., Sano, S., Okano, T., Kitamura, S., and Mori, H. "Monolayered mesenchymal stem cells repair scarred myocardium after myocardial infarction." *Nat Med* 12, no. 4 (2006): 459-65.

Morritt, A. N., Bortolotto, S. K., Dilley, R. J., Han, X., Kompa, A. R., McCombe, D., Wright, C. E., Itescu, S., Angus, J. A., and Morrison, W. A. "Cardiac tissue engineering in an in vivo vascularized chamber." *Circulation* 115, no. 3 (2007): 353-60.

Mueller-Stahl, K., Kofidis, T., Akhyari, P., Lee, D. H., Lenz, A., Martinez, E. C., Woitek, F., and Haverich, A. "Determinants of bioartificial myocardial graft survival and engraftment in vivo." *J Heart Lung Transplant* 27, no. 11 (2008): 1242-50.

Muller-Ehmsen, J., Whittaker, P., Kloner, R. A., Dow, J. S., Sakoda, T., Long, T. I., Laird, P. W., and Kedes, L. "Survival and development of neonatal rat cardiomyocytes transplanted into adult myocardium." *J Mol Cell Cardiol* 34, no. 2 (2002): 107-16.

Muller-Werdan, U., Schumann, H., Fuchs, R., Reithmann, C., Loppnow, H., Koch, S., Zimny-Arndt, U., He, C., Darmer, D., Jungblut, P., Stadler, J., Holtz, J., and Werdan, K. "Tumor necrosis factor alpha (TNF alpha) is cardiodepressant in pathophysiologically relevant concentrations without inducing inducible nitric oxide-(NO)-synthase (iNOS) or triggering serious cytotoxicity." *J Mol Cell Cardiol* 29, no. 11 (1997): 2915-23.

Muschler, G. F., Nakamoto, C., and Griffith, L. G. "Engineering principles of clinical cell-based tissue engineering." *J Bone Joint Surg Am* 86-A, no. 7 (2004): 1541-58.

Nabeebaccus, A., Zhang, M., and Shah, A. M. "NADPH oxidases and cardiac remodelling." *Heart Fail Rev* (2010).

Nagaya, N., Kangawa, K., Itoh, T., Iwase, T., Murakami, S., Miyahara, Y., Fujii, T., Uematsu, M., Ohgushi, H., Yamagishi, M., Tokudome, T., Mori, H., Miyatake, K., and Kitamura, S. "Transplantation of mesenchymal stem cells improves cardiac function in a rat model of dilated cardiomyopathy." *Circulation* 112, no. 8 (2005): 1128-35.

Naito, H., Melnychenko, I., Didie, M., Schneiderbanger, K., Schubert, P., Rosenkranz, S., Eschenhagen, T., and Zimmermann, W. H. "Optimizing engineered heart tissue for therapeutic applications as surrogate heart muscle." *Circulation* 114, no. 1 Suppl (2006): I72-8.

Nakanishi, C., Yamagishi, M., Yamahara, K., Hagino, I., Mori, H., Sawa, Y., Yagihara, T., Kitamura, S., and Nagaya, N. "Activation of cardiac progenitor cells through paracrine effects of mesenchymal stem cells." *Biochem Biophys Res Commun* 374, no. 1 (2008): 11-6.

Nandan, D., Clarke, E. P., Ball, E. H., and Sanwal, B. D. "Ethyl-3,4-dihydroxybenzoate inhibits myoblast differentiation: evidence for an essential role of collagen." *J Cell Biol* 110, no. 5 (1990): 1673-9.

Narmoneva, D. A., Vukmirovic, R., Davis, M. E., Kamm, R. D., and Lee, R. T. "Endothelial cells promote cardiac myocyte survival and spatial

reorganization: implications for cardiac regeneration." *Circulation* 110, no. 8 (2004): 962-8.

Nor, J. E., Peters, M. C., Christensen, J. B., Sutorik, M. M., Linn, S., Khan, M. K., Addison, C. L., Mooney, D. J., and Polverini, P. J. "Engineering and characterization of functional human microvessels in immunodeficient mice." *Lab Invest* 81, no. 4 (2001): 453-63.

O'Shaughnessy, L. "Surgical treatment of cardiac ischemia." *Lancet* 232, (1937): 185-94.

Omeroglu, S., Peker, T., Turkozkan, N., and Omeroglu, H. "High-dose vitamin C supplementation accelerates the Achilles tendon healing in healthy rats." *Arch Orthop Trauma Surg* 2, (2008): 281-86.

Ott, H. C., Matthiesen, T. S., Goh, S. K., Black, L. D., Kren, S. M., Netoff, T. I., and Taylor, D. A. "Perfusion-decellularized matrix: using nature's platform to engineer a bioartificial heart." *Nat Med* 14, no. 2 (2008): 213-21.

Pereira, G. M., Miller, J. F., and Shevach, E. M. "Mechanism of action of cyclosporine A in vivo. II. T cell priming in vivo to alloantigen can be mediated by an IL-2-independent cyclosporine A-resistant pathway." *J Immunol* 144, no. 6 (1990): 2109-16.

Pfeffer, M. A., and Braunwald, E. "Ventricular remodeling after myocardial infarction. Experimental observations and clinical implications." *Circulation* 81, no. 4 (1990): 1161-72.

Phua, H. P., Chua, A. V., Ma, S., Heng, D., and Chew, S. K. "Singapore's burden of disease and injury 2004." *Singapore Med J* 50, no. 5 (2009): 468-78.

Piao, H., Kwon, J. S., Piao, S., Sohn, J. H., Lee, Y. S., Bae, J. W., Hwang, K. K., Kim, D. W., Jeon, O., Kim, B. S., Park, Y. B., and Cho, M. C. "Effects of cardiac patches engineered with bone marrow-derived mononuclear cells and PGCL scaffolds in a rat myocardial infarction model." *Biomaterials* 28, no. 4 (2007): 641-9.

Planat-Benard, V., Menard, C., Andre, M., Puceat, M., Perez, A., Garcia-Verdugo, J. M., Penicaud, L., and Casteilla, L. "Spontaneous cardiomyocyte differentiation from adipose tissue stroma cells." *Circ Res* 94, no. 2 (2004): 223-9.

Platell, C., Cooper, D., Papadimitriou, J. M., and Hall, J. C. "The omentum." *World J Gastroenterol* 6, no. 2 (2000): 169-76.

Polykandriotis, E., Arkudas, A., Horch, R. E., and Kneser, U. "To matrigel or not to matrigel." *Am J Pathol* 172, no. 5 (2008): 1441; author reply 41-2.

Puskas, F., Gergely, P., Jr., Banki, K., and Perl, A. "Stimulation of the pentose phosphate pathway and glutathione levels by dehydroascorbate, the oxidized form of vitamin C." *FASEB J* 14, no. 10 (2000): 1352-61.

Radisic, M., Park, H., Gerecht, S., Cannizzaro, C., Langer, R., and Vunjak-Novakovic, G. "Biomimetic approach to cardiac tissue engineering." *Philos Trans R Soc Lond B Biol Sci* 362, no. 1484 (2007): 1357-68.

Reinecke, H., and Murry, C. E. "Taking the death toll after cardiomyocyte grafting: a reminder of the importance of quantitative biology." *J Mol Cell Cardiol* 34, no. 3 (2002): 251-3.

Robey, T. E., Saiget, M. K., Reinecke, H., and Murry, C. E. "Systems approaches to preventing transplanted cell death in cardiac repair." *J Mol Cell Cardiol* 45, no. 4 (2008): 567-81.

Rohanizadeh, R., Swain, M. V., and Mason, R. S. "Gelatin sponges (Gelfoam) as a scaffold for osteoblasts." *J Mater Sci Mater Med* 19, no. 3 (2008): 1173-82.

Ryu, J. H., Kim, I. K., Cho, S. W., Cho, M. C., Hwang, K. K., Piao, H., Piao, S., Lim, S. H., Hong, Y. S., Choi, C. Y., Yoo, K. J., and Kim, B. S. "Implantation of bone marrow mononuclear cells using injectable fibrin matrix enhances neovascularization in infarcted myocardium." *Biomaterials* 26, no. 3 (2005): 319-26.

Sam, F., Kerstetter, D. L., Pimental, D. R., Mulukutla, S., Tabaee, A., Bristow, M. R., Colucci, W. S., and Sawyer, D. B. "Increased reactive oxygen species production and functional alterations in antioxidant enzymes in human failing myocardium." *J Card Fail* 11, no. 6 (2005): 473-80.

Sato, H., Takahashi, M., Ise, H., Yamada, A., Hirose, S., Tagawa, Y., Morimoto, H., Izawa, A., and Ikeda, U. "Collagen synthesis is required for ascorbic acid-enhanced differentiation of mouse embryonic stem cells into cardiomyocytes." *Biochem Biophys Res Commun* 342, no. 1 (2006): 107-12.

Schachinger, V., Assmus, B., Britten, M. B., Honold, J., Lehmann, R., Teupe, C., Abolmaali, N. D., Vogl, T. J., Hofmann, W. K., Martin, H., Dimmeler, S., and Zeiher, A. M. "Transplantation of progenitor cells and regeneration enhancement in acute myocardial infarction: final one-year results of the TOPCARE-AMI Trial." *J Am Coll Cardiol* 44, no. 8 (2004): 1690-9.

Schaefer, A., Zwadlo, C., Fuchs, M., Meyer, G. P., Lippolt, P., Wollert, K. C., and Drexler, H. "Long-term effects of intracoronary bone marrow cell transfer on diastolic function in patients after acute myocardial infarction: 5-year results from the randomized-controlled BOOST trial--an echocardiographic study." *Eur J Echocardiogr* 11, no. 2 (2009): 165-71.

Schenke-Layland, K., Strem, B. M., Jordan, M. C., Deemedio, M. T., Hedrick, M. H., Roos, K. P., Fraser, J. K., and Maclellan, W. R. "Adipose tissue-derived cells improve cardiac function following myocardial infarction." *J Surg Res* 153, no. 2 (2009): 217-23.

Schnee, J. M., and Hsueh, W. A. "Angiotensin II, adhesion, and cardiac fibrosis." *Cardiovasc Res* 46, no. 2 (2000): 264-8.

Sekine, H., Shimizu, T., Hobo, K., Sekiya, S., Yang, J., Yamato, M., Kurosawa, H., Kobayashi, E., and Okano, T. "Endothelial cell coculture within tissue-engineered cardiomyocyte sheets enhances neovascularization and improves cardiac function of ischemic hearts." *Circulation* 118, no. 14 Suppl (2008): S145-52.

Sekiya, S., Shimizu, T., Yamato, M., Kikuchi, A., and Okano, T. "Bioengineered cardiac cell sheet grafts have intrinsic angiogenic potential." *Biochem Biophys Res Commun* 341, no. 2 (2006): 573-82.

Shah, R. V., and Fifer, M. A. "Heart Failure." In *Pathophysiology of heart disease: a collaborative project of medical students and faculty*, edited by L. S. Lilly, p. 225-51. Baltimore: Lippincott Williams & Wilkins, 2007.

Shao, Z. Q., Kawasuji, M., Takaji, K., Katayama, Y., and Matsukawa, M. "Therapeutic angiogenesis with autologous hepatic tissue implantation and omental wrapping." *Circ J* 72, no. 11 (2008): 1894-9.

Shim, W. S., Jiang, S., Wong, P., Tan, J., Chua, Y. L., Tan, Y. S., Sin, Y. K., Lim, C. H., Chua, T., Teh, M., Liu, T. C., and Sim, E. "Ex vivo differentiation of human adult bone marrow stem cells into cardiomyocyte-like cells." *Biochem Biophys Res Commun* 324, no. 2 (2004): 481-8.

Shimizu, T., Sekine, H., Yang, J., Isoi, Y., Yamato, M., Kikuchi, A., Kobayashi, E., and Okano, T. "Polysurgery of cell sheet grafts overcomes diffusion limits to produce thick, vascularized myocardial tissues." *FASEB J* 20, no. 6 (2006): 708-10.

Shimizu, T., Yamato, M., Isoi, Y., Akutsu, T., Setomaru, T., Abe, K., Kikuchi, A., Umezu, M., and Okano, T. "Fabrication of pulsatile cardiac tissue grafts using a novel 3-dimensional cell sheet manipulation technique and temperature-responsive cell culture surfaces." *Circ Res* 90, no. 3 (2002): e40.

Shinde, R., Perkins, J., and Contag, C. H. "Luciferin derivatives for enhanced in vitro and in vivo bioluminescence assays." *Biochemistry* 45, no. 37 (2006): 11103-12.

Simpson, D., Liu, H., Fan, T. H., Nerem, R., and Dudley, S. C., Jr. "A tissue engineering approach to progenitor cell delivery results in significant cell engraftment and improved myocardial remodeling." *Stem Cells* 25, no. 9 (2007): 2350-7.

Smith, R. R., Barile, L., Messina, E., and Marban, E. "Stem cells in the heart: what's the buzz all about? Part 2: Arrhythmic risks and clinical studies." *Heart Rhythm* 5, no. 6 (2008): 880-7.

Souders, C. A., Bowers, S. L., and Baudino, T. A. "Cardiac fibroblast: the renaissance cell." *Circ Res* 105, no. 12 (2009): 1164-76.

Sunderkotter, C., Goebeler, M., Schulze-Osthoff, K., Bhardwaj, R., and Sorg, C. "Macrophage-derived angiogenesis factors." *Pharmacol Ther* 51, no. 2 (1991): 195-216.

Suzuki, K., Murtuza, B., Beauchamp, J. R., Brand, N. J., Barton, P. J., Varela-Carver, A., Fukushima, S., Coppen, S. R., Partridge, T. A., and Yacoub, M. H. "Role of interleukin-1beta in acute inflammation and graft death after cell transplantation to the heart." *Circulation* 110, no. 11 Suppl 1 (2004): II219-24.

Swedberg, K. "Importance of neuroendocrine activation in chronic heart failure. Impact on treatment strategies." *Eur J Heart Fail* 2, no. 3 (2000): 229-33.

Tabibiazar, R., and Rockson, S. G. "Angiogenesis and the ischaemic heart." *Eur Heart J* 22, no. 11 (2001): 903-18.

Takahashi, T., Lord, B., Schulze, P. C., Fryer, R. M., Sarang, S. S., Gullans, S. R., and Lee, R. T. "Ascorbic acid enhances differentiation of embryonic stem cells into cardiac myocytes." *Circulation* 107, no. 14 (2003): 1912-6.

Tan, M. Y., Zhi, W., Wei, R. Q., Huang, Y. C., Zhou, K. P., Tan, B., Deng, L., Luo, J. C., Li, X. Q., Xie, H. Q., and Yang, Z. M. "Repair of infarcted myocardium using mesenchymal stem cell seeded small intestinal submucosa in rabbits." *Biomaterials* 19, (2009): 3234-40

Tanaka, M., Muto, N., Gohda, E., and Yamamoto, I. "Enhancement by ascorbic acid 2-glucoside or repeated additions of ascorbate of mitogen-induced IgM and IgG productions by human peripheral blood lymphocytes." *Jpn J Pharmacol* 66, no. 4 (1994): 451-6.

Tang, W. H., Shrestha, K., Martin, M. G., Borowski, A. G., Jasper, S., Yandle, T. G., Richards, A. M., Klein, A. L., and Troughton, R. W. "Clinical significance of endogenous vasoactive neurohormones in chronic systolic heart failure." *J Card Fail* 16, no. 8 (2010): 635-40.

Telang, S., Clem, A. L., Eaton, J. W., and Chesney, J. "Depletion of ascorbic acid restricts angiogenesis and retards tumor growth in a mouse model." *Neoplasia* 9, no. 1 (2007): 47-56.

Teng, C. J., Luo, J., Chiu, R. C., and Shum-Tim, D. "Massive mechanical loss of microspheres with direct intramyocardial injection in the beating heart: implications for cellular cardiomyoplasty." *J Thorac Cardiovasc Surg* 132, no. 3 (2006): 628-32.

Toma, C., Pittenger, M. F., Cahill, K. S., Byrne, B. J., and Kessler, P. D. "Human mesenchymal stem cells differentiate to a cardiomyocyte phenotype in the adult murine heart." *Circulation* 105, no. 1 (2002): 93-8.

Trappe, H. J. "Tachyarrhythmias, bradyarrhythmias and acute coronary syndromes." *J Emerg Trauma Shock* 3, no. 2 (2010): 137-42.

Ueyama, K., Bing, G., Tabata, Y., Ozeki, M., Doi, K., Nishimura, K., Suma, H., and Komeda, M. "Development of biologic coronary artery bypass grafting in a rabbit model: revival of a classic concept with modern biotechnology." *J Thorac Cardiovasc Surg* 127, no. 6 (2004): 1608-15.

Vacanti, C. A. "The history of tissue engineering." *J Cell Mol Med* 10, no. 3 (2006): 569-76.

Vassilopoulos, A., and Papazafiri, P. "Attenuation of oxidative stress in HL-1 cardiomyocytes improves mitochondrial function and stabilizes Hif-1alpha." *Free Radic Res* 39, no. 12 (2005): 1273-84.

Vissers, M. C., Gunningham, S. P., Morrison, M. J., Dachs, G. U., and Currie, M. J. "Modulation of hypoxia-inducible factor-1 alpha in cultured primary cells by intracellular ascorbate." *Free Radic Biol Med* 42, no. 6 (2007): 765-72.

Wang, C. C., Chen, C. H., Lin, W. W., Hwang, S. M., Hsieh, P. C., Lai, P. H., Yeh, Y. C., Chang, Y., and Sung, H. W. "Direct intramyocardial injection of mesenchymal stem cell sheet fragments improves cardiac functions after infarction." *Cardiovasc Res* 77, no. 3 (2008): 515-24.

Wang, H., Zhou, J., Liu, Z., and Wang, C. "Injectable cardiac tissue engineering for the treatment of myocardial infarction." *J Cell Mol Med* 5(2010): 1044-55.

Wei, H. J., Chen, C. H., Lee, W. Y., Chiu, I., Hwang, S. M., Lin, W. W., Huang, C. C., Yeh, Y. C., Chang, Y., and Sung, H. W. "Bioengineered cardiac patch constructed from multilayered mesenchymal stem cells for myocardial repair." *Biomaterials* 29, no. 26 (2008): 3547-56.

Weytjens, C., Cosyns, B., D'Hooge, J., Gallez, C., Droogmans, S., Lahoute, T., Franken, P., and Van Camp, G. "Doppler myocardial imaging in adult male rats: reference values and reproducibility of velocity and deformation parameters." *Eur J Echocardiogr* 7, no. 6 (2006): 411-7.

White, H. D., Norris, R. M., Brown, M. A., Brandt, P. W., Whitlock, R. M., and Wild, C. J. "Left ventricular end-systolic volume as the major determinant of survival after recovery from myocardial infarction." *Circulation* 76, no. 1 (1987): 44-51.

WHO, World Health Organization. "Singapore health situation and trend." http://www.wpro.who.int/countries/sin/2009/health_situation.htm Access date: July 30, 2010.

Wollert, K. C., Meyer, G. P., Lotz, J., Ringes-Lichtenberg, S., Lippolt, P., Breidenbach, C., Fichtner, S., Korte, T., Hornig, B., Messinger, D., Arseniev, L., Hertenstein, B., Ganser, A., and Drexler, H. "Intracoronary autologous bone-marrow cell transfer after myocardial infarction: the BOOST randomised controlled clinical trial." *Lancet* 364, no. 9429 (2004): 141-8.

Wu, J. C., Chen, I. Y., Sundaresan, G., Min, J. J., De, A., Qiao, J. H., Fishbein, M. C., and Gambhir, S. S. "Molecular imaging of cardiac cell transplantation in living animals using optical bioluminescence and positron emission tomography." *Circulation* 108, no. 11 (2003): 1302-5.

Wu, X. M., Branford-White, C. J., Yu, D. G., Chatterton, N. P., and Zhu, L. M. "Preparation of core-shell PAN nanofibers encapsulated alpha-tocopherol acetate and ascorbic acid 2-phosphate for photoprotection." *Colloids Surf B Biointerfaces* 82, no. 1 (2011): 247-52.

Xiang, Z., Liao, R., Kelly, M. S., and Spector, M. "Collagen-GAG scaffolds grafted onto myocardial infarcts in a rat model: a delivery vehicle for mesenchymal stem cells." *Tissue Eng* 12, no. 9 (2006): 2467-78.

Yoshida, H., Matsusaki, M., and Akashi, M. "Development of thick and highly cell-incorporated engineered tissues by hydrogel template approach with basic fibroblast growth factor or ascorbic acid." *J Biomater Sci Polym Ed* 21, no. 4 (2010): 415-28.

Zhang, H., Song, P., Tang, Y., Zhang, X. L., Zhao, S. H., Wei, Y. J., and Hu, S. S. "Injection of bone marrow mesenchymal stem cells in the borderline area of infarcted myocardium: heart status and cell distribution." *J Thorac Cardiovasc Surg* 134, no. 5 (2007): 1234-40.

Zhang, J. Y., Doll, B. A., Beckman, E. J., and Hollinger, J. O. "Three-dimensional biocompatible ascorbic acid-containing scaffold for bone tissue engineering." *Tissue Eng* 9, no. 6 (2003): 1143-57.

Zimmermann, W. H. "Remuscularizing Failing Hearts with Tissue Engineered Myocardium." *Antioxid Redox Signal* 8, (2009): 2011-23.

Zimmermann, W. H., and Eschenhagen, T. "Embryonic stem cells for cardiac muscle engineering." *Trends Cardiovasc Med* 17, no. 4 (2007): 134-40.

Zimmermann, W. H., Melnychenko, I., Wasmeier, G., Didie, M., Naito, H., Nixdorff, U., Hess, A., Budinsky, L., Brune, K., Michaelis, B., Dhein, S., Schwoerer, A., Ehmke, H., and Eschenhagen, T. "Engineered heart tissue grafts improve systolic and diastolic function in infarcted rat hearts." *Nat Med* 12, no. 4 (2006): 452-8.